STRATIGRAPHIC DISTRIBUTION AND PALEOENVIRONMENTAL IMPLICATIONS OF PEDOGENIC FEATURES AND TRACE FOSSILS FROM THE LOWER PERMIAN OF KANSAS

By

John Waldon Counts

B.S., Auburn University, 2005

Submitted to the Department of Geology and the Faculty of the Graduate School of the
University of Kansas in partial fulfillment of the requirements for the degree of
Master of Science

Advisory Committee:

Chairman: Stephen T. Hasiotis

W. Lynn Watney

Robert H. Goldstein

Date Defended: November 16th, 2012

The thesis committee for John W. Counts certifies
that this is the approved version of the following thesis:

STRATIGRAPHIC DISTRIBUTION AND PALEOENVIRONMENTAL IMPLICATIONS OF PEDOGENIC FEATURES AND TRACE FOSSILS FROM THE LOWER PERMIAN OF KANSAS

Advisory Committee:

____

Stephen T. Hasiotis, Chairman

____

W. Lynn Watney

____

Robert H. Goldstein

Date submitted: November 21st, 2012

ABSTRACT

John W. Counts, M.S.
Department of Geology, November 2012
University of Kansas

Paleosols in the Lower Permian (Asselian–Sakmarian) Council Grove Group from western Kansas, USA, contain numerous pedogenic features, including carbonate nodules (caliche), redoximorphic coloration, rhizoliths, and trace fossils, which can be used to reconstruct the paleoenvironmental and paleoclimatic conditions during the interval of soil formation. Due to the paleogeographic setting of the Hugoton Basin, 5th-order cycles recorded in distant Council Grove Group outcrops are condensed in the study area into cumulic paleosols that contain pedogenic features signifying both wet and dry climates. Wet/dry cycles are interpreted to be the product of eustatically driven climate change, as well as seasonal changes related to monsoonal weather variability. Statistical analyses of the distribution of pedogenic features indicate a change from drier to wetter conditions over the upper Council Grove Group interval. Detailed study of trace fossils revealed unique morphologies that warrant the erection of a new ichnospecies, proposed here as *Naktodemasis krausi*. These assemblages are the oldest known occurrence of the genus *Naktodemasis*. Trace fossils were interpreted as the burrows of soil-dwelling insects or insect larvae that colonized semiarid coastal plain environments during periods of subaerial exposure, creating topography and reducing accommodation, thereby preventing the formation of discrete 5th-order lithologic cycles. In order to provide further evidence for the origin of trace fossils, neoichnological experiments were conducted to compare ancient burrows to those of modern fossorial insects. Experimental results showed that the burrows of modern coleopterans belonging to the masked chafer beetles (*Cyclocephala* sp.) are convincing analogs for Permian trace fossils, and provide some general constraints on moisture tolerances for potential Permian tracemakers. The presence of these traces in Permian sediments, therefore, indicate that soil moisture levels during sea-level lowstands were high enough to support sustained populations of similar organisms. This study also conclusively demonstrates that burrows of this type could be constructed in subaerial settings, and documents the unique burrowing mechanism of the masked chafer beetle.

ACKNOWLEDGEMENTS

This thesis would not be possible without the never-ending patience and encouragement of my friends, family, and colleagues. During the many years that it was in preparation, there were countless times when I would have given up if it was not for the support I received along the way. More than anyone else, I am forever in debted to Dr. Stephen (Steve) Hasiotis. None of my success today would have been possible if he had not taken a chance with me in 2005, and I could never have finished without his help or the fact that he never gave up on me through the years that I was away. I also thank the faculty of the University of Kansas, especially my committee members Bob Goldstein and Lynn Watney, for their reviews of my work. Many of my fellow graduate students deserve thanks as well—Brian Platt, Justin Fairchild, David Lobue, Aisha Al-Suwaidi, and Kenny Bader (among many others) all contributed to my geologic understanding and provided helpful support along the way. Marty Dubois and Jon Smith were instrumental in laying the groundwork for different parts of this study and deserve special recognition. I also wish to thank Ian Rowell at the KU Geology department, Jill Krebs at the KUMIP, and Mike Cormack and Jill Hardesty at the Paleontological Institute for all their help throughout the years.

Of the many people who have inspired me throughout the years, my parents were the first to instill in me a love and appreciation of science. Through their encouragement, I knew from a young age that I wanted to be involved with the sciences for the rest of my life. Drs. Charles Savrda and Ron Lewis at Auburn University were pretty much solely responsible for my geological career—without their support I probably never would have become a geologist, much less been accepted to graduate school.

Finally, I thank my loving wife, Shelagh Morrissey Jessop, for supporting me in many ways over the past six years. Without her I would have given up on this thesis long ago.

TABLE OF CONTENTS

FIGURES AND TABLES

Tables

Appendices

CHAPTER ONE. INTRODUCTION

The purpose of this study is to describe and interpret the character of pedogenic features and trace fossil assemblages in Lower Permian (Asselian–Sakmarian; Wolfcampian) paleosols of western Kansas, and to establish constraints on soil moisture and climate regimes in the study area through the detailed examination of trace fossils and their modern analogs. Although outcrops of Permian strata in Kansas have been well studied, this study focuses on subsurface core in the Hugoton-Panoma gas field, an area that has received less academic attention. Paleosols and trace fossils in the study area are significantly different than those seen in equivalent strata in outcrop and, thus, provide new insights into the paleoenvironmental and paleoclimatic variability in the Early Permian of the midcontinent.

Cyclical sedimentation in the late Paleozoic of Kansas has been recognized as eustatically driven for decades (Wanless and Shepard, 1936), and lowstand intervals have long been interpreted as having been subaerially exposed and pedogenically modified. Only in the last 20 years, however, has debate arisen regarding the nature of potential climate changes associated with these global sea level changes (e.g., Soreghan, 1994; Miller et al., 1999; Rankey, 1997; Olszewski and Patzkowsky, 2003, and many others). A variety of interpretations, some mutually exclusive, have been proposed for the relationship between sea level and climate. At issue is whether sea-level lowstands, consisting of clastics or paleosols, are associated with drier or wetter conditions relative to transgressive or highstand limestones. Here, we examine a number of pedogenic features in a series of continental intervals in the upper Council Grove Group that can be used as proxies for soil moisture and paleoclimate, and the stratigraphic change in these climate proxies across three formations. We also examine the differences in paleosol character and stratigraphic architecture between the study area and equivalent outcrops in eastern Kansas in order to determine the influence of paleogeographic setting on soil formation.

Trace fossils found in continental intervals proved especially interesting, and were the subject of further study. Traces in the upper Council Grove consist solely of small, unbranching, cylindrical burrows with tortuous axes and meniscate backfill, which are highly abundant in most studied intervals. Detailed examination of traces revealed a number of morphologic features that distinguish these trace fossils from other known ichnospecies; notable differences include the shape of internal menisci and the bundling of menisci into groups or packets. Permian traces were proposed to be placed into a new ichnospecies *Naktodemasis krausi*, described in this thesis for the first time.

Although meniscate burrows of this type have traditionally been thought to be formed solely in subaqueous settings, a growing body of research is demonstrating that such burrows can also be formed subaerially by soil-dwelling organisms (e.g., Smith and Hasiotis, 2008). The Permian traces described here are only found in continental intervals, and are often associated with rhizoliths, providing strong evidence that they were formed contemporaneously with paleosols. In the final part of this study, experiments were conducted with modern soil-dwelling organisms in order to provide a possible modern analog for trace fossils, and to understand better the burrowing mechanism by which they were created. Experiments were created to study the trace morphology and burrowing behavior of all life cycle stages of the masked chafer beetle, with the goal of comparing these modern traces to the fossil record. These traces provide convincing analogs to ancient traces seen throughout the US midcontinent, including those described here.

REFERENCES

MILLER, K.B., WEST, R.R., and RANKEY, E.C., 1999, Relations between relative changes in sea level and climate shifts: Pennsylvanian-Permian mixed carbonate-siliciclastic strata, western United States: Discussion and reply, Geological Society of America Bulletin, v. 111, p. 467-472.

OLSZEWSKI, T. D. and M. E. PATZKOWSKY, 2003, From Cyclothems to sequences: the record of eustacy and climate on an icehouse epeiric platform (Pennsylvanian-Permian, North American Midcontinent): Journal of Sedimentary Research, vol. 73, no. 1, p.15-30.

RANKEY, E. C., 1997, Relations between relative changes in sea level and climate shifts; Pennsylvanian-Permian mixed carbonate-siliciclastic strata, Western United States. GSA Bulletin 109:9, p. 1089-1100.

SMITH, J.J., and HASIOTIS, S.T., 2008, Traces and burrowing behaviors of the cicada nymph *Cicadetta calliope*: Neoichnology and paleoecological significance of extant soil-dwelling insects: PALAIOS, v. 23, p. 503–513.

SOREGHAN, G.S., 1994, The impact of glacioclimatic change on Pennsylvanian cyclostratigraphy, *in* Embry, A.E., Beauchamp, B., and Glass, D.J., eds., Pangea: Global Environments and Resources: Canadian Society of Petroleum Geologists Memoir 17, p.523–543.

WANLESS, H.R., and SHEPARD, F.P., 1936, Sea level and climatic changes related to late Paleozoic cycles, Geological Society of America Bulletin, v. 47, p. 1177-1206.

CHAPTER TWO. DISTRIBUTION, PALEOENVIRONMENTAL IMPLICATIONS, AND SEQUENCE STRATIGRAPHIC SIGNIFICANCE OF TRACE FOSSILS AND PALEOSOLS IN LOWER PERMIAN CONTINENTAL DEPOSITS OF WESTERN KANSAS

ABSTRACT

Cumulative paleosols in core from the Lower Permian (Asselian-Sakmarian) Council Grove Group of western Kansas contain a diverse suite of pedogenic features, including carbonate nodules, gleying, trace fossils, rhizoliths, rhizohalos, peds, and cutans. Climatic variability during the interval of soil formation resulted in overprinting and close stratigraphic juxtaposition of both humid and arid climate indicators. Variability is likely the result of exposure to multiple 5th-order eustatic and climatic cycles during the lowstands of 4th-order cycles. The distribution of pedogenic features across formations also indicates a shift toward more humid conditions during a larger 3rd-order regression. Paleosol character was strongly influenced by regional topography and paleogeographic position, as well as the climate changes accompanying these hierarchical glacioeustatic cycles. Abundant trace fossils (Naktodemasis isp.) were likely produced during soil formation by root-feeding insect larvae. Biologic activity assisted in consolidation and stabilization of eolian and alluvially deposited sediments, creating updip topography that reduced accommodation for subsequent deposition. Lack of accommodation prevented the deposition of small-scale, 5th-order cycles that are expressed as lithologic changes in stratigraphically equivalent outcrops across the state. These outcrops reveal a series of stacked paleosols with discrete exposure surfaces that are separated by thin limestones, rather than the thin, cumulic paleosols seen in core. The lack of biostabilization and topography, and the generally lower relief outside of the Anadarko Basin made these areas more susceptible to small-scale variations in sea-level and climate.

This study emphasizes that detailed, quantitative study of pedogenic features can reveal important paleoclimatic and paleoenvironmental information in otherwise lithologically homogeneous paleosols. Paleoenvironmental reconstructions based on these features should take into account the full suite of pedogenic characteristics, as opposed any one specific feature (e.g., soil carbonate nodules as indicators of aridity). This study also adds additional evidence to the hypothesis of a link between sea-level change and climate change in the Early Permian. The midcontinent, however, may not have been as arid as previously thought—abundant gleying, burrowing by organisms with a high soil moisture requirement, and extensive plant growth are evidence of increased soil moisture during this time.

Introduction

The purpose of this paper is to document the characteristics and distribution of trace fossils and other pedogenic features within Lower Permian (Asselian-Sakmarian) cyclothemic strata in western Kansas, USA, and to interpret their paleoenvironmental and sequence stratigraphic implications. This study examines three formation-level lithostratigraphic units from the upper portion of the Council Grove Group that were deposited in a continental setting. The Speiser, Blue Rapids, and Easly Creek shales are units consisting primarily of fine sand- to silt-sized sediments characterized by varying degrees of pedogenic modification, including prominent zones of gleying, rooting, and bioturbation composed of *Naktodemasis* isp. These features are a valuable source of paleoenvironmental information that can be used to reconstruct hydrologic and climatic conditions in continental settings during periods of soil formation (Kraus, 1999; Retallack, 2001; Hasiotis, 2002, Hasiotis and Platt, 2012).

Pennsylvanian and Permian strata in Kansas have long been recognized as cyclical in nature (Moore, 1931, 1936), and have often been interpreted as the product of eustatic change driven by orbital forcing (Heckel, 1977, 1986). Hierarchical, cyclic sedimentation patterns allow for identification of multiple scales of sequences within Paleozoic strata of the midcontinent, which can be linked to both eustatic and climatic change (Miller and West, 1993; Soreghan, 1994; Miller et al., 1996; Soreghan, 1997; Boardman and Nestell, 2000). Outcrops showing smaller scale lithofacies changes and repeated soil profiles within composite paleosols have been interpreted as 5th or 6th order stratigraphic cycles—the meter scale cycles of Miller et al. (1996) and punctuated aggradational cycles of Goodwin and Anderson (1985), and may represent time periods of 10–100 ka (Miller and West 1993, 1998; Boardman and Nestell 2000). These repeated 5th- or 6th-order sequences comprise longer-term 4th-order sequences (0.1–1 ma) that are expressed as regional, formation-level lithologic units that are correlatable across Kansas and beyond. The change in distribution, thickness, and character of lithofacies within 4th-order cycles can, in turn, be linked to much longer 3rd-order (1–10 ma) changes in global sea level (Busch and West, 1987; Youle et al., 1994; Puckette et al., 1995).

The distribution and stratigraphic succession of ichnocoenoses (trace fossil assemblages) and pedogenic features record environmental, hydrologic, and climatic changes that have the potential to preserve smaller scale eustatic cycles within relatively homogeneous formations when major lithologic changes are not present. These features may also be the only indicators of environmental change within more recognizable larger order cycles. Although both outcrop and core of Lower Permian rocks in Kansas have been described (e.g., Miller and West, 1993; Miller et al., 1996; Dubois et al., 2012), paleosol variability between outcrop and core has not yet been described in detail. Previous studies have not quantified the distribution of trace fossils and other pedogenic features with respect to changes in climate and sea level.

Geologic Setting

The Lower Permian Council Grove Group is ~75 m thick, and consists of alternating marine and continental deposits divided into 14 formations and representing less than 10 million years of deposition (Baars 1990) (Fig. 1). The Council Grove Group is the principle source of petroleum from the highly productive Hugoton-Panoma gas field. Numerous studies of the stratigraphy, depositional environments, and paleoecology of formations within the Council Grove Group have been conducted (e.g., Mudge and Yochelson 1962; Lane 1964; Abdullah 1985; Schultze 1985; Miller and West, 1993; Miller et al., 1996; Rankey, 1997; Miller and West, 1998; Boardman and Nestell, 2000; Olszewski and Patzowsky, 2003), but were mainly limited to outcrops in the eastern portion of the state.

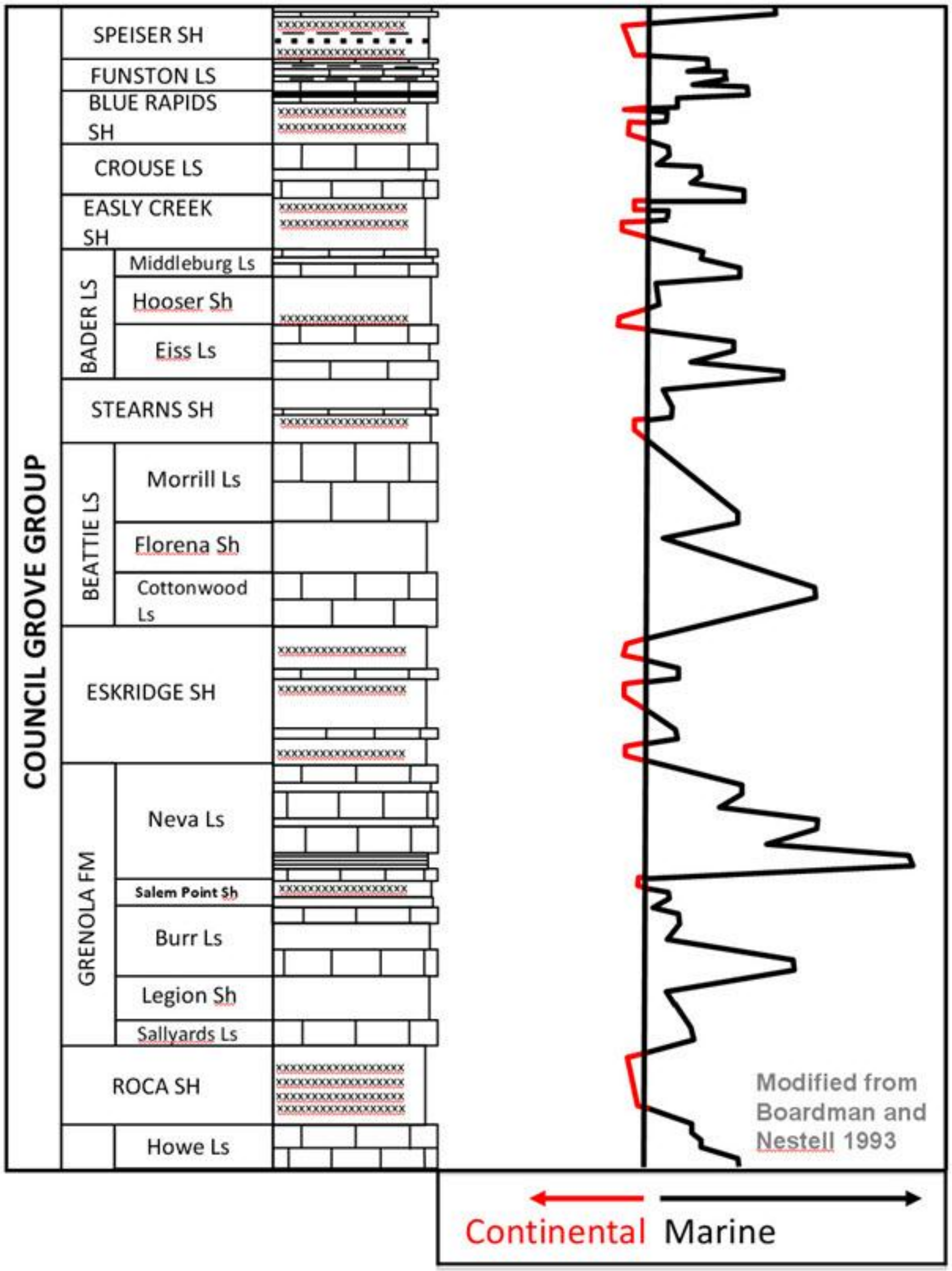

Figure 1: Stratigraphic column showing studied interval within Council Grove Group and generalized sea level. Modified from Boardman and Nestell (2000).

Deposits of the Council Grove Group in Kansas are relatively flat lying, dipping shallowly to the west at roughly ~ 4 m per 1.6 km (13 feet per mile; 0.15 to 0.25 degrees), and outcropping in a north–south trending belt near the city of Manhattan (Fig. 2). Current dip direction and magnitude are likely not reflective of original slope steepness during deposition, which was probably < 1 m per km and oriented to the south (Rascoe and Adler 1983, Olszewski and Patzkowsky 2003). In the study area, Permian deposits dip to the southeast as a result of subsidence associated with the Hugoton extension of the Anadarko basin, an asymmetric foreland–intracratonic basin that began activity in the late Cambrian, continued subsiding until the Pennsylvanian, and was mostly filled in by the Middle Permian (Garner and Turcotte, 1984; Sorenson, 2005).

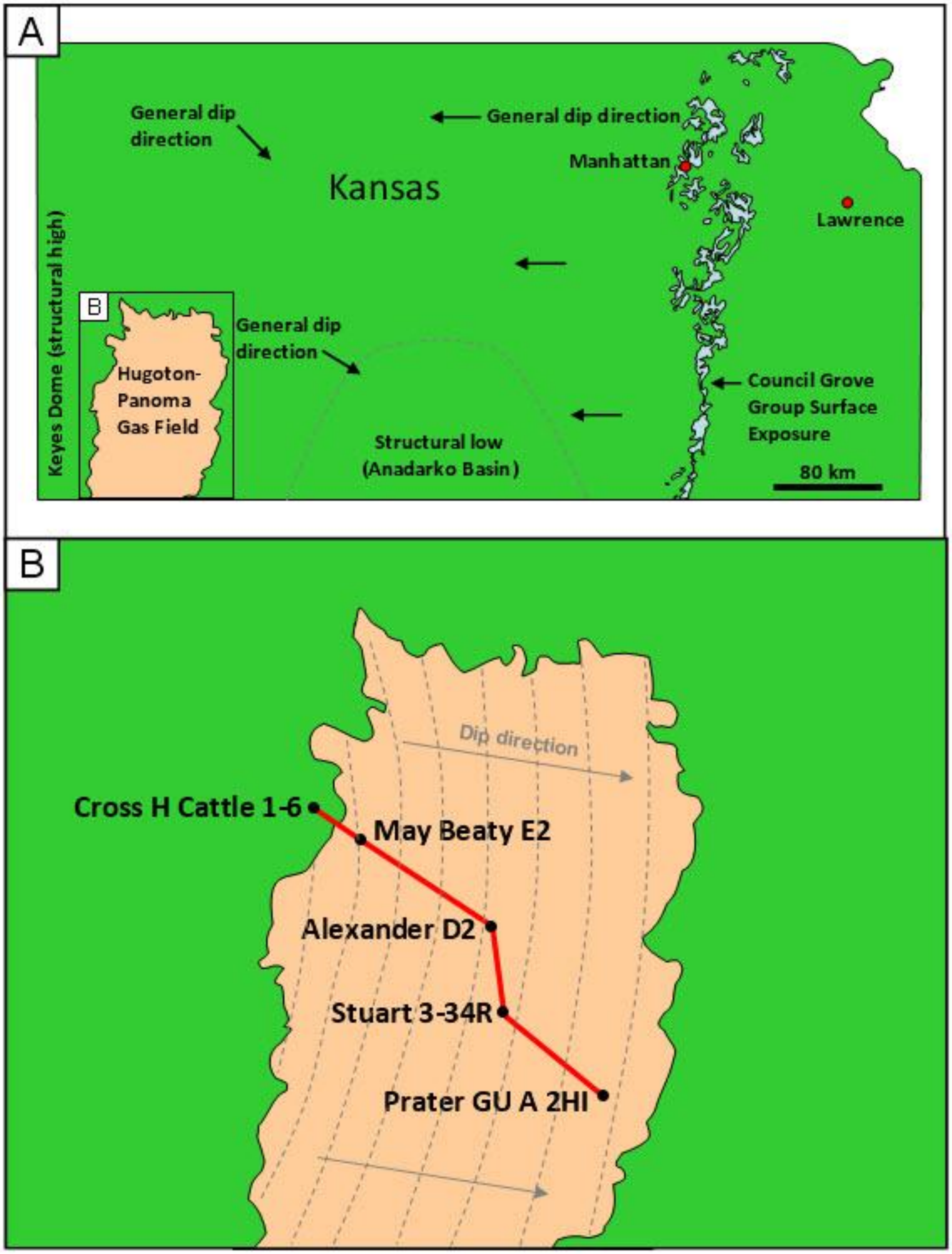

Figure 2: Map showing current geographic location of upper Council Grove group outcrops in Kansas, Hugoton-Panoma gas field, and location of core transect.

Kansas in the Late Pennsylvanian and Early Permian was roughly centered in the Pangean supercontinent, and located slightly north of the equator (Scotese, 2002; Blakey, 2011) (Fig. 3). Overall high sea levels led to repeated flooding and exposure of the continental interior. Pennsylvanian and Permian depositional environments in Kansas were especially sensitive to climatic and eustatic variations due to their setting on a broad, shallow, gently dipping carbonate ramp, which resulted in regionally extensive cyclothem deposition (Heckel, 1977; Puckette et al., 1995; Mazzullo, 1998; Olszewski and Patzkowsky, 2003; Feldman et al., 2005). The Hugoton area was adjacent to the eroding Ancestral Rocky Mountains to the northwest (Rascoe and Adler, 1983; Johnson, 1989; Boardman and Nestell, 2000), which likely provided a source for much of the clastic sedimentation in the region (Soreghan et al., 2002). In the Hugoton basin, an inverse relationship exists between the thicknesses of limestone and continental units, where limestones thicken basinward and continental deposits thicken towards the hinterland, with a concomitant thinning in marine limestones. This pattern can be seen in the selected core transect (Fig. 4).

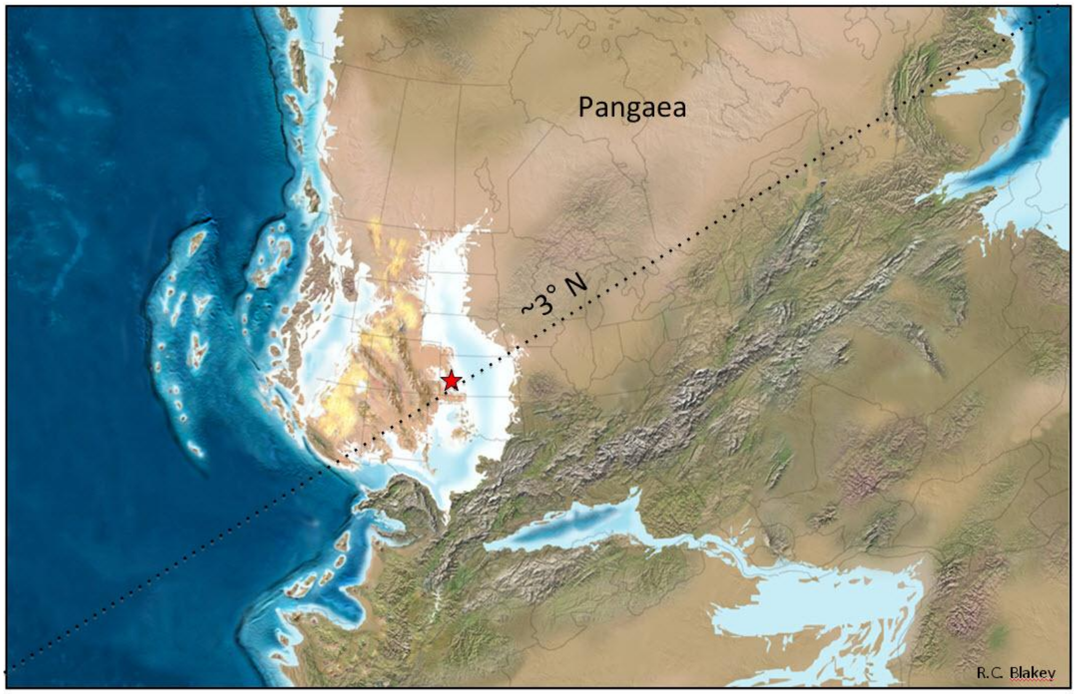

Figure 3: Paleogeographic map showing position of focus area within North America at the approximate time of deposition of upper Council Grove Group sediments. Modified from Blakey (2012).

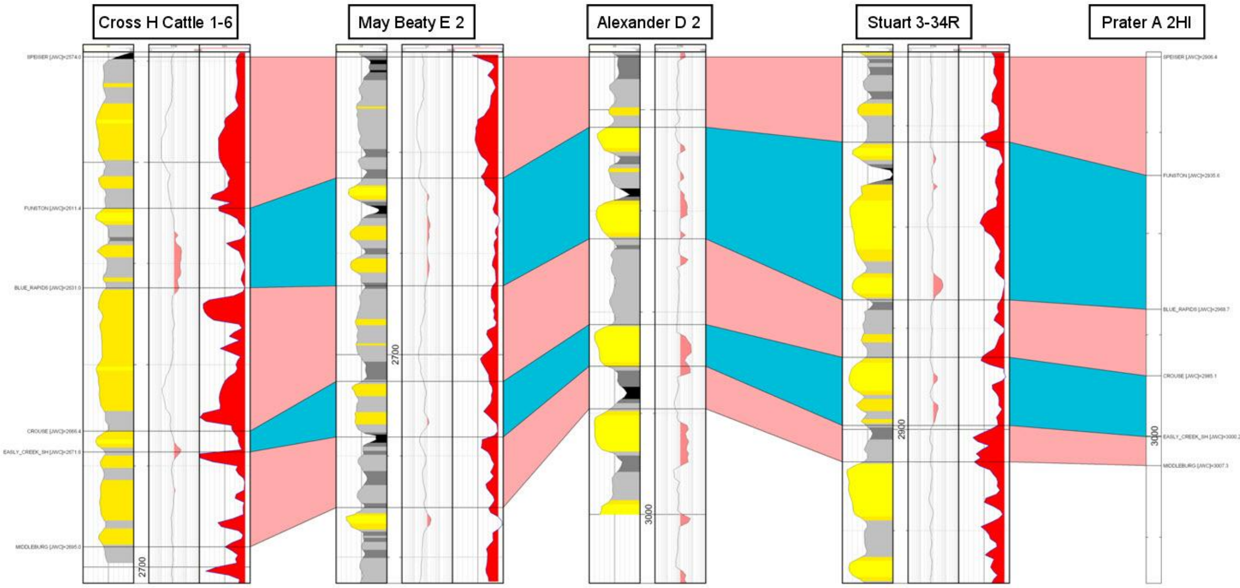

Figure 4: Cross section of core transect used in this study, showing formation tops and Gamma Ray, Induction, and Density Porosity electric logs.

Background

Stratigraphic Cycles in Kansas Paleozoic Strata

The late Paleozoic strata of the midcontinent have played an important role in the evolution of the cyclothem concept. Cyclothems were initially proposed by Moore (1931), and the term was coined by Wanless and Weller (1932), who defined it as “a series of beds deposited during a single sedimentary cycle” in reference to Pennsylvanian rocks of Illinois. The definition was later modified to define a specific succession of rocks bound by unconformities, which is the generally accepted definition today (Weibel, 2004). Moore (1936) was the first to apply the term to the midcontinent area, and Heckel (1977) defined the classic Kansas type cyclothem based on the Pennsylvanian and Permian outcrops in the eastern part of the state.

Wanless and Shepard (1936) initially postulated glacioeustatic change as the mechanism responsible for cyclic sedimentation. Elias (1937) proposed an alternate explanation wherein cycles were the product of local epiorogenic effects rather than global sea-level change. Diastrophism or periodic tectonism remained the favored mechanism behind cyclic sedimentation for many years. Correlation of hypothetical sea level curves in other midcontinent basins in the 1950s and 1960s, especially Schenk’s (1967) recognition of black shales as continuous across large areas, led to a resurrection of the eustasy model. Currently, the most widely accepted mechanism for cyclothem deposition is a combination of eustatic and climatic change driven by orbital forcing.

The Kansas-type cyclothem consists of four repeating lithologic units (Heckel, 1977) (Fig. 5). The lowermost unit in the cycle, the “middle” or transgressive limestone, is a carbonate mudstone containing a diverse suite of open marine fauna deposited during a period of deepening sea level. Above the middle limestone is the core shale, a laminated, black phosphatic shale deposited when sea level was at its highest. The sequence-defining offshore core shales are noticeably absent from Council Grove Group cyclothems in outcrop, thus, marking a distinct difference from the Pennsylvanian strata that form the basis of the Heckel (1977) model (Boardman, 1999). Above the black core shale, the upper, or regressive, limestone is a thick marine carbonate produced in shallow, high-energy waters during early regression. Later stages of regression and maximum lowstand led to deposition of the outside shale or nearshore shale, a red to grey sandy shale that records either subaerial exposure or nearshore deposition. The presence of marine fossils in the outside shale indicates that these units were deposited subaqueously and subsequently pedogenically modified.

Although this model forms the basis for much of the subsequent discussion of Paleozoic cyclothems, many individual cycles differ from this idealized model. Heckel (1984) modified this original model to account for lithologic differences in Upper Pennsylvanian and Lower Permian strata. Asselian–Sakmarian cycles of the Council Grove Group, in particular, are lacking certain important members in the series, and also contain other lithologic units not incorporated into the original model. These later cycles generally record shallower depositional environments and more rapid sea-level fluctuations than those seen in the underlying Missourian and Desmoinesian rocks and contain more prominent paleosols (Miller and West 1993, Olszewski and Patzkowsky 2003). Miller and West (1993) interpret the Upper Council Grove formations studied here to be parts of three distinct cyclothems—Middleburg-Easly Creek, Crouse-Blue Rapids, and Funston-Speiser.

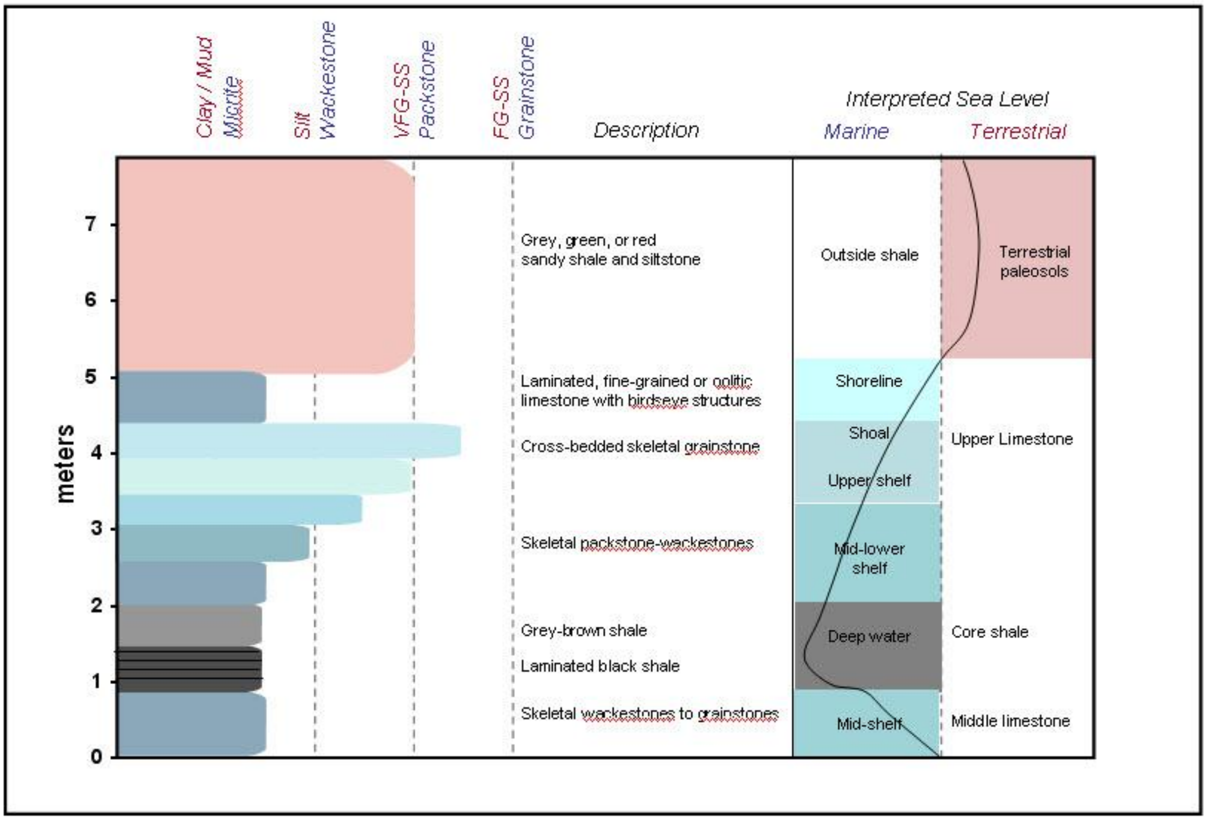

Figure 5: Primary lithostratigraphic components of the Kansas-type cyclothem model, as originally described by Heckel (1977). In the upper Council Grove cyclothems described in this study, the core shale is absent, leaving only the outside shale consisting of the paleosols described here, and the merged middle/upper limestones.

Cyclothems are still considered a useful concept, but the advent of sequence stratigraphy has made the term somewhat obsolete. Modern research has focused on both the lithologic sequence and the nature of the bounding surfaces, referencing cyclothems in a historic sense and applying sequence stratigraphic principles to cyclic strata (e.g., Miller and West 1993,1998; Mazzullo et al. 1995; Puckette et al., 1995; Mazzullo, 1998; Boardman and Nestell 2000; Olszewski and Patzkowsky, 2003; Feldman et al. 2005; West et al. 2010).

Puckette et al. (1995) examined upper Council Grove core in the Oklahoma panhandle and interpreted the depositional setting and sequence stratigraphic context of each formation-level unit. They interpreted the lower sections of upper Council Grove limestones as small-scale transgressive systems tracts in 4th-order sequences, upper limestones as highstand or forced regression systems tracts, and paleosols (redbeds) as lowstand systems tracts. The uppermost formations in the Council Grove were interpreted as being part of a larger, 3rd-order regressive-sequence set. Lithologies seen in Oklahoma Council Grove core were similar to those seen in the Hugoton area.

Olszewski and Patzkowsky (2003) also attempted to put the stratigraphic architecture of cyclothems into a sequence stratigraphic framework. In their model, the smallest-scale depositional sequence consists of very thin units composed of alternating carbonate and clastic couplets, which are interpreted to be very thin fifth-order sequences. The transgressive systems tract is generally composed of carbonate, followed by marine clastics of the highstand systems tract. Highstand clastics are pedogenically modified during lowstand, forming paleosols and the sequence boundary. Lowstand systems tracts are present as incised valley fills, which are only present in Pennsylvanian strata. Fourth-order sequences can be inferred from the stacking patterns and changing lithologies of 5th-order cycles, and are bounded by unconformities. These 4th-order composite sequences are generally equivalent to Heckel's Kansas-type cyclothem.

Cyclicity and Climate Change

Perlmutter (2007) emphasized the link between orbital cycles, climate change, and paleolatitude. Most paleoclimatic and paleogeographic reconstructions agree that Upper Pennsylvanian and Lower Permian strata in the midcontinent were deposited near the paleoequator, under variable climatic conditions with seasonal variations in rainfall (e.g., Miller et al., 1996; Rankey, 1997; Kessler et al. 2001). Other authors, however, differ in their interpretations of how specifically climate change relates to eustasy. The Council Grove Group, in particular, has been the focus of numerous hypotheses regarding the relationship between sea level and climate in the Permian.

Miller and West (1993) recognized that the carbonate to clastic alternations within 5th-order sequences cannot be explained by eustatic change alone. They propose a model wherein eustasy was accompanied by a concomitant change in regional paleoclimate. Eustatic lowstands (glacial maximums) corresponded to periods of weakened monsoonal intensity that allowed warm, moist subtropical airmasses to carry moisture further into the continental interior, thus, increasing weathering and erosion that favored deposition of clastics and the formation of paleosols. Eustatic highstand deposits (glacial minimums) corresponded to stronger monsoon intensity, diverting moisture to subtropical latitudes and causing increased aridity near the equator, which led to deposition of thin carbonates. The cycles delineated by these surfaces can be considered parasequences rather than sequences.

Olszewski and Patzkowsky (2003) also examined climate changes associated with midcontinent cyclothems. They also favor an interpretation where transgressive carbonates were deposited during the most arid conditions. Marine siliciclastics, deposited during highstand, represent the most humid climates. Paleosols formed during lowstand and subaerial exposure, and represent a transition from wetter to drier conditions. They cite the transition from vertic to calcic paleosols in the Speiser Shale as evidence for increasing aridity as conditions begin to move toward those that favor limestone deposition.

Dubois et al. (2012) are one of few studies to examine core from the Hugoton basin, including several of the same cores that are described in this study. In their model, continental units are the product of concurrent loess deposition and pedogenic modification during sea-level lowstands. Windblown silt and fine-grained sand sourced from the Ancestral Rocky Mountains are stabilized by soil development—including bioturbation and rooting—resulting in siliciclastic aggradation that reduced available space for carbonate deposition landward during sea-level rise. Their interpretations support a climate pattern that is opposite to that of Miller et al. (1996), favoring an interpretation where most arid climates occurred during falling sea level and eolian deposition, with maximum lowstand and aridity occurring in roughly the center of continental intervals. Limestones and the upper portions of continental units are interpreted as having been deposited during the wettest time periods during sea level rise. No lithologic changes that could be interpreted as representing smaller-scale cycles (i.e., a series of discrete exposure surfaces or thin limestones) are seen in the Hugoton cores.

5th-Order Cycles in Council Grove Group Outcrops

Miller and West (1993) and Miller et al. (1996) provided detailed stratigraphic sections of measured Council Grove Group outcrops in Riley County, Kansas, ~480 km (300 miles) northeast of the Hugoton Basin (Fig. 6). Although individual formations are correlative across the state, the character of paleosol-bearing units in outcrop sections is noticeably different than that seen in core. Most notably, the Speiser, Blue Rapids, and Easly Creek shales contain thin limestones that separate each formation into a series of paleosol profiles. Miller and West (1993) noted the spatial extent of intraformational lithologic changes within Upper Council Grove Group outcrops, and were the first to recognize them as small, 5th-order cycles that had previously been noted in Pennsylvanian rocks (e.g., West and Busch, 1985) By focusing on discontinuity surfaces rather than lithofacies, they recognized multiple discrete cycles within both marine and continental intervals.

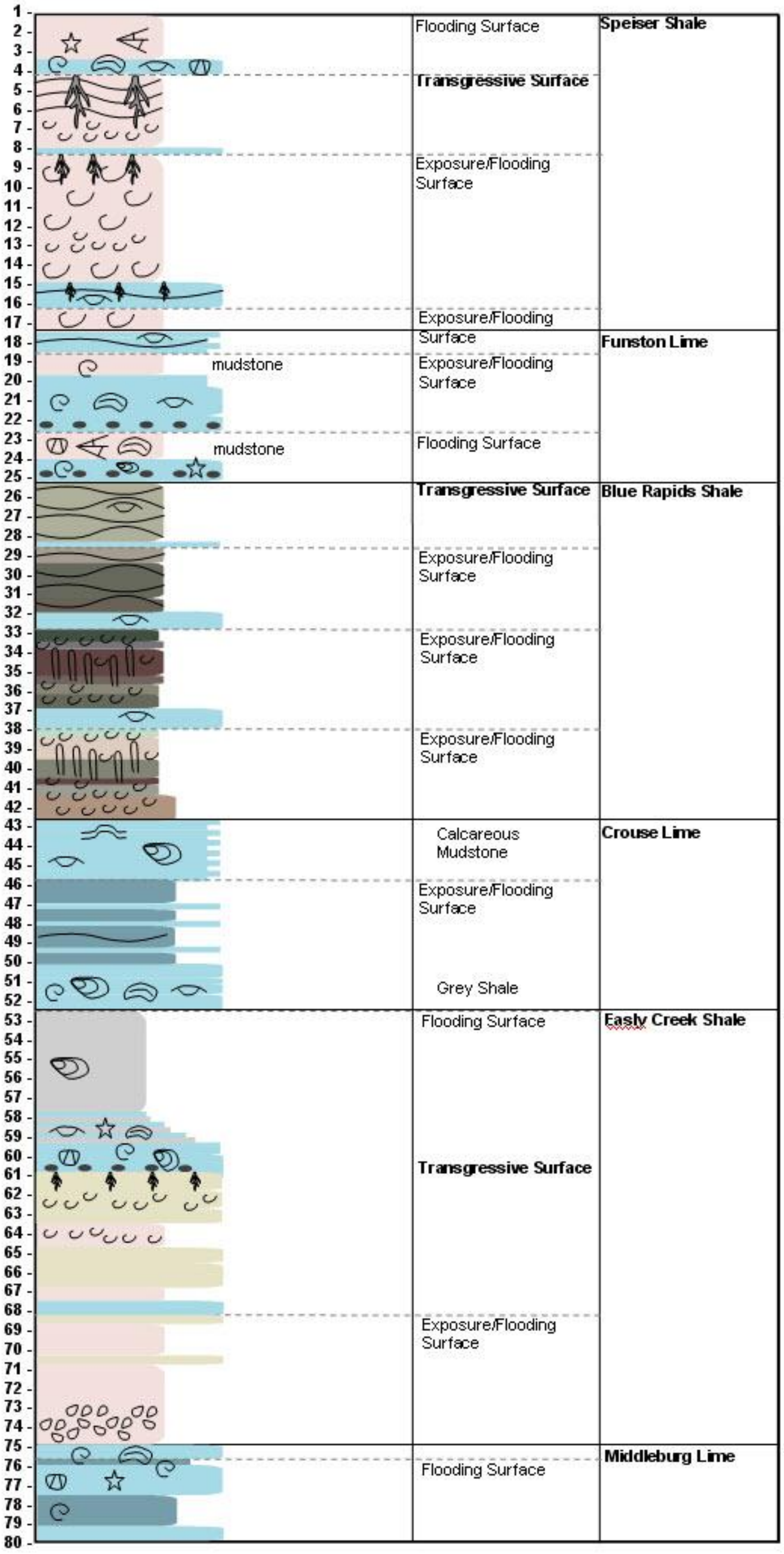
1 2 3 4 5 6 7 8 9 10 11 12 13 14 15 16 17 18 19 20 21 22 23 24 25 26 27 28 29 30 31 32 33 34 35 36 37 38 39 40 41 42 43 44 45 46 47 48 49 50 51 52 53 54 55 56 57 58 59 60 61 62 63 64 65 66 67 68 69 70 71 72 73 74 75 76 77 78 79 80
Flooding Surface
Speiser Shale
Transgressive Surface
Exposure/Flooding Surface
Exposure/Flooding Surface
Funston Lime
mudstone
Exposure/Flooding Surface
Flooding Surface
mudstone
Transgressive Surface
Blue Rapids Shale
Exposure/Flooding Surface
Exposure/Flooding Surface
Exposure/Flooding Surface
Calcareous Mudstone
Crouse Lime
Exposure/Flooding Surface
Grey Shale
Flooding Surface
Easly Creek Shale
Transgressive Surface
Exposure/Flooding Surface
Flooding Surface
Middleburg Lime

Figure 6: Composite upper Council Grove outcrop section as described by Miller and West (1993). Vertical scale same as described core in figs. 9-13.

The Easly Creek Shale in outcrop is lithologically heterogeneous, containing limestone, mudstone, and siltstone. The lower section lies above the gastropod packstone and wackestone of the Middleburg Limestone, and contains pedogenically modified mudstone clasts and gypsum crystals that likely represent a solution-collapse breccia. The overlying interval is characterized by grey to brown mudstone containing thin, sandier intervals with evidence of soft-sediment deformation. A unit of thin limestone containing rhizoliths and plant debris overlies this sequence. Above these, thin carbonates are decimeter-scale, grayish yellow siltstone beds containing blocky and columnar ped structures, capped by a distinct exposure surface. Another series of intraclastic limestone and grey mudstone form the uppermost sequence in the Easly Creek Shale.

The Blue Rapids Shale is separated into four smaller units, each containing a variegated mudstone showing evidence of pedogenic modification with a marine carbonate at the base. The lowest sequence overlies the Crouse Limestone, and contains numerous pedogenic features including peds, rhizoliths, and color horizonation. This sequence is interpreted to represent a complete individual soil profile. The next overlying sequence is similar and lies above a thin carbonate containing ostracodes and fish bones. Both of these paleosols record a transition from blocky peds at the base to columnar ped structures near the top of each mudstone unit. Above these are two additional limestone to mudstone sequences, the lower of which contains a grayish green mudstone with prominent pseudoanticlines—a pedogenic feature formed by repeated subaerial shrinking and swelling of clay-rich sediments. Thin, wavy carbonate beds within a yellowish mudstone dominate the uppermost sequence in the Blue Rapids Shale. The thicker carbonate at the base of both of these upper sequences contains marine fossils.

In the Speiser Shale, four distinct sequences can be recognized, at least three of which can be correlated in outcrop across multiple counties (e.g., Cunningham, 1989). The lowermost sequence sits atop the Funston Limestone and is composed of red- and green-banded clastics with abundant ped structures and rhizoliths. The next sequence begins with a sharp-based, carbonate mudstone with rhizoliths overlain by more than 2 m of greenish grey mudstone with small blocky peds. This unit, in turn, is overlain by another mudstone with peds, pseudoanticlines, and compacted rhizoliths. The uppermost sequence in the Speiser Shale is composed of a limestone with a diverse marine fauna at the base, followed by a grey mudstone with occasional tepee structures at the top. Other authors report additional continental features of the Speiser Shale, including ephemeral ponds (Hembree et al., 2004) and the presence of lungfish (*Gnathoriza*) aestivation burrows (Schultze, 1985; Hasiotis et al., 2004; Hembree et al., 2005).

Pedogenic Features and their Implications

Gleying is the product of bacterially mediated iron reduction in soil minerals from Fe^{3+} to Fe^{2+}, a process that can only occur in anaerobic conditions (Retallack, 1990). Gleyed zones in both modern and ancient soils are usually colored green or grey and are often caused by complete water saturation or high concentrations of organic matter (Vespraskas, 2004). Gleying in waterlogged soils can happen relatively quickly, with color change occurring in as little as five years (Vespraskas et al., 1999). Extensive gleying in continental sediments is, thus, an indicator of precipitation in areas with poor drainage, high subterranean water tables, or subaqueous anoxic environments, including lakes, marshes, or ponds (Sheldon and Tabor, 2009). Localized gleying can also form in close proximity to decaying organic matter, such as plant roots (Retallack, 2001). Mottled red-green color patterns result from partial gleying or gleyed sediments that are also been exposed to air, often through fluctuation of subterranean water tables (Crown and Hoffman, 1970; Ponnamperuma, 1972). Soils dominated by gleying or gleysols are distributed worldwide in a wide range of different climates, but are dominant in tropical regions near the equator (0° latitude) and in subpolar and temperate regions in Eurasia and North America (~60° latitude) (Driessen et al., 2001). Although the relationship between gleysol formation and mean annual precipitation has not been quantified, gleying is notably less common in arid regions like the Middle East, North Africa, and Australia (Micheli, 2006).

Carbonate nodules in paleosols are the product of subaerial carbonate precipitation. Calcium carbonate typically enters soils as windblown particulate matter or dissolved calcium in rainwater (Royer, 1999). Soil carbonate forms as carbonate minerals are leached from overlying A-horizons and percolate downward during rainfall, and are then reprecipitated in B-horizons (Reeves, 1976). The presence of carbonate nodules is, thus, an indicator of at least some degree of soil maturity, although individual nodules and aggradations of nodules require less time to form than massive or bedded carbonate. The formation of nodular carbonate is estimated to take 1,000 to 10,000 yrs (Retallack, 2001), depending on local conditions. Pedogenic carbonate is also thought to be an indicator of dry or seasonal climates since it requires both rainfall and periodic evaporation in order to form (Retallack, 1994). Calcic soils, or Calcisols, however, can form in a wide range of climatic conditions. They are distributed worldwide, but are most common in subtropical latitudes at approximately 30° N and S. Arid, semiarid, and Mediterranean climates, such as the Middle East, north Africa, Australia, and the southwestern

USA contain the highest abundance of calcisols (Driessen et al., 2001). In the Midcontinent of the US, modern soils only contain carbonate in areas where annual precipitation falls below 500-600 mm (Retallack 2001), although they may be found less commonly in environments with > 1000 mm (Royer, 1999). Marion (1989), however, estimated that $CaCO_3$ precipitation would cease at a mean annual precipitation < 37 mm in the American southwest. The depth from the soil surface to the calcium-rich horizon can be used to approximate mean annual rainfall, with deeper calcic deposits forming in areas of higher precipitation (Retallack, 1994; Royer, 1999 and subsequent discussion and reply). This relationship, however, likely does not apply to cumulic soils that are constantly aggrading.

Root traces, or rhizoliths, reflect colonization of exposed sediments by land plants, and can be used to infer a variety of environmental and climatic parameters. Plant colonization can happen relatively quickly after subaerial exposure, and occurs in a wide range of environments and climates, but requires at least some amount of moisture within the soil. The mineralogy and mode of rhizolith preservation can be used to determine drainage conditions within paleosols—well-drained paleosols are characterized by carbonate rhizocretions, and iron-depleted haloes (Kraus and Hasiotis, 2006). Paleosols with poor drainage are typified by carbonaceous debris within the rhizoliths and Mn-enriched haloes. Abundant rhizoliths can also be an indicator of increased plant growth in an area. The amount of vegetation cover in modern environments is directly affected by the amount of effective precipitation, which is a relationship between the amount of true precipitation and the degree of evaporation (Barry and Chorley, 2009). Arid biomes, such as deserts and tundra, support less vegetation overall than those receiving higher amounts of rainfall (Park, 1997). In order for plant growth to occur, soil moisture must be continually above the permanent wilting point—the point at which plants can no longer recover from desiccation. This varies for both plant type and soil composition (Tolk, 2003), but even at wilting point, soil moisture is > 0% due to both hygroscopic water on particle surfaces and a small amount of capillary water held in micropores that is unavailable to plants. In modern desert environments, growth of grasses begins in climates with a mean annual precipitation of ~20 mm, and trees at ~100 mm (Ward, 2009). Although plant communities have changed in structure through geologic time, similar moisture tolerances to modern communities are reasonable to assume. Abundant rhizoliths in paleosols, therefore, indicate sustained levels of mobile water in the soil that support plant communities over long time spans. This can be an indicator of semiarid to temperate climates, as sparse vegetative cover is typical of xeric or arid climates (e.g., Ward, 2009).

Blocky peds and their associated cutans are present in both outcrop and core. Outcrop exposures also occasionally contain columnar peds and gilgai structures, forming vertisols that are not seen in core. Vertisols are found today only in temperate to tropical latitudes, typically in hot climates, and form only in soils with high clay content and shrink/swell potential (Driessen et al., 2001; Retallack 2001). Blocky peds also reflect shrinking and swelling clays, but to a lesser degree than columnar ped structures. Both ped structures are representative of climates with fluctuating seasonal moisture conditions.

Meniscate backfilled trace fossils in paleosols are likely formed by the burrowing action of fossorial insects or insect larvae (Smith and Hasiotis, 2008; Counts and Hasiotis, 2009). Insects and their larvae are found in a wide range of climates worldwide, from arctic to arid regions. Insects can colonize a newly exposed soil relatively quickly, and may feed on the roots of plants or on detrital organic material within the soil. Experiments with extant subterranean insects show that these organisms have a very low tolerance for soil moisture outside of a relatively narrow range. Chafer beetle larvae, juvenile and adult dung beetles (order Coleoptera), cicada nymphs and soil bugs (order Hemiptera) have all been shown to be extremely susceptible to desiccation. Although individual species have different tolerances in different soil compositions and field capacities, most of these insects show increased survival, preference, or reproduction at a moisture range of approximately 18-40 % (Willis and Roth, 1962; Potter, 1983; Potter and Gordon, 1984; Villani and Wright 1990; Vessby, 2001; Riis et al., 2005). Many modern fossorial insects have a multiyear life cycle, most of which is spent underground. Extensive assemblages of backfilled trace fossils in cumulic paleosols, therefore, indicate that environmental conditions remained favorable with enough adequate moisture to support multiple generations of insect populations.

Methods and Materials

Five core were used for this study from Grant, Kearny, and Hamilton counties in Kansas—Cross H Cattle 1-6 (API 15-075-20543), May Beaty E2 (API 15-093-20134), Stuart 3-34R (API 15-067-21415), Alexander D2 (API 15-067-20338) and Prater Gas Unit A 2HI (API 15-175-20250). Core were selected to form a roughly northwest to southeast transect trending down dip into the Hugoton extension of the Anadarko basin across approximately 80 km (50 miles), with varying distances between individual core (Fig. 2).

The three uppermost continental units in all wells—the Speiser, Blue Rapids, and Easly Creek shales—were selected for study. Here, we focus on certain quantifiable characteristics of paleosols that may provide additional insight into paleoenvironment and paleoclimate of the Hugoton area in the Early Permian (Figs. 7-8). We discussed trace fossil morphology, ichnotaxonomy, and modern analogs in earlier papers (Counts and Hasiotis, 2009, in review), and Dubois et al. (2012) qualitatively cataloged pedogenic features.

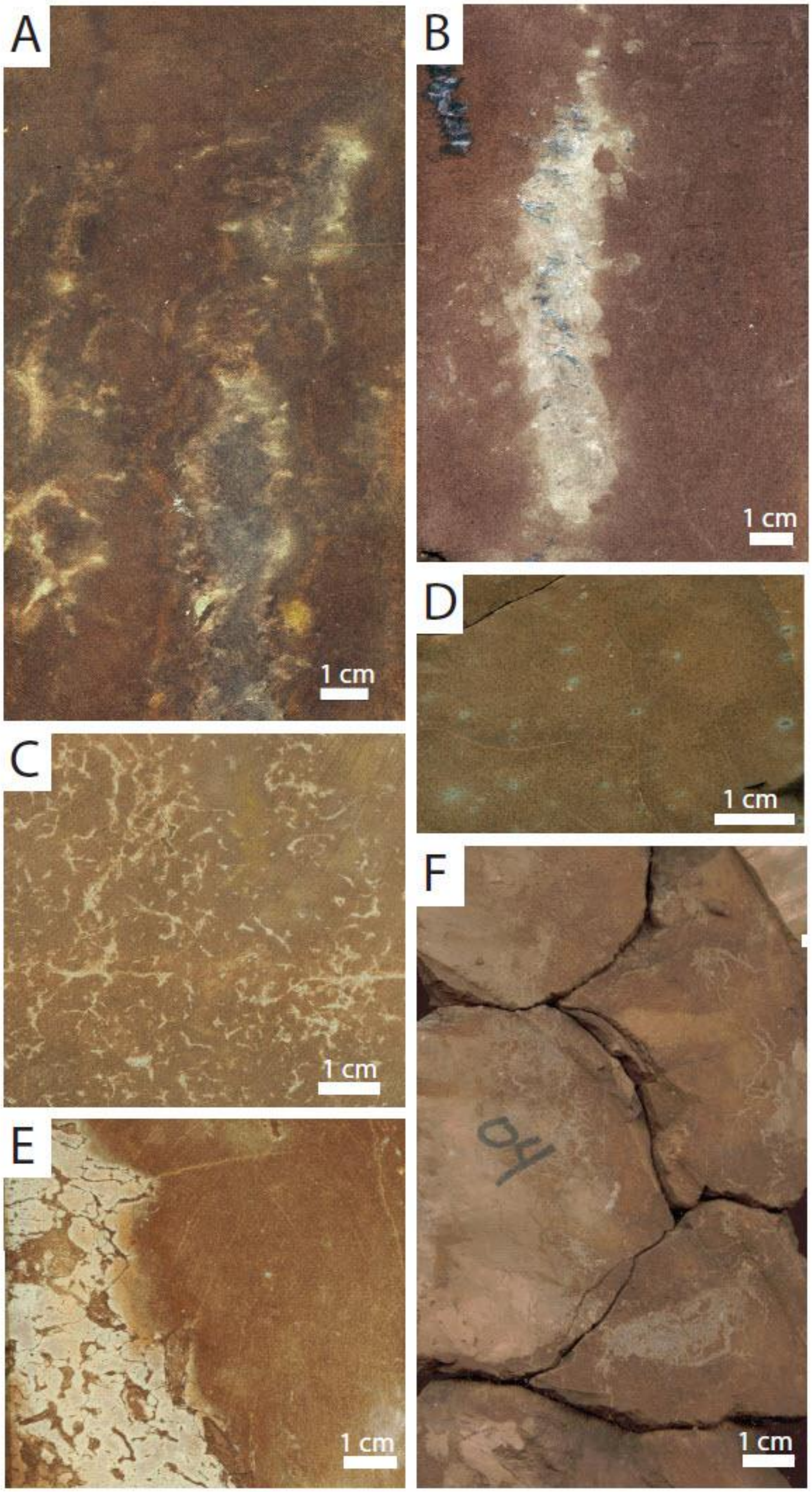
A
B
1 cm
1 cm
D
1 cm
C
1 cm
E
F
1 cm
1 cm

Figure 7: Soil features in upper Council Grove Group paleosols, showing a variety of rhizolith morphologies and ped structures; A) large vertical rhizolith with multiple redoximorphic halos; Cross H Cattle 787 m (2582’); B) vertical, anhydrite-filled rhizolith surrounded by faint *Naktodemasis* burrows within the rhizohalos; Cross H Cattle Cross H Cattle core, 791 m (2596’); C) fine network of small rhizoliths; May Beaty E 2, 829 m (2723’); D) small, isolated rhizoliths with carbonaceous interiors and grey reduced halos; . D Alexander, 905 m (2970’); E) subvertical network of small, branching rhizoliths; Stuart 3-34R, 897 m (2942’); F) ped structures in core--breaks in core face follow clay-rich cutans along ped surfaces; Prater, 946 m (3104’).

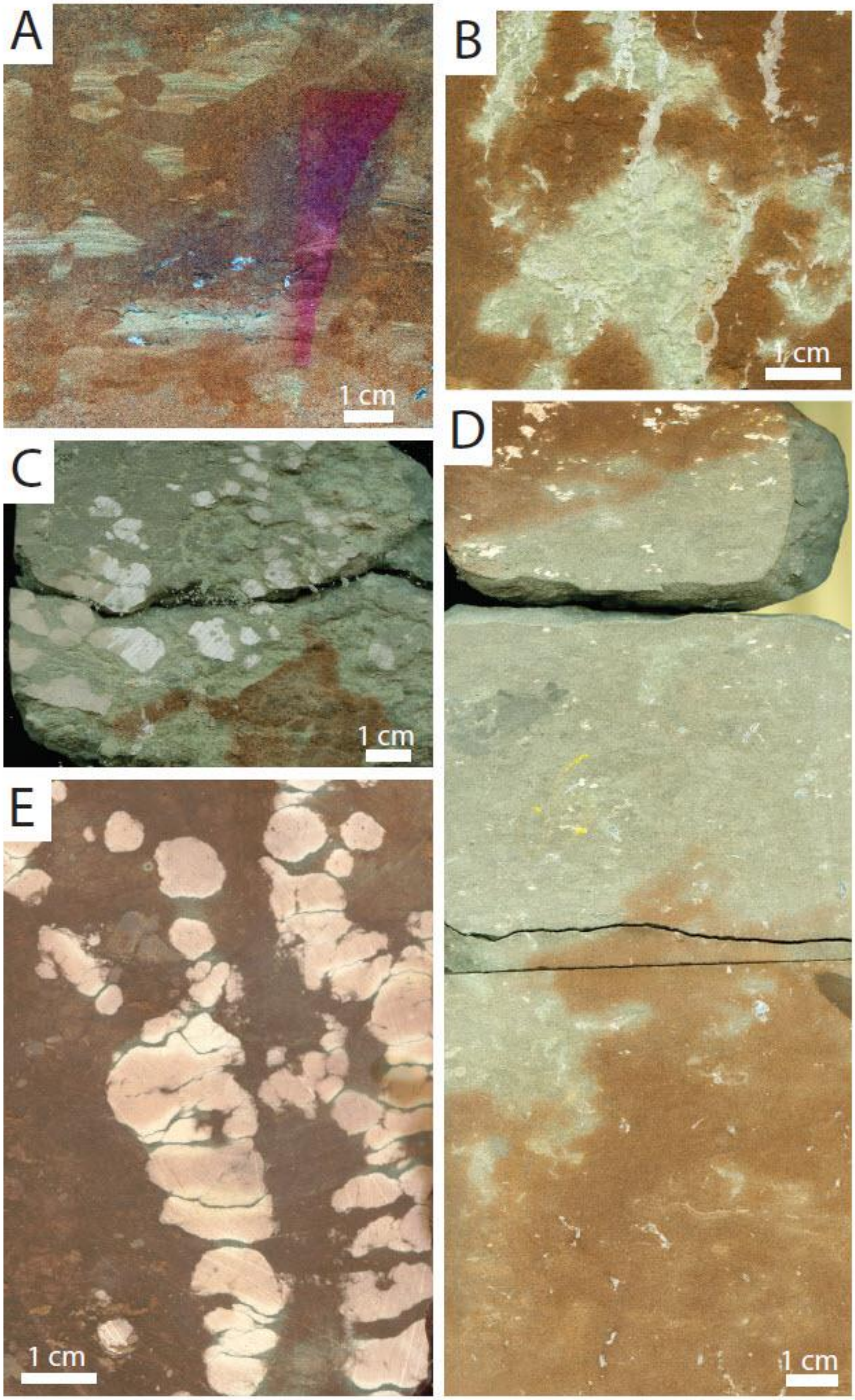
A
1 cm
B
1 cm
C
1 cm
D
1 cm
E
1 cm

Figure 8: Additional soil features in upper Council Grove Group paleosols, showing primary sedimentary structures, soil carbonate, and gleying. A) remnant horizontal laminae interrupted by later bioturbation; Stuart 3-34R, 859 m (2820’); B) patchy, mottled intervals of gleyed silt, unassociated with other soil features; Stuart 3-34R, 886 m (2906’); C) carbonate nodules in gleyed interval, indicating variable soil moisture; D Alexander 907 m (2977’); D) larger, discrete area of gleyed sediment reflecting greater extent of iron reduction; Cross H Cattle 824 m (2704’); E) vertical strings of round soil carbonate nodules associated with minor gleying Stuart 3-34R, 909 m (2982’).

In each core, continental units were analyzed with regard to pedogenic features, including trace fossils (Table 1). Pedogenic features were quantitatively indexed using a modified version of Folks’ (1951) visual estimation chart. Indices were created by measuring the percentage of each feature covering the slabbed core face for every 15 cm (6 in) interval of core. Each of the primary indicators of pedogenesis—bioturbation, rooting, soil carbonate, and gleying, as well as an index for displacive diagenetic anhydrite—were indexed. This resulted in over 2,500 individual measurements in 77 m (total 254 ft) of core (Appendix 1). Pedogenic characteristics were then plotted by depth for each core (Figs. 9–13), and were also averaged and crossplotted by formation and grain size so that larger scale trends could be seen (Figs. 14-15). Indices, qualitative descriptions, and interpretations were used to correlate individual features across core and generate hypothetical sea-level curves. Within each formation, some general patterns of pedogenic feature distribution are consistent throughout the basin. Other pedogenic features were qualitatively noted (Figs. 7–8, Table 1). Discrete trace fossils were also measured where possible. For each visible trace fossil, the diameter and length were measured, and orientation was noted. All data were then plotted, correlated across core, and statistically analyzed when appropriate.

In addition to core, several outcrops of the same stratigraphic interval were reconnoitered in order to examine the section for discrete pedogenic features, and specifically for trace fossils. Those outcrops, however, have been thoroughly described in detail by numerous authors (e.g., Miller and West, 1993; Miller, 1994; Miller et al., 1996; Mazzullo, 1998; Boardman and Nestell, 2000; West et al., 2010; and many others), so measuring numerous sections was unnecessary.

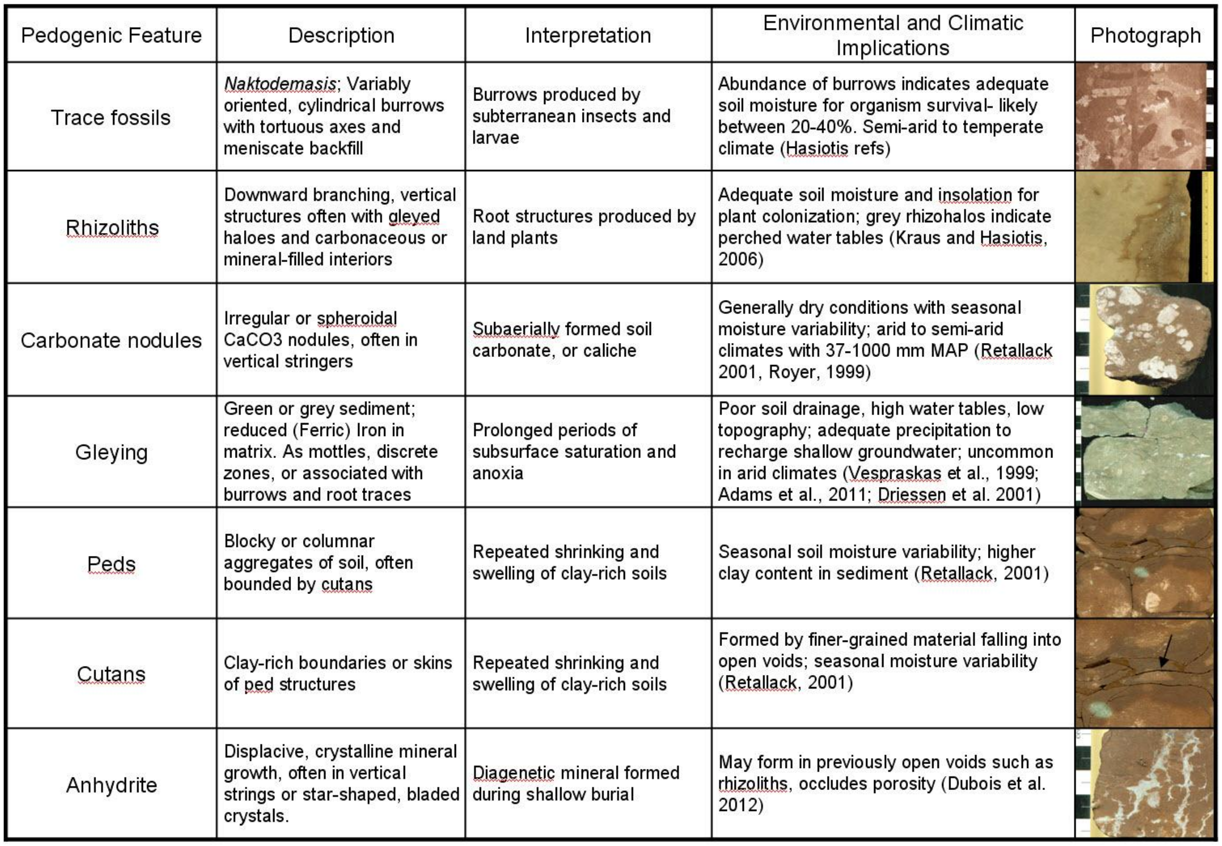

Pedogenic Feature	Description	Interpretation	Environmental and Climatic Implications	Photograph
Trace fossils	*Naktodemasis*; Variably oriented, cylindrical burrows with tortuous axes and meniscate backfill	Burrows produced by subterranean insects and larvae	Abundance of burrows indicates adequate soil moisture for organism survival- likely between 20-40%. Semi-arid to temperate climate (Hasiotis refs)	
Rhizoliths	Downward branching, vertical structures often with gleyed haloes and carbonaceous or mineral-filled interiors	Root structures produced by land plants	Adequate soil moisture and insolation for plant colonization; grey rhizohalos indicate perched water tables (Kraus and Hasiotis, 2006)	
Carbonate nodules	Irregular or spheroidal CaCO3 nodules, often in vertical stringers	Subaerially formed soil carbonate, or caliche	Generally dry conditions with seasonal moisture variability; arid to semi-arid climates with 37-1000 mm MAP (Retallack 2001, Royer, 1999)	
Gleying	Green or grey sediment; reduced (Ferric) Iron in matrix. As mottles, discrete zones, or associated with burrows and root traces	Prolonged periods of subsurface saturation and anoxia	Poor soil drainage, high water tables, low topography; adequate precipitation to recharge shallow groundwater; uncommon in arid climates (Vespraskas et al., 1999; Adams et al., 2011; Driessen et al. 2001)	
Peds	Blocky or columnar aggregates of soil, often bounded by cutans	Repeated shrinking and swelling of clay-rich soils	Seasonal soil moisture variability; higher clay content in sediment (Retallack, 2001)	
Cutans	Clay-rich boundaries or skins of ped structures	Repeated shrinking and swelling of clay-rich soils	Formed by finer-grained material falling into open voids; seasonal moisture variability (Retallack, 2001)	
Anhydrite	Displacive, crystalline mineral growth, often in vertical strings or star-shaped, bladed crystals.	Diagenetic mineral formed during shallow burial	May form in previously open voids such as rhizoliths, occludes porosity (Dubois et al. 2012)	

Table 1. Pedogenic features indexed for this study and their significance

Following pages:

Figure 9: Stratigraphic column, detailed descriptions, representative photographs, interpreted sea level curve, and depositional environments for the Amoco Cross H Cattle core, API 15-075-20543.

Figure 10: Stratigraphic column, detailed descriptions, representative photographs, interpreted sea level curve, and depositional environments for the Amoco May Beaty E 2 core, API 15-093-20134.

Figure 11: Stratigraphic column, detailed descriptions, representative photographs, interpreted sea level curve, and depositional environments for the Cities Service Alexander D 2 core, API 15-067-20338.

Figure 12: Stratigraphic column, detailed descriptions, representative photographs, interpreted sea level curve, and depositional environments for the Pioneer Stuart 3-34R core, API 15-067-21415.

Figure 13: Stratigraphic column, detailed descriptions, representative photographs, interpreted sea level curve, and depositional environments for the Amoco Prater Gas Unit A 2HI core, API 15-175-20250.

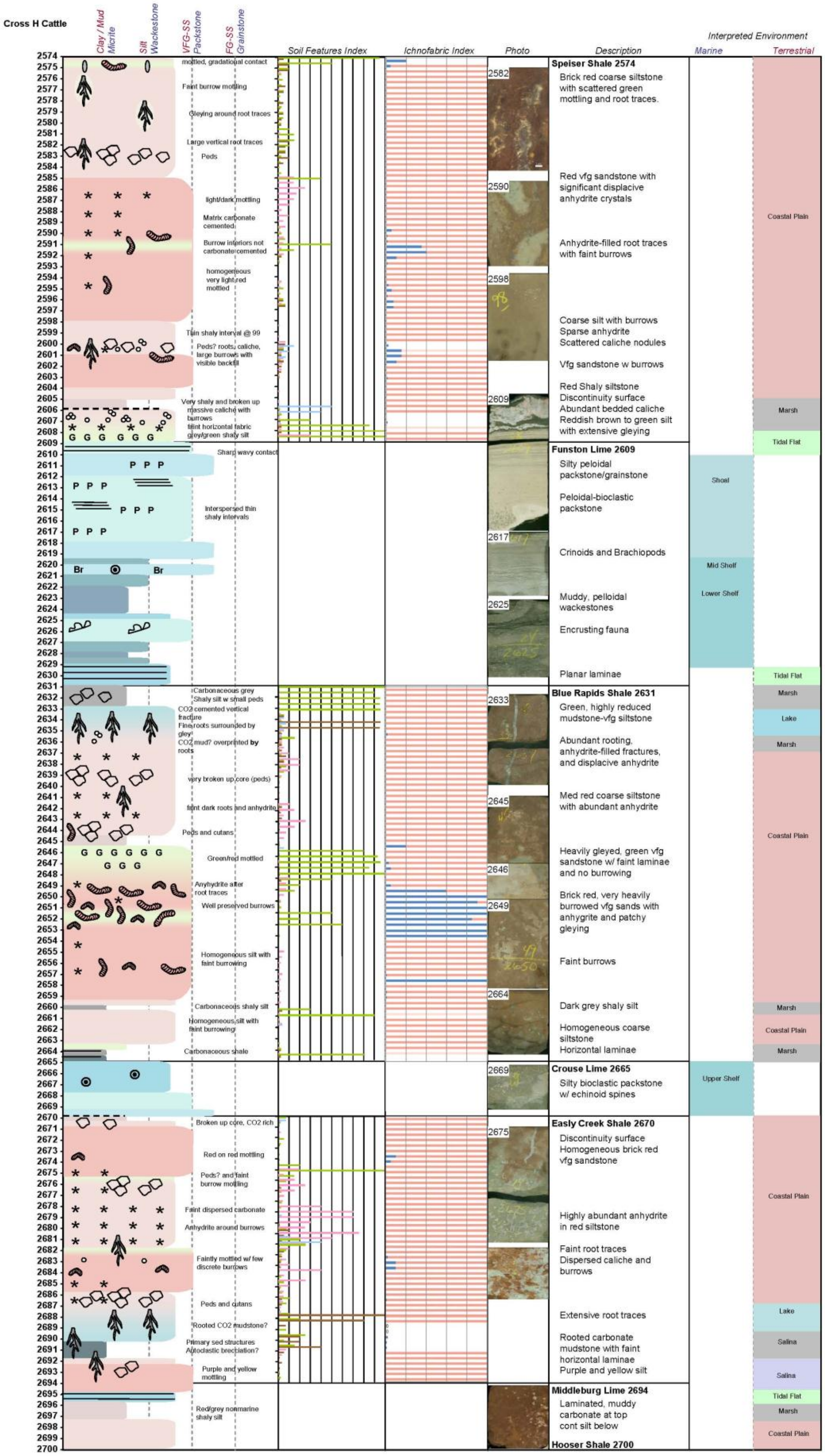
Cross H Cattle
Clay / Mud
Micrite
Silt
Wackestone
VFG-SS
Packstone
FG-SS
Grainstone
Soil Features Index
Ichnofabric Index
Photo
Description
Interpreted Environment
Marine
Terrestrial
2574
2575
2576
2577
2578
2579
2580
2581
2582
2583
2584
2585
2586
2587
2588
2589
2590
2591
2592
2593
2594
2595
2596
2597
2598
2599
2600
2601
2602
2603
2604
2605
2606
2607
2608
2609
2610
2611
2612
2613
2614
2615
2616
2617
2618
2619
2620
2621
2622
2623
2624
2625
2626
2627
2628
2629
2630
2631
2632
2633
2634
2635
2636
2637
2638
2639
2640
2641
2642
2643
2644
2645
2646
2647
2648
2649
2650
2651
2652
2653
2654
2655
2656
2657
2658
2659
2660
2661
2662
2663
2664
2665
2666
2667
2668
2669
2670
2671
2672
2673
2674
2675
2676
2677
2678
2679
2680
2681
2682
2683
2684
2685
2686
2687
2688
2689
2690
2691
2692
2693
2694
2695
2696
2697
2698
2699
2700
mottled, gradational contact
Faint burrow mottling
Gleying around root traces
Large vertical root traces
Peds
light/dark mottling
Matrix carbonate cemented
Burrow interiors not carbonate cemented
homogeneous very light red mottled
Thin shaly interval @ 99
Peds? roots, caliche, large burrows with visible backfill
Very shaly and broken up massive caliche with burrows faint horizontal fabric grey/green shaly silt
G G G G G G
Sharp wavy contact
P P P
Interspersed thin shaly intervals
Br
Br
Carbonaceous grey Shaly silt w small peds
CO2 cemented vertical fracture
Fine roots surrounded by gley
CO2 mud? overprinted by roots
very broken up core (peds)
faint dark roots and anhydrite
Peds and cutans
Green/red mottled
Anyhydrite after root traces
Well preserved burrows
Homogeneous silt with faint burrowing
Carbonaceous shaly silt
Homogeneous silt with faint burrowing
Carbonaceous shale
Broken up core, CO2 rich
Red on red mottling
Peds? and faint burrow mottling
Faint dispersed carbonate
Anhydrite around burrows
Faintly mottled w/ few discrete burrows
Peds and cutans
Rooted CO2 mudstone?
Primary sed structures
Autoclastic brecciation?
Purple and yellow mottling
Red/grey nonmarine shaly silt
2582
2590
2598
2609
2617
2625
2633
2645
2646
2649
2664
2669
2675
Speiser Shale 2574
Brick red coarse siltstone with scattered green mottling and root traces.
Red vfg sandstone with significant displacive anhydrite crystals
Anhydrite-filled root traces with faint burrows
Coarse silt with burrows
Sparse anhydrite
Scattered caliche nodules
Vfg sandstone w burrows
Red Shaly siltstone
Discontinuity surface
Abundant bedded caliche
Reddish brown to green silt with extensive gleying
Funston Lime 2609
Silty peloidal packstone/grainstone
Peloidal-bioclastic packstone
Crinoids and Brachiopods
Muddy, pelloidal wackestones
Encrusting fauna
Planar laminae
Blue Rapids Shale 2631
Green, highly reduced mudstone-vfg siltstone
Abundant rooting, anhydrite-filled fractures, and displacive anhydrite
Med red coarse siltstone with abundant anhydrite
Heavily gleyed, green vfg sandstone w/ faint laminae and no burrowing
Brick red, very heavily burrowed vfg sands with anhygrite and patchy gleying
Faint burrows
Dark grey shaly silt
Homogeneous coarse siltstone
Horizontal laminae
Crouse Lime 2665
Silty bioclastic packstone w/ echinoid spines
Easly Creek Shale 2670
Discontinuity surface
Homogeneous brick red vfg sandstone
Highly abundant anhydrite in red siltstone
Faint root traces
Dispersed caliche and burrows
Extensive root traces
Rooted carbonate mudstone with faint horizontal laminae
Purple and yellow silt
Middleburg Lime 2694
Laminated, muddy carbonate at top
cont silt below
Hooser Shale 2700
Coastal Plain
Marsh
Tidal Flat
Shoal
Mid Shelf
Lower Shelf
Tidal Flat
Marsh
Lake
Marsh
Coastal Plain
Marsh
Coastal Plain
Marsh
Upper Shelf
Coastal Plain
Lake
Salina
Salina
Tidal Flat
Marsh
Coastal Plain

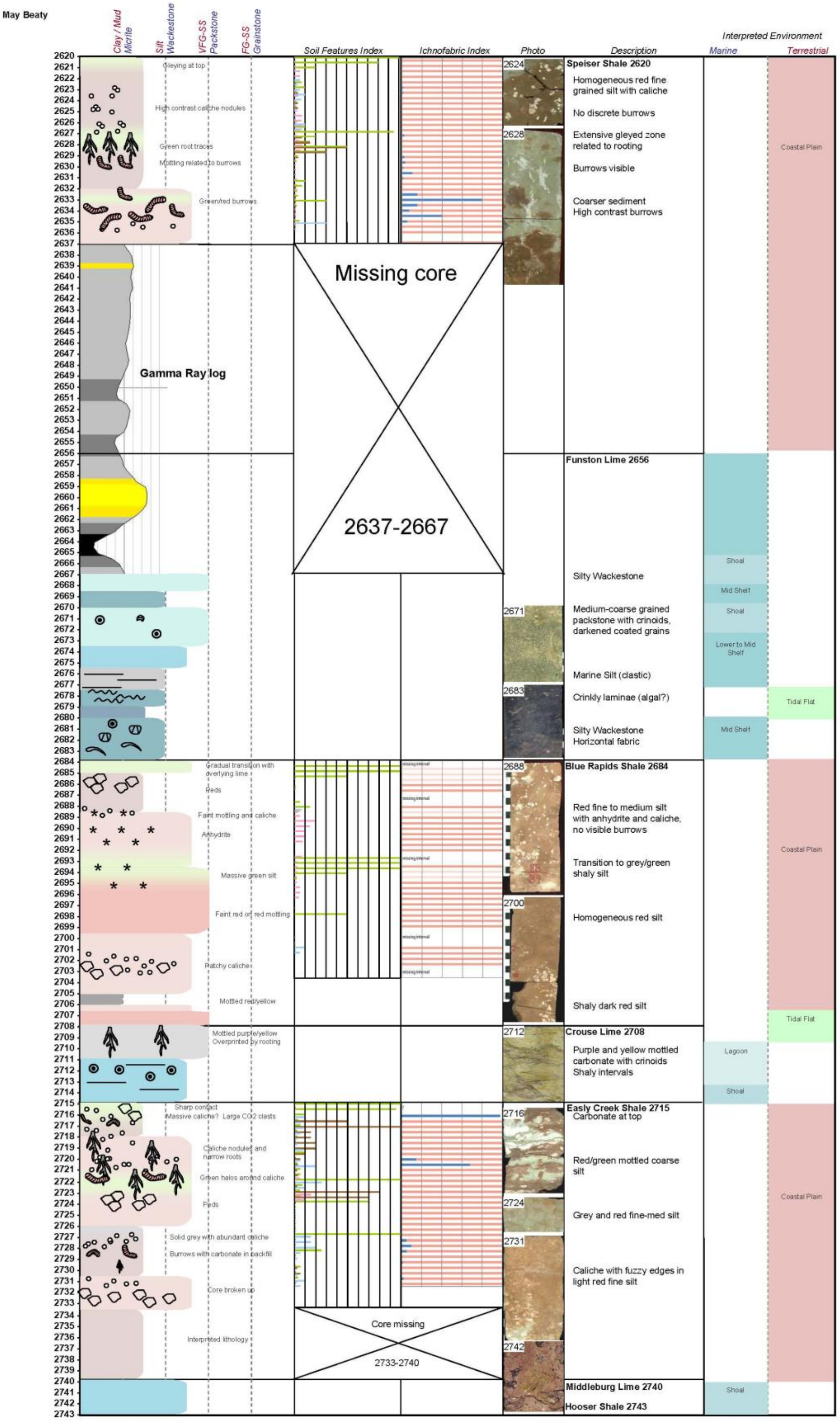
May Beaty
Clay / Mud
Micrite
Silt
Wackestone
VFG-SS
Packstone
FG-SS
Grainstone
Soil Features Index
Ichnofabric Index
Photo
Description
Interpreted Environment
Marine
Terrestrial
Gleying at top
High contrast caliche nodules
Green root traces
Mottling related to burrows
Green/red burrows
Speiser Shale 2620
Homogeneous red fine grained silt with caliche
No discrete burrows
Extensive gleyed zone related to rooting
Burrows visible
Coarser sediment
High contrast burrows
2624
2628
Coastal Plain
Missing core
2637-2667
Gamma Ray log
Funston Lime 2656
Silty Wackestone
Medium-coarse grained packstone with crinoids, darkened coated grains
Marine Silt (clastic)
Crinkly laminae (algal?)
Silty Wackestone
Horizontal fabric
2671
2683
Shoal
Mid Shelf
Shoal
Lower to Mid Shelf
Tidal Flat
Mid Shelf
Gradual transition with overlying lime
Reds
Faint mottling and caliche
Anhydrite
Massive green silt
Faint red on red mottling
Patchy caliche
Mottled red/yellow
missing interval
Blue Rapids Shale 2684
Red fine to medium silt with anhydrite and caliche, no visible burrows
Transition to grey/green shaly silt
Homogeneous red silt
Shaly dark red silt
2688
2700
Coastal Plain
Tidal Flat
Mottled purple/yellow
Overprinted by rooting
Crouse Lime 2708
Purple and yellow mottled carbonate with crinoids
Shaly intervals
2712
Lagoon
Shoal
Sharp contact
Massive caliche? Large CO2 clasts
Caliche nodules and narrow roots
Green halos around caliche
Peds
Solid grey with abundant caliche
Burrows with carbonate in backfill
Core broken up
Interpreted lithology
Easly Creek Shale 2715
Carbonate at top
Red/green mottled coarse silt
Grey and red fine-med silt
Caliche with fuzzy edges in light red fine silt
2716
2724
2731
2742
Coastal Plain
Core missing
2733-2740
Middleburg Lime 2740
Hooser Shale 2743
Shoal

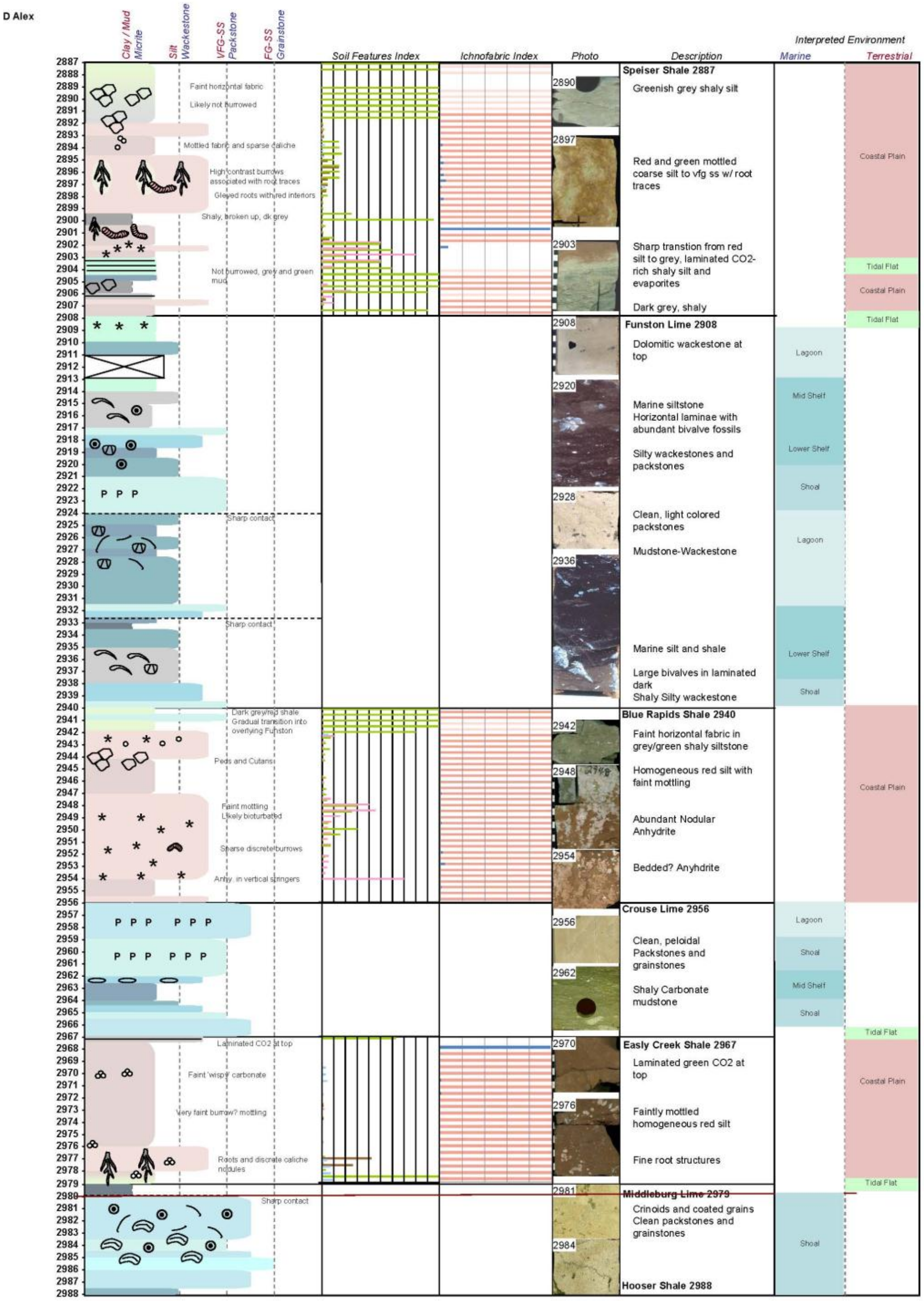
D Alex
Clay / Mud
Micrite
Silt
Wackestone
VFG-SS
Packstone
FG-SS
Grainstone
Soil Features Index
Ichnofabric Index
Photo
Description
Interpreted Environment
Marine
Terrestrial
2887
2888
2889
2890
2891
2892
2893
2894
2895
2896
2897
2898
2899
2900
2901
2902
2903
2904
2905
2906
2907
2908
2909
2910
2911
2912
2913
2914
2915
2916
2917
2918
2919
2920
2921
2922
2923
2924
2925
2926
2927
2928
2929
2930
2931
2932
2933
2934
2935
2936
2937
2938
2939
2940
2941
2942
2943
2944
2945
2946
2947
2948
2949
2950
2951
2952
2953
2954
2955
2956
2957
2958
2959
2960
2961
2962
2963
2964
2965
2966
2967
2968
2969
2970
2971
2972
2973
2974
2975
2976
2977
2978
2979
2980
2981
2982
2983
2984
2985
2986
2987
2988
Faint horizontal fabric
Likely not burrowed
Mottled fabric and sparse caliche
High contrast burrows associated with root traces
Gleyed roots with red interiors
Shaly, broken up, dk grey
Not burrowed, grey and green mud
P P P
Sharp contact
Sharp contact
Dark grey/red shale
Gradual transition into overlying Funston
Peds and Cutans
Faint mottling
Likely bioturbated
Sparse discrete burrows
Anhy. in vertical stringers
P P P P P P
P P P P P P
Laminated CO2 at top
Faint 'wispy' carbonate
Very faint burrow? mottling
Roots and discrete caliche nodules
Sharp contact
2890
2897
2903
2908
2920
2928
2936
2942
2948
2954
2956
2962
2970
2976
2981
2984
Speiser Shale 2887
Greenish grey shaly silt
Red and green mottled coarse silt to vfg ss w/ root traces
Sharp transtion from red silt to grey, laminated CO2-rich shaly silt and evaporites
Dark grey, shaly
Funston Lime 2908
Dolomitic wackestone at top
Marine siltstone
Horizontal laminae with abundant bivalve fossils
Silty wackestones and packstones
Clean, light colored packstones
Mudstone-Wackestone
Marine silt and shale
Large bivalves in laminated dark
Shaly Silty wackestone
Blue Rapids Shale 2940
Faint horizontal fabric in grey/green shaly siltstone
Homogeneous red silt with faint mottling
Abundant Nodular Anhydrite
Bedded? Anyhdrite
Crouse Lime 2956
Clean, peloidal Packstones and grainstones
Shaly Carbonate mudstone
Easly Creek Shale 2967
Laminated green CO2 at top
Faintly mottled homogeneous red silt
Fine root structures
Middleburg Lime 2979
Crinoids and coated grains
Clean packstones and grainstones
Hooser Shale 2988
Coastal Plain
Tidal Flat
Coastal Plain
Tidal Flat
Lagoon
Mid Shelf
Lower Shelf
Shoal
Lagoon
Lower Shelf
Shoal
Coastal Plain
Lagoon
Shoal
Mid Shelf
Shoal
Tidal Flat
Coastal Plain
Tidal Flat
Shoal

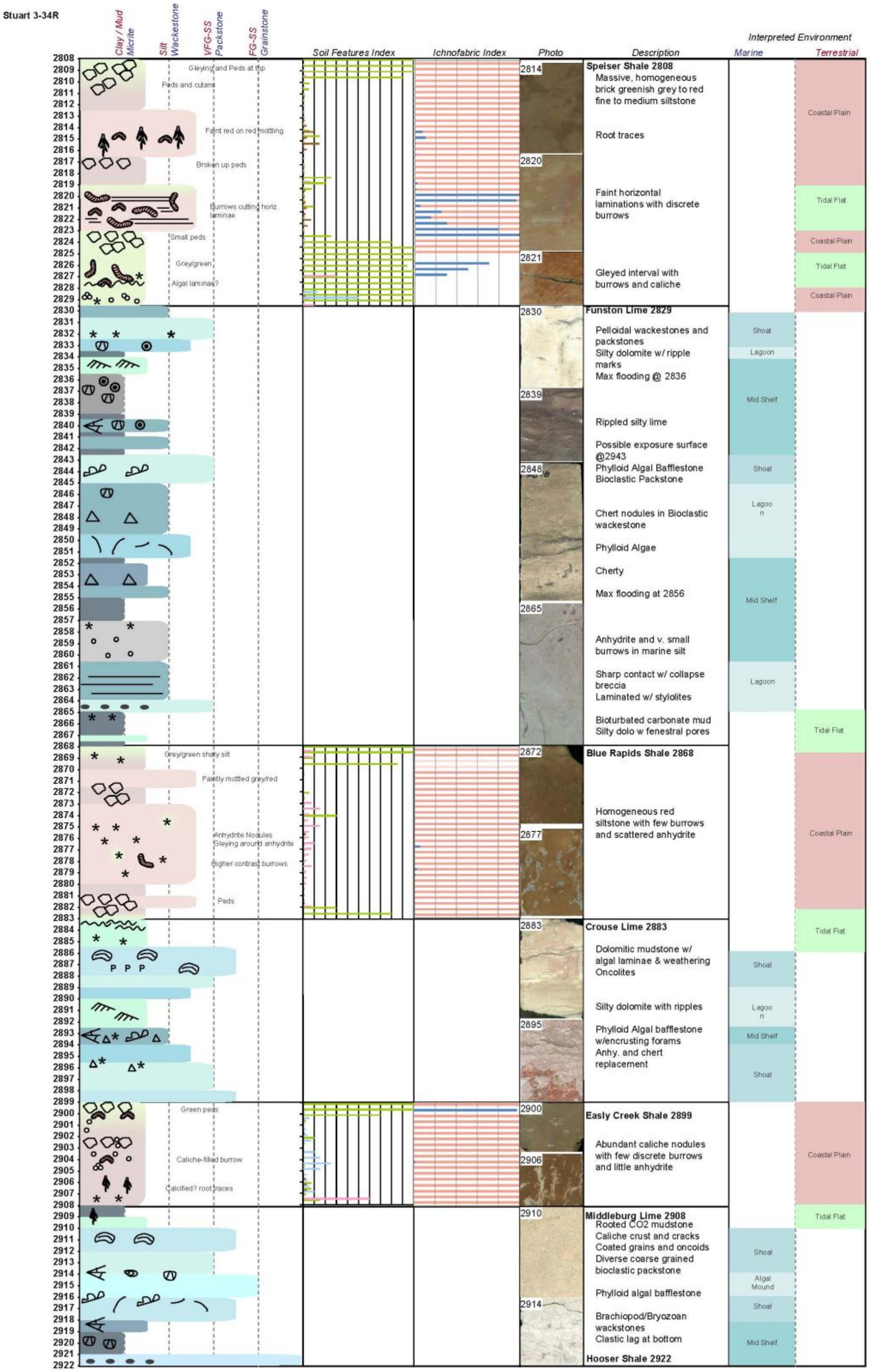
Stuart 3-34R
Clay / Mud
Micrite
Silt
Wackestone
VFG-SS
Packstone
FG-SS
Grainstone
Soil Features Index
Ichnofabric Index
Photo
Description
Interpreted Environment
Marine
Terrestrial
2808
2809
2810
2811
2812
2813
2814
2815
2816
2817
2818
2819
2820
2821
2822
2823
2824
2825
2826
2827
2828
2829
2830
2831
2832
2833
2834
2835
2836
2837
2838
2839
2840
2841
2842
2843
2844
2845
2846
2847
2848
2849
2850
2851
2852
2853
2854
2855
2856
2857
2858
2859
2860
2861
2862
2863
2864
2865
2866
2867
2868
2869
2870
2871
2872
2873
2874
2875
2876
2877
2878
2879
2880
2881
2882
2883
2884
2885
2886
2887
2888
2889
2890
2891
2892
2893
2894
2895
2896
2897
2898
2899
2900
2901
2902
2903
2904
2905
2906
2907
2908
2909
2910
2911
2912
2913
2914
2915
2916
2917
2918
2919
2920
2921
2922
Gleying and Peds at top
Peds and cutans
Faint red on red mottling
Broken up peds
Burrows cutting horiz. laminae
Small peds
Grey/green
Algal laminae?
Grey/green shaly silt
Faintly mottled grey/red
Anhydrite Nodules
Gleying around anhydrite
Higher contrast burrows
Peds
P P P
Green peds
Caliche-filled burrow
Calcified? root traces
2814
2820
2821
2830
2839
2848
2865
2872
2877
2883
2895
2900
2906
2910
2914
Speiser Shale 2808
Massive, homogeneous brick greenish grey to red fine to medium siltstone
Root traces
Faint horizontal laminations with discrete burrows
Gleyed interval with burrows and caliche
Funston Lime 2829
Pelloidal wackestones and packstones
Silty dolomite w/ ripple marks
Max flooding @ 2836
Rippled silty lime
Possible exposure surface @2943
Phylloid Algal Bafflestone
Bioclastic Packstone
Chert nodules in Bioclastic wackestone
Phylloid Algae
Cherty
Max flooding at 2856
Anhydrite and v. small burrows in marine silt
Sharp contact w/ collapse breccia
Laminated w/ stylolites
Bioturbated carbonate mud
Silty dolo w fenestral pores
Blue Rapids Shale 2868
Homogeneous red siltstone with few burrows and scattered anhydrite
Crouse Lime 2883
Dolomitic mudstone w/ algal laminae & weathering
Oncolites
Silty dolomite with ripples
Phylloid Algal bafflestone w/encrusting forams
Anhy. and chert replacement
Easly Creek Shale 2899
Abundant caliche nodules with few discrete burrows and little anhydrite
Middleburg Lime 2908
Rooted CO2 mudstone
Caliche crust and cracks
Coated grains and oncoids
Diverse coarse grained bioclastic packstone
Phylloid algal bafflestone
Brachiopod/Bryozoan wackstones
Clastic lag at bottom
Hooser Shale 2922
Coastal Plain
Tidal Flat
Coastal Plain
Tidal Flat
Coastal Plain
Shoal
Lagoon
Mid Shelf
Shoal
Lagoo n
Mid Shelf
Lagoon
Tidal Flat
Coastal Plain
Tidal Flat
Shoal
Lagoo n
Mid Shelf
Shoal
Coastal Plain
Tidal Flat
Shoal
Algal Mound
Shoal
Mid Shelf

Prater A2

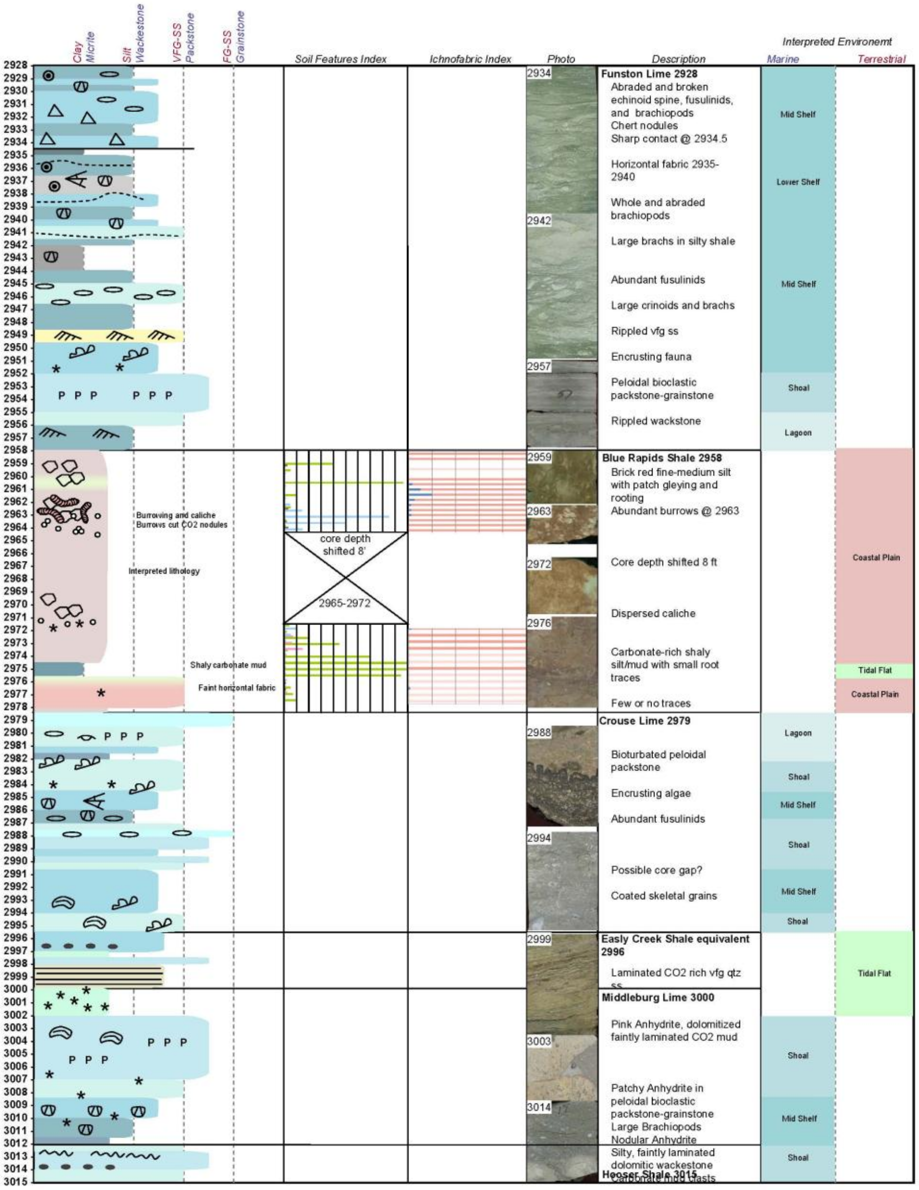
Clay
Micrite
Silt
Wackestone
VFG-SS
Packstone
FG-SS
Grainstone
Soil Features Index
Ichnofabric Index
Photo
Description
Interpreted Environemt
Marine
Terrestrial
2928
2929
2930
2931
2932
2933
2934
2935
2936
2937
2938
2939
2940
2941
2942
2943
2944
2945
2946
2947
2948
2949
2950
2951
2952
2953
2954
2955
2956
2957
2958
2959
2960
2961
2962
2963
2964
2965
2966
2967
2968
2969
2970
2971
2972
2973
2974
2975
2976
2977
2978
2979
2980
2981
2982
2983
2984
2985
2986
2987
2988
2989
2990
2991
2992
2993
2994
2995
2996
2997
2998
2999
3000
3001
3002
3003
3004
3005
3006
3007
3008
3009
3010
3011
3012
3013
3014
3015
P P P P P P
Burrowing and caliche
Burrows cut CO2 nodules
Interpreted lithology
Shaly carbonate mud
Faint horizontal fabric
P P P
P P P
P P P
core depth shifted 8'
2965-2972
2934
2942
2957
2959
2963
2972
2976
2988
2994
2999
3003
3014
Funston Lime 2928
Abraded and broken echinoid spine, fusulinids, and brachiopods
Chert nodules
Sharp contact @ 2934.5
Horizontal fabric 2935-2940
Whole and abraded brachiopods
Large brachs in silty shale
Abundant fusulinids
Large crinoids and brachs
Rippled vfg ss
Encrusting fauna
Peloidal bioclastic packstone-grainstone
Rippled wackstone
Blue Rapids Shale 2958
Brick red fine-medium silt with patch gleying and rooting
Abundant burrows @ 2963
Core depth shifted 8 ft
Dispersed caliche
Carbonate-rich shaly silt/mud with small root traces
Few or no traces
Crouse Lime 2979
Bioturbated peloidal packstone
Encrusting algae
Abundant fusulinids
Possible core gap?
Coated skeletal grains
Easly Creek Shale equivalent 2996
Laminated CO2 rich vfg qtz ss
Middleburg Lime 3000
Pink Anhydrite, dolomitized faintly laminated CO2 mud
Patchy Anhydrite in peloidal bioclastic packstone-grainstone
Large Brachiopods
Nodular Anhydrite
Silty, faintly laminated dolomitic wackestone
Carbonate mud clasts
Hooser Shale 3015
Mid Shelf
Lower Shelf
Mid Shelf
Shoal
Lagoon
Coastal Plain
Tidal Flat
Coastal Plain
Lagoon
Shoal
Mid Shelf
Shoal
Mid Shelf
Shoal
Tidal Flat
Shoal
Mid Shelf
Shoal

Legend

	*Naktodemasis* burrows (AMB)		Coated grains
	Rhizoliths	⊙ ⊙	Echinoderms
	Peds and cutans	∼ ∼	Algal laminae
* * *	Anhydrite	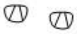	Brachiopods
G G G	Gleying		Bivalves
△ △ △	Chert	- - - -	Discontinuity surface
	Bryozoans	P P P	Peloids
	Ostracods		Encrusting fauna
● ● ●	Rip-up clasts		Fusulinids
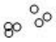	Carbonate nodules		Phylloid algae
≡	Horizontal laminations		Ripple marks

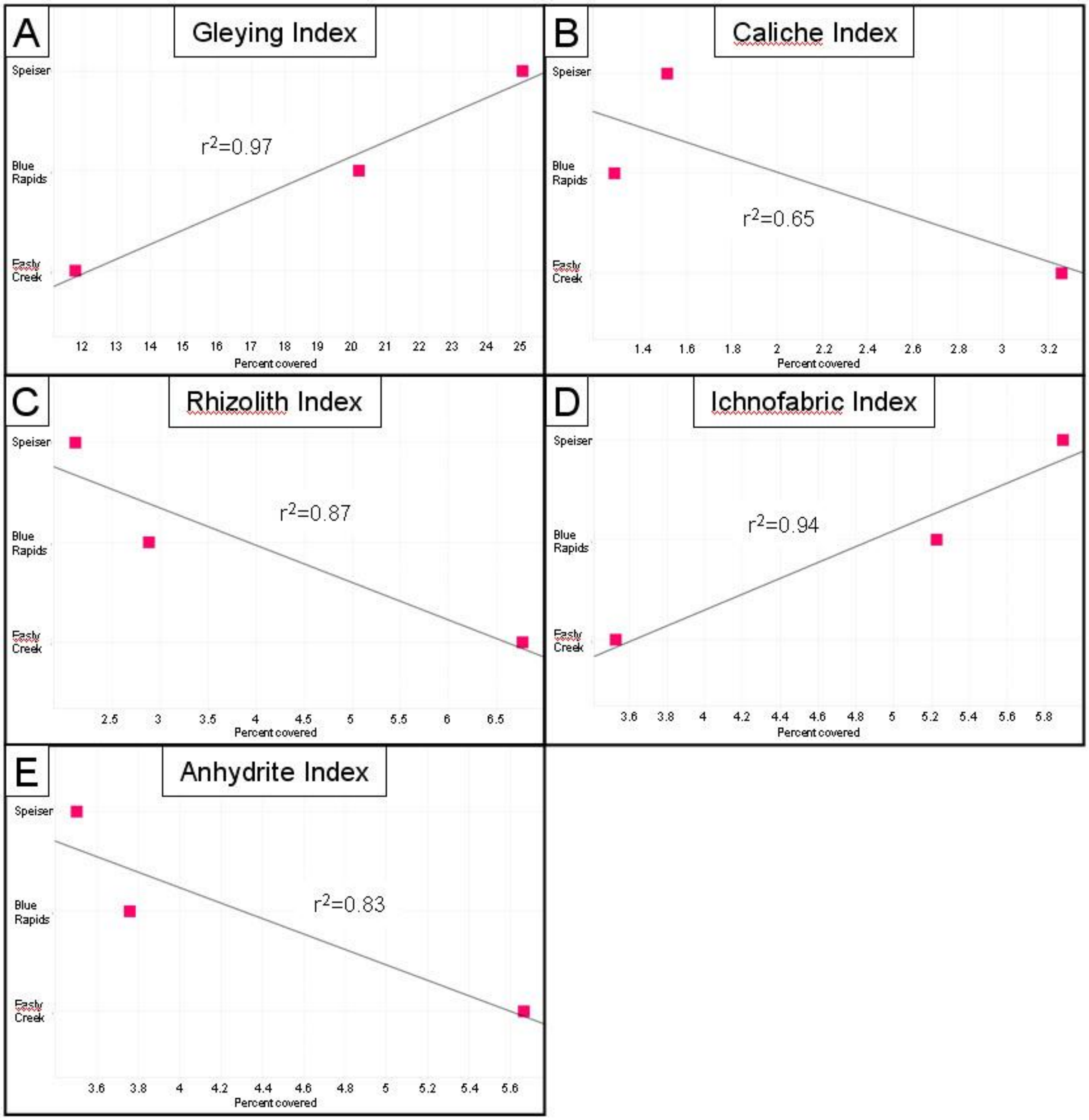

Figure 14: Crossplots showing total percentage of pedogenic features in each formation. Percentages shown are the total area of the core face covered by each soil feature, divided by the total slab area in each formation.

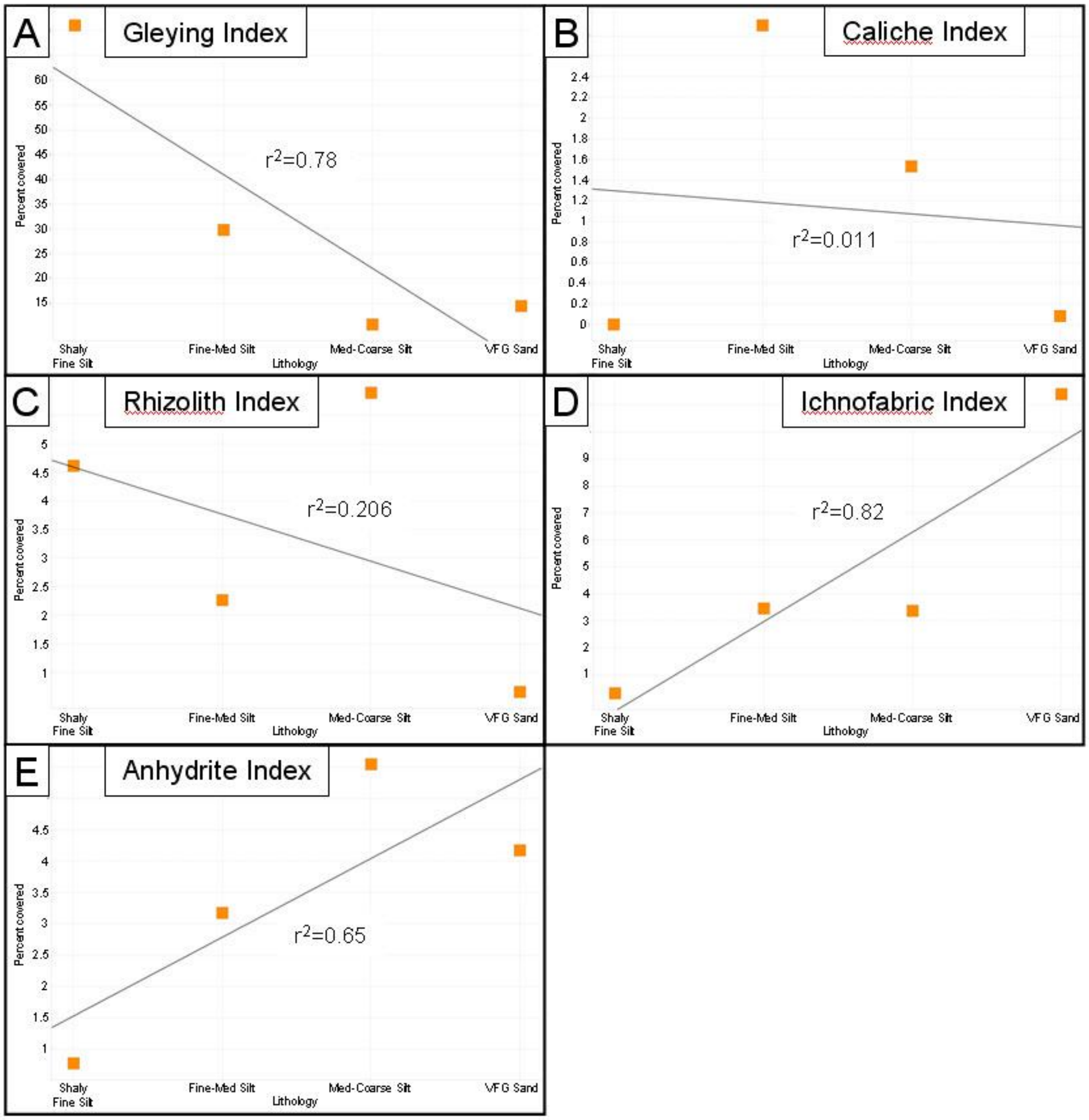

Figure 15: Crossplots showing total percentage of pedogenic features in each of the four major lithologies in paleosols. Percentages shown are the total area of the core face covered by each soil feature, divided by the total slab area determined to consist of each particular lithology, regardless of core or formation.

Spatial and Stratigraphic Distribution of Observed Paleosol Characteristics

Hugoton Area

All formations studied consist primarily of fine to coarse siltstone and very fine-grained sandstone with interbedded, intermittent, shalier intervals of varying thickness (Table 2). Coarser grain sizes are more common in stratigraphically higher formations (Dubois et al., 2012). Siltstones and sandstones of the Council Grove Group generally are weakly cemented by cryptocrystalline iron oxide, which fills the majority of existing pore space (Fig. 16). Calcite cements are also common, although not as ubiquitous as iron oxide cement, and are most abundant in sediments adjacent to, over, or underlying limestone. Iron oxides typically result in rocks that are dark red to brown red in color, with increasing amounts of calcite causing increasingly lighter shades of red.

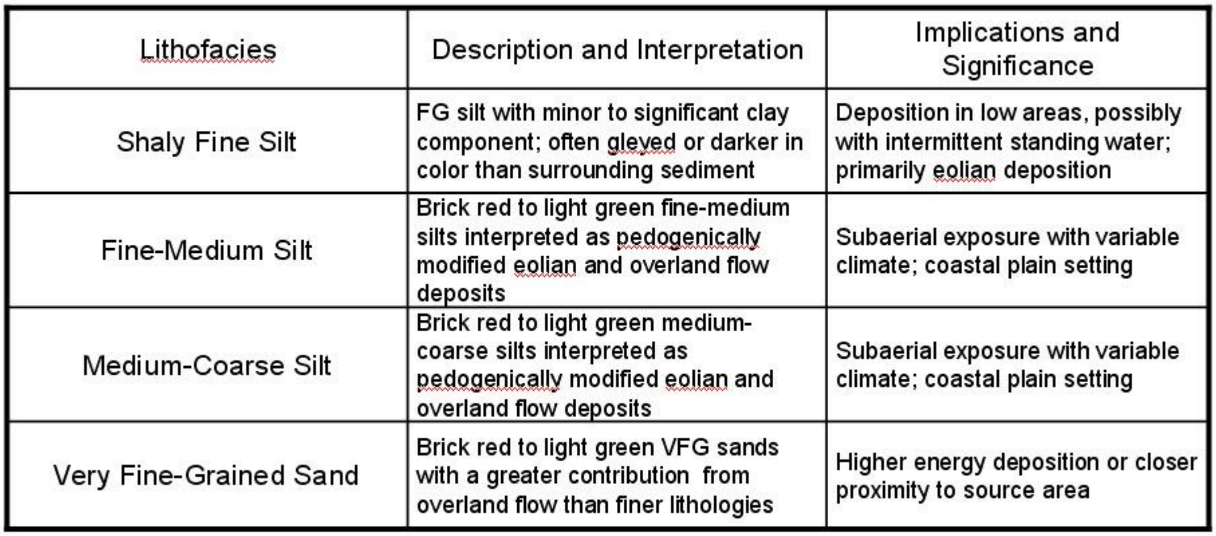

Lithofacies	Description and Interpretation	Implications and Significance
Shaly Fine Silt	FG silt with minor to significant clay component; often gleyed or darker in color than surrounding sediment	Deposition in low areas, possibly with intermittent standing water; primarily eolian deposition
Fine-Medium Silt	Brick red to light green fine-medium silts interpreted as pedogenically modified eolian and overland flow deposits	Subaerial exposure with variable climate; coastal plain setting
Medium-Coarse Silt	Brick red to light green medium-coarse silts interpreted as pedogenically modified eolian and overland flow deposits	Subaerial exposure with variable climate; coastal plain setting
Very Fine-Grained Sand	Brick red to light green VFG sands with a greater contribution from overland flow than finer lithologies	Higher energy deposition or closer proximity to source area

Table 2: Major lithofacies found in continental units; implications and significance

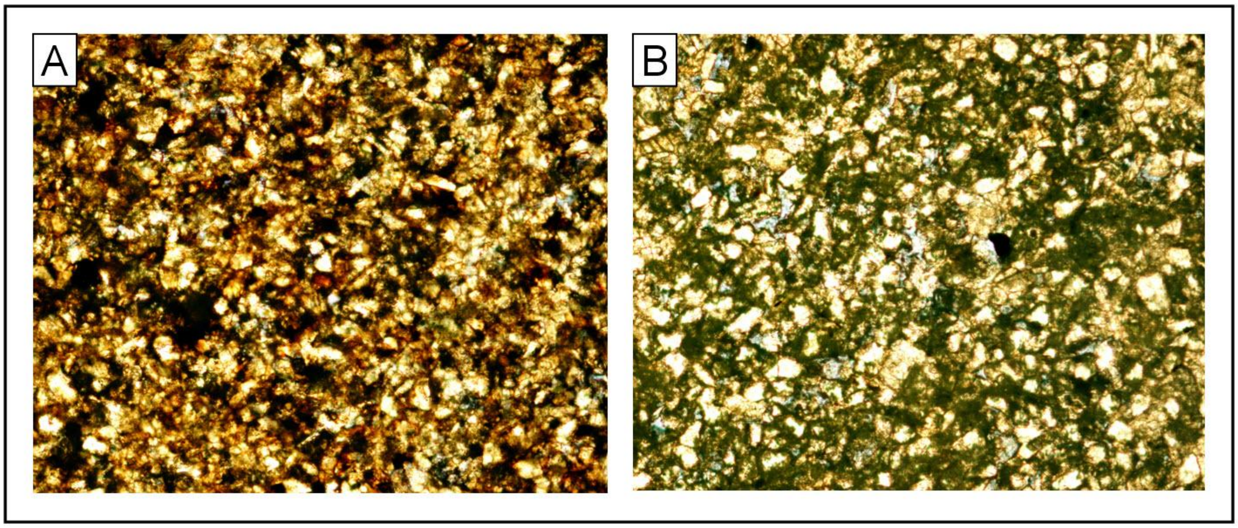

Figure 16: Thin section photos showing general nature of iron oxide cemented siltstone, the most common lithology in Council Grove Group paleosols. A) Oxidized sediment, Cross H Cattle 2716.2, PPL 10X, B) Gleyed sediment, Cross H Cattle, 2651.5, PPL 10X

Several zones within paleosols are composed of similar or identical lithologies but are light green to light grey in color. These zones are the product of gleying. At least some degree of gleying is present in all formations in all core (Fig. 17). Notably, gleying is present usually in the uppermost portions of all continental intervals. The lowermost formation studied, the Easly Creek Shale, is generally thinner than the overlying continental units and does not contain any discernable pattern of gleying other than a narrow band at the top of the formation. In addition to gleying at the formation top, both the Speiser and Blue Rapids shales show a distinct interval of gleyed sediments in a roughly correlative interval near the upper middle of the formation. The Speiser Shale also contains a higher incidence of gleyed strata near the base. On a larger scale, the average percentage of gleyed strata in each formation increases upward from the Easly Creek Shale to the Speiser Shale (Figure 14a). Increased gleying also shows a strong correlation with finer grained deposits (Fig 15a).

Figure 17: Bar graphs showing distribution of pedogenic characteristics in all formations in all core. A) Speiser Shale; B) Blue Rapids Shale; C) Easly Creek Shale. Datum for each set of graphs is the top of each formation.

Upper Council Grove Group paleosols also contain numerous associations of cm-scale discrete carbonate nodules, but bedded or massive carbonate is rare. Nodules are present and patchily distributed in all formations, although definitive correlative zones within paleosols are not present. The Speiser Shale contains concentrations of carbonate nodules ranging from the lower to the upper parts of the formation, with little consistency between cores. In the Blue Rapids Shale, the most significant concentration of carbonate nodules is in the most basinward core, the Prater A 1—other core only contain small quantities of nodules 1–1.3 m (3–4 ft) below the formation top. The Easly Creek Shale, however, contains significant amounts of carbonate nodules dispersed throughout each core along the transect. No significant trend in carbonate nodule distribution is seen between formations, although the Easly Creek Shale generally contains less carbonate than the overlying formations (Fig 14b). Carbonate nodules are also more likely to occur in finer grained rocks, with the exception of muddy siltstones (Fig. 15b).

Rhizoliths are also common, though not abundant, throughout the studied intervals. Rhizoliths are often preserved as gleyed rhizohalos that surround the original root cast, which is sometimes preserved as carbonaceous debris. Rhizolith morphologies are highly variable, ranging from a large, single taproot, to very small, isolated, carbon-filled traces, to fine networks of thin interlocking tubules. Rhizoliths are present in all core and are most abundant in the upper halves of continental intervals. In the Speiser Shale, rhizoliths can be correlated in a 0.6–1.3 m (2–4 ft) thick zone approximately 3 m (10 ft) from the top of the interval. Rhizoliths are present both above and below this zone, but much less frequent. In the Blue Rapids Shale, rhizoliths are rare overall. Significant numbers are present near the top of the Blue Rapids in the most landward core (Cross H Cattle) and are present but sparse in the most basinward (Prater), while core in between these two locations show little or no rhizoliths. In the Easly Creek Shale, rhizoliths are more common than in all other formations, and are distributed throughout the formation. Overall, rhizolith abundance generally decreases stratigraphically upward between formations, with the Easly Creek Shale recording the highest percentage of rhizoturbation and the Speiser Shale the least (Fig. 14c).

Trace fossils are common in Permian paleosols in the form of adhesive meniscate backfilled burrows (AMBs) (Fig. 18). AMBs in Permian paleosols, including the traces and sections described here, were referred to the newly erected ichnogenus *Naktodemasis* (Smith et al., 2008) and a possible new ichnospecies (Counts and Hasiotis, in review) based on of their unique internal morphology. No other ichnospecies or type of trace fossil was observed in continental units in any of the studied core. Traces are often visible as high-contrast, brick red burrow outlines and meniscate fill within gleyed zones, or lighter colored burrows within red-oxidized sediment. Almost all continental siltstone and sandstone of the upper Council Grove Group show some degree of mottling that is likely related to bioturbation. Visible bioturbation in the Speiser Shale is concentrated approximately ~3.6–5.5 m (12–18 ft) from the top of the formation, although much of the formation has likely been completely bioturbated. While the majority of the deposits appear homogeneous, reaction with dilute HCl reveals a mottled appearance created by differential carbonate cementation within and around ghost burrows. Near the bottom of the Speiser Shale, however, there is a higher incidence of gleyed sediments with faint horizontal laminations. The Blue Rapids and Easly Creek shales contain fewer assemblages of trace fossils than the Speiser Shale; the amount of visible bioturbation increases in each successively higher formation (Fig. 14d). Traces are also more likely to be found more frequently in coarser grain sizes (Fig. 15d), an observation reported in Dubois et al. (2012) but not statistically quantified.


A
Speiser Ichnofabric Index - XHC
Speiser Ichnofabric Index - MBE2
Speiser Ichnofabric Index - D Alex
missing interval
missing interval
Speiser Ichnofabric Index - Stuart
B
Blue Rapids Ichnofabric Index - XHC
Blue Rapids Ichnofabric Index - MBE2
missing interval
missing interval
missing interval
missing interval
missing interval
Blue Rapids Ichnofabric Index - D Alex
Blue Rapids Ichnofabric Index - Stuart
Blue Rapids Ichnofabric Index - Prater
missing interval
missing interval
C
Easly Creek Ichnofabric Index - XHC
Easly Creek Ichnofabric Index - MBE2
Easly Creek Ichnofabric Index - D Alex
Easly Creek Ichnofabric Index - Stuart
Easly Creek Ichnofabric Index - Prater
missing interval
0
20
40
60
80
100%

Figure 18: Bar graphs showing distribution of trace fossils in all formations in all core. A) Speiser Shale; B) Blue Rapids Shale; C) Easly Creek Shale. Datum for each set of graphs is the top of each formation.

Anhydrite crystals of varying size are found scattered throughout the section (Fig 17), and were likely formed after burial. Anhydrite is distributed patchily and is often found only as star-shaped, bladed crystals, though it may be concentrated into denser areas with higher concentrations of crystal aggradations. Although bedded anhydrite is rare, most crystals are displacive and, thus, had to have been formed before significant compaction and lithification. Anhydrite occasionally forms the core of rhizoliths. The exact timing of anhydrite formation is difficult to ascertain, but it must have been shortly after deposition. Like bioturbation, anhydrite is most common in stratigraphically higher formations and in coarser grain sizes (Figs. 14e, 15e).

Discussion

Paleoenvironmental and Paleoclimatic Significance of Paleosol Characteristics

Pedogenesis is a complex process based on the interaction of the prevailing climate, local organisms, topographic relief, parent lithology, and time of exposure (Jenny, 1941). The paleosols, their stratigraphic architecture, and their internal characteristics preserve sufficient soil features to reconstruct at least some of these parameters for the Lower Permian of western Kansas, which are useful in larger-scale paleoecological, paleogeographic, and paleoclimatic reconstructions.

Analysis of Upper Council Grove deposits supports the assertion that these units are cumulic paleosols formed primarily from the deposition of silt- and sand-sized particles throughout the time interval of soil formation. These deposits would likely be classified as Inceptisols if found in modern environments based on the lack of horizonation and incipient soil structures. Deposition rates were likely high enough that the exposure surface was rapidly aggrading; continual deposition made sure that sediments were buried below the pedogenic window before significant maturation could occur. Lithologies in thin section bear a resemblance to modern loess deposits (Dubois et al., 2012), indicating a possible eolian origin for sediment deposition. Subaqueous methods of deposition, including periodic overland sheet flow, cannot be ruled out—all continental units are generally lacking in primary sedimentary structures that would provide clues as to the initial mechanism of deposition. This is most likely because they have been completely bioturbated. General patterns of lithologic change can still be discerned, however; coarsest grain sizes are typically concentrated near the middle of each formation, indicating closer proximity to the source area or increased energy of deposition during times of lowest sea level. Across formations, the upward trend of increasing coarser sediment indicates a longer-term shift in the relative position of the Hugoton Basin toward the source area.

The abundance of gleying within Council Grove Group paleosols is partially due to the differences in drainage ability of different soil lithologies. Gleying is more common in finer-grained sediments, which are more likely to retain water due to decreased porosity and increased capillarity. Additionally, some finer-grained sediments, such as muddy silts, were likely deposited in topographic lows with ponded water, leading to saturated conditions. In many cases, though, gleying occurs immediately adjacent to oxidized sediment with no visible change in grain size. These types of gleying are likely not the result of poor drainage, but instead are interpreted to be associated with high subterranean water tables, which may in turn be related to smaller scale sea-level fluctuations that are not recorded by lithologic change. 5th-order sea level rise may have led to an overall rise in base level and, thus, decreased the distance from surface to the top of the water table. Gleying at formation tops is also likely due to a raised water table resulting from higher base level as sea level rose in the transgressive portion of each 4th order cycle. Gleying at the base of the Speiser Shale is probably due to a remnant high water table as sea level falls from the preceding highstand. In addition to base level changes, eustatic change was likely accompanied by changes in regional climate. The interval of time during which soil formation occurred was likely subject to multiple smaller scale climate cycles that favored either drier or wetter conditions, resulting in gleyed and oxidized intervals in close proximity to one another. Aggradation was, therefore, slow enough to record climate changes before active soil horizons could be buried below the zone of active soil formation. Gleying in coarser-grained sediments increases up section from the Easly Creek Shale to the Speiser Shale; this likely indicates increasingly high water tables or wetter climates as sea level fell within the larger scale, 3rd-order cycle that encompasses much of the Upper Council Grove Group. The abundance of gleying in coarser-grained intervals suggests that increased water saturation was not a product of changing depositional environment, but rather a climatic shift toward wetter conditions. .

Carbonate nodules found in paleosols are interpreted to be subaerially formed pedogenic carbonate. Since the physical processes responsible for pedogenic carbonate formation remain relatively constant through time, modern precipitation limits to paleosols containing carbonate nodules can be reasonably applied. The modern range of calcic soil formation occurs at a range of between 40 and 1100 mm per year (Marion, 1989; Retallack, 1994; Royer, 1999). While this range is relatively large, carbonate nodules are less common on either extreme—in both the most arid environments (e.g., Sahara-type deserts) as well the more tropical and temperate areas that receive higher amounts of rainfall. The vast majority of soil carbonate in these studies forms in areas with a mean annual precipitation of between 100 and 800 mm per year. It is likely, therefore, that the Early Permian of southwestern Kansas likely had an average rainfall within this range. Methods used to quantify mean annual precipitation based on depth to the Bk (carbonate-rich) horizon are not applicable here due to the cumulative nature of the paleosols in question, however, future studies may be able to further refine this range using geochemical methods (e.g., those described in Sheldon and Tabor, 2009). Most pedogenic carbonate in the upper Council Grove Group is nodular, indicating it was not able to fully develop into massive or layered beds. This also indicates either suboptimal conditions for pedogenic carbonate formation, or rapid aggradation that buried incipient nodules before significant development. No indices have been published quantifying the relationship between soil carbonate morphology and MAP. The distribution of carbonate nodules in vertical stringers indicates continual aggradation of the soil surface and associated rising of the Bk horizon. The percentage of carbonate nodules in the coarser sediments of each formation decreases stratigraphically upward, indicating a change to increasingly wetter climates where carbonate precipitation is not favored.

Plant communities colonized Council Grove Group soils repeatedly and over a wide area—rhizoliths are common in all formations studied and throughout the core transect. Rhizolith abundance shows no clear relationship to lithofacies and grain size, indicating that such other factors as soil moisture and sedimentation rate controlled plant distribution in continental settings. Rhizoliths are proportionately more abundant in the Easly Creek Shale, and less common in the Speiser Shale. Conditions became less favorable for plant growth over the Easly Creek Shale to Speiser Shale time span, possibly due to poorer drainage as evidenced by increased gleying and fewer carbonate nodules. Individual plants, however, may have been widely spaced—rhizoliths usually form less than 10% of the total area of the core face and are most often found as isolated traces. The lack of ubiquitous rhizoturbation might indicate that plant communities did not always dominate the landscape but provides additional evidence that soil moisture was likely higher than modern arid environments, where plant growth is more limited—e.g., B climates as defined in the Koppen system (Trewartha, 1982). The absence of rhizoliths, however, can also be attributed to the destruction by *Naktodemasis*. Multiple rhizolith morphologies do exist, however, indicating that plant communities were at least somewhat diverse.

Trace fossil assemblages in Permian paleosols are interpreted to be the work of insects or insect larvae that lived within the soil vadose zone for an extended period of time, based on morphological similarities with modern burrows (Smith and Hasiotis, 2008; Counts and Hasiotis, 2009). The association between trace fossils and rhizoliths provides additional evidence for this hypothesis; many modern fossorial insects feed on plant roots and organic matter disseminated in the soil. By using these modern insects as analogs, the approximate range of soil moisture in Permian sediments can be deduced from the moisture tolerances of these organisms. Like their modern counterparts, the constructors of *Naktodemasis* would have been susceptible to desiccation and could not have survived even limited amounts of time in completely dry sediments. Permian sediments, thus, likely retained some amount of water even during the dry season. Conversely, sediments unlikely were completely saturated for long periods of time, since many fossorial insects can neither survive in fully subaqueous conditions. Numerous studies of moisture variation tolerances in modern insects and insect larvae find that highest survival of these organisms occurs at soil moisture levels of roughly 20–40% water by weight (see references and discussion in Counts and Hasiotis, 2009). Ambient soil moisture was, therefore, likely most often within this range in upper Council Grove Group paleosols. The lack of visible primary sedimentary structures in the majority of continental units suggests that sediments have been completely bioturbated during pedogenesis. Although multiple generations of organisms repeatedly colonized these soils, visible burrow assemblages are likely only the most recent generation of burrowing. Decreased abundance of traces upward throughout the studied section may be related to increasing soil moisture content through time, as evidenced by increased gleying and decreased pedogenic carbonate. Burrowing activity is also more common in coarser grain sizes. Since Dubois et al. (2012) interpret coarser lithofacies as being deposited in more arid conditions, traces that require higher soil moisture would not be expected to be most abundant in the coarsest sediments. We interpret this as evidence that "arid" climates may not have been truly arid. Arid climates with consistently dry soils do not support large populations of subterranean insects (Hasiotis et al., 2012); large numbers of insect burrows in paleosols, therefore, are not suggestive of arid climates.

Anhydrite is likely diagenetic in origin, but would not be unexpected in a seasonally dry climate. The lack of bedded anhydrite indicates it did not originate from large-scale evaporative events. Since the anhydrite does displace silt grains, however, it likely formed early enough that sediment had not completely lithified. Anhydrite is more common in coarser grain sizes, and increases in abundance downward from the Speiser Shale to the Easly Creek Shale. The interiors of rhizoliths are often filled with anhydrite, indicating that anhydrite precipitation occurred in the void space after the root had decayed.

The combination of pedogenic features and trace fossils within the studied interval indicates an environment with a variable climate that was capable of supporting a substantial ecosystem of plant and animal communities. Such communities require more rainfall than is currently seen in modern arid climates, which have an upper limit of 380mm per year MAP. We therefore favor an interpretation wherein precipitation in the Early Permian of the Midcontinent reached a minimum of several hundred millimeters per year, the approximate range of modern semiarid climates (Peel et al., 2007). The repeated occurrence of features supporting this interpretation across multiple formations indicates that environmental conditions were relatively similar over time, but variations in their abundance indicate a change from drier to wetter conditions within the observed stratigraphic interval.

Hugoton-Area Depositional Mechanisms and Stratigraphic Architecture

Evidence of soil moisture in paleosols suggests that mechanisms other than eolian deposition were responsible for initial sedimentation of silts and fine sands in continental units Modern semiarid environments with higher amounts of precipitation contain at least some proportion of sediment deposited through overland flow, when rivers and streams overtop natural levees or the boundaries of incised channels in low-relief areas during flooding events. Large amounts of rainfall in upland areas can also flow basinward faster than water can infiltrate into the ground. Our observations of paleosols are consistent with contributions from both sheetflood and eolian deposition; coarser grain sizes may have been deposited during higher energy flooding events, with fine silts being deposited by wind action or reworked from lower-energy environments within the fluvial cycle. Alluvial and eolian depositional mechanisms for similar paleosols have been proposed for the similar paleosols, such as the underlying D-zone in the Lansing-Kansas City Groups (Prather, 1985). Sediments were continually bioturbated and pedogenically modified before, during, and after deposition, creating cumulative paleosol profiles without well-defined horizons. Although sedimentation and pedogenesis were roughly equal, sedimentation rate was slightly higher, enough to build thick successions of compound paleosols in some areas (e.g., Hasiotis and Platt, 2012).

Isopach mapping of continental units shows a clear increase in thickness landward (Fig 4). Extensive subaerial burrowing and plant colonization may have an impact on stratigraphic architecture—biostabilization of the landscape by these organisms likely played a role in the updip aggradation and thickening of continental units. This pattern of updip thickening, however, also follows expected trends of continental sediment thickness in settings with very low slope. Updip portions of the clastic wedges that form continental units are thicker and coarser overall, since they were deposited closer to sediment source areas. The decreasing relief of the coastal plain setting slowed the deposition of sediment as fluvial energy decreased in the hinterland. Accommodation for subsequent cycles was created by subsidence associated with the Hugoton basin, which was an isostatic response to sea-level change and was relatively consistent across the region (Johnson, 1989). The alternating clastic-carbonate wedge architecture of the area is thus a function of biostabilization, variation in sedimentation rate, depositional environment, and subsidence.

Regional Changes in Cyclothems and Sequence Stratigraphy

The internal changes in continental units over the ~480 km (~300 mile) span between core and outcrop represent fundamentally different mechanisms of soil formation in the two areas (Figure 19- see comment). Outcrop paleosols contain distinct exposure surfaces at the base of thin limestones and are not interpreted as cumulic. Each of the stacked paleosols seen in outcrops was likely formed through pedogenic modification of existing marine clastics that were deposited during 5th-order cycles, with little or no accumulation of additional sediment during soil formation. This mechanism of paleosol formation is also well known in other midcontinent cyclic strata, e.g., the underlying Pennsylvanian Roca Shale (Rankey and Farr, 1997). Since these cycles are likely related to global sea level change, evidence of 5th-order cyclicity should be present in the Hugoton area as well. The lack of internal, cyclic changes in lithology in continental units in core, however, suggests that the Hugoton area was less sensitive to these smaller-scale sea-level changes. Stratigraphic variations in pedogenic features in Hugoton-area sediments are evidence that the parameters affecting soil formation change significantly over the time interval during which each unit was formed. These variations in soil characteristics may be related to differences in water table height or climate change, which in turn may be influenced by 5th-order cycles. These variations, however, lack the regularity that would indicate a strong relationship to cyclical sea level change.

.

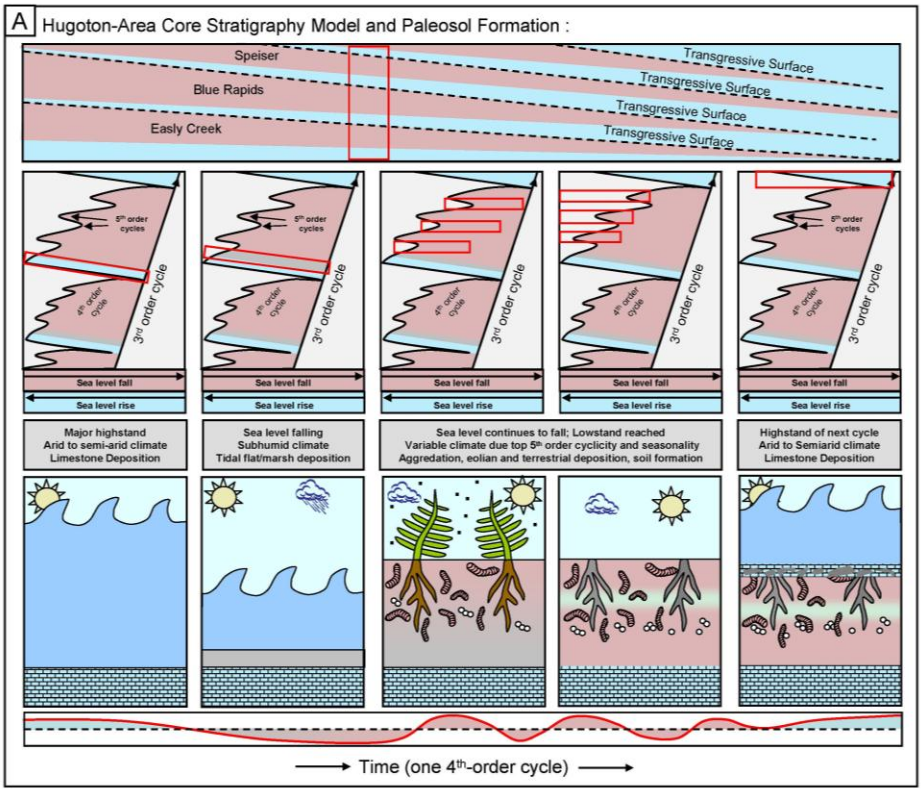
A
Hugoton-Area Core Stratigraphy Model and Paleosol Formation :
Speiser
Blue Rapids
Easly Creek
Transgressive Surface
Transgressive Surface
Transgressive Surface
Transgressive Surface
5th order cycles
4th order cycle
3rd order cycle
Sea level fall
Sea level rise
Major highstand
Arid to semi-arid climate
Limestone Deposition
Sea level falling
Subhumid climate
Tidal flat/marsh deposition
Sea level continues to fall; Lowstand reached
Variable climate due top 5th order cyclicity and seasonality
Aggredation, eolian and terrestrial deposition, soil formation
Highstand of next cycle
Arid to Semiarid climate
Limestone Deposition
Time (one 4th-order cycle)

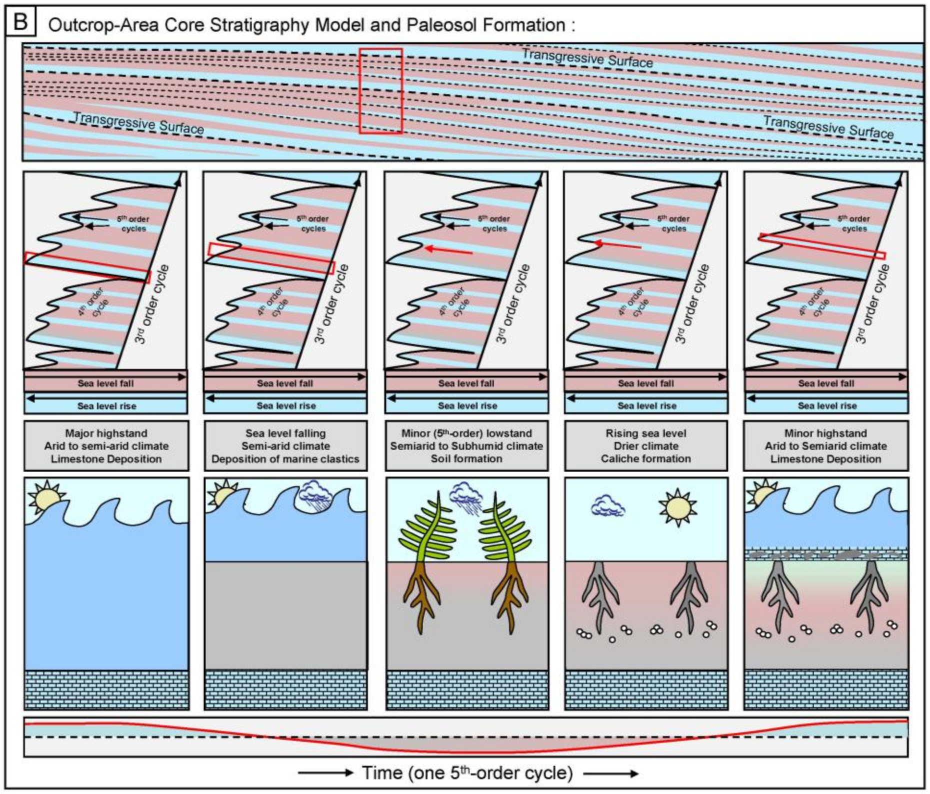
B
Outcrop-Area Core Stratigraphy Model and Paleosol Formation :
Transgressive Surface
Transgressive Surface
Transgressive Surface
5th order cycles
4th order cycle
3rd order cycle
Sea level fall
Sea level rise
Major highstand
Arid to semi-arid climate
Limestone Deposition
Sea level falling
Semi-arid climate
Deposition of marine clastics
Minor (5th-order) lowstand
Semiarid to Subhumid climate
Soil formation
Rising sea level
Drier climate
Caliche formation
Minor highstand
Arid to Semiarid climate
Limestone Deposition
Time (one 5th-order cycle)

Figure 19: Cycle hierarchies recorded in paleosols, and hypothesized mechanisms of soil formation in upper Council Grove Group paleosols in both Eastern Kansas outcrops and Hugoton-area core. Outcrop model modified from Miller et al. (1996). Although sea level change was consistent in both areas, 5th-order cycles are not visible in the Hugoton area as lithologic changes due to paleogeographic differences. Soil formation was also different in each area, with outcrop paleosols being the result of pedogenic modification of marine clastics, and Hugoton-area soils accumulating and aggrading throughout the interval of subaerial exposure.

Several factors may influence the reasons that fifth-order cycles do not consistently affect Hugoton-area paleosols. Our observations support the model proposed by Dubois et al. (2012), wherein biostabilization of the landscape results in topographic aggradation and reduced accommodation. Positive relief created through aggradation prevented all but the largest sea level changes from affecting updip sediments. Although small-scale (5th order) sea-level fluctuations occur, little or no accommodation exists to allow for extensive flooding and limestone deposition like that seen in outcrop. Neither is there space for the marine clastics that form the basis for outcrop paleosols to be deposited during late-stage highstand and early regression (Figure 19b). Additionally, the lack of *Naktodemasis* burrow assemblages in outcrop may indicate that little or no biostabilization took place. Topographic relief was not able to be created in the outcrop area, as the lesser degree of biologic activity would not have allowed significant stabilization and aggradation. The abundance of *Naktodemasis* burrows in Hugoton area indicates that enough moisture was present in sediments to support plant growth, soil biota life cycles, and biostabilization of the landscape via pedogenesis, resulting in the building of relief. Future sequence stratigraphic models should incorporate extensive burrowing, aggradation, and reduced accommodation in the updip portions of continental cycles. The uniform nature of continental formations in core, however, is also likely a function of geographic position on the broad, low relief ramp. The overall Hugoton area was likely located further from the basin center than outcrops, decreasing the influence of sea level on the area, while experiencing greater sediment input from the source area (i.e., Ancestral Rocky Mountains). In addition, the Hugoton basin most likely had a steeper slope than the outcrop area to the east due to higher rates of subsidence within the tectonically active basin. Small changes in sea level would, thus, have affected a smaller spatial area than the flatter passive margin to the east, which had little large-scale tectonic activity.

Implications for Early Permian Paleoclimate

Although existing paleoclimate models are based on data sets from a broad geographical and spatial range, our more detailed observations can lend support to specific aspects of models proposed by others (e.g., Miller and West, 1993; Miller et al., 1996; Rankey, 1997; Soreghan, 1997; Olszewski and Patzkowsky, 2003) Although some of these studies favor an interpretation of an arid climate during lowstands, our observed characteristics of continental units in the Upper Council Grove Group suggest that paleosol formation took place during a time when climate was generally semiarid. Juxtaposition of soil features interpreted to represent both high and low amounts of soil moisture, however, indicates climatic variability within the time interval of soil formation. These interpretations are consistent with the model proposed by Miller et al. (1996), wherein 5th-order lowstands allow formation of a monsoonal climate, leading to increased seasonality and precipitation, and 5th-order highstands are coincident with dryer conditions. During the time of formation of each cumulative paleosol, several of these smaller cycles would have occurred. The observed pedogenic characteristics are thus a result of seasonality within the lowstand portions of 5th order cycles, as well as the climatic variability between the lowstand and highstand portions of these cycles. Difference between wetter lowstand and drier highstand climates likely contributed to a greater contribution to pedogenic variability than seasonal variations within monsoonal climates.

Given the intraformational climate variability, our interpretations do not support the assertion that Hugoton-area continental units were deposited solely in times of arid climates. If climate change was occurring at 5th-order time scales in outcrops 300 km to the east, then some degree of climate cyclicity would also be seen in Hugoton area, regardless of the particular depositional environment, paleogeography, or ramp position. The interpretations of Dubois et al. (2012) do not take into account climatic variations on these time scales. Rankey (1997) applied the same climate model—drier lowstands and wetter highstands—to examples of both 4th and 5th-order cycles, although Miller et al. (1996) noted that the two cycle scales would not necessarily have the same climate signature. Our studies show that models of cyclic climate change need to incorporate cycle hierarchies and more rapid variations in climate in order to fully explain observed pedogenic features. These smaller scale cycles may play an important role in determining the characteristics of cumulic paleosols. Although our detailed observations cannot comment on the climate moisture levels of highstand phases, they support an overall semiarid climate during lowstand. Even during the drier portions of 5th-order cycles, soil moisture would have to be high enough to support the continued presence of stable communities of organisms. Sedimentation and pedogenesis may have alternated with climate as the predominant soil-forming factors, with sedimentation have a greater contribution in drier times, and pedogenic alteration in the wetter.

Changes in paleosol features across formations are also indicative of climate change, but on a larger scale. The Speiser Shale has been interpreted as the terminal end of a larger 3rd-order cycle that encompasses most of the Council Grove Group (Boardman and Nestell, 2000). Trends in paleosol features across continental units from the Easly Creek to the Speiser Shale can, thus, be used to determine climatic response to 3rd-order sea level regression during late-stage highstand. Both gleying and total bioturbation increase stratigraphically upward across the formations studied--we interpret this as evidence of increasing soil moisture as sea level fell over 3rd-order time scales. Additionally, pedogenic carbonate, an indicator of climates where precipitation is less than evapotranspiration, is proportionally less abundant in the Speiser and Blue Rapids Shales than in the underlying Easly Creek. This increase in soil moisture is likely related to a more humid climate and not increasingly higher water tables, as falling sea level would have lowered overall base level. Generally coarser grain sizes in the Speiser Shale also could indicate increased contribution from overland flow, since coarser grain sizes require higher energy for deposition and may not be eolian in origin. Our observations support the interpretation that larger scale regressions are coincident with changes to a more humid or seasonal climate with increased precipitation.

Conclusions

Permian continental deposits in Hugoton core are interpreted as cumulative paleosols that are the product of continual aggradation and pedogenic modification of both windblown and floodplain silts and very fine sands. Paleosol characteristics, including trace fossils, rhizoliths, carbonate nodules, and gleying, indicate a variable, seasonally wet climate in the western interior of Pangaea. By comparing trace fossils to modern analogs, Hugoton-area paleosols are thought to have consistently contained adequate soil moisture to allow for continued survival of infauna. Soil features are not consistently distributed throughout continental units, and cannot be tied directly to smaller scale cyclicity, but are ultimately the product of climate variability related to smaller, 5th-order cycles. Differences in character between outcrops and core reflect different mechanisms of soil formation that are related to both the time scales of formation, the paleogeographic setting, and the presence of topography-building organisms that reduce accommodation space in the Hugoton basin. Our observations indicate that a completely arid climate during deposition of continental units is not supported for the Hugoton area. This study also underscores the need to account for cycle hierarchies and intra-cycle climate variability when reconstructing paleoclimates.

Acknowledgements

This research was supported by the University of Kansas Joseph M. Patterson scholarship, a University of Kansas summer field research award, the AAPG Raymond C. Moore Memorial Grant, and a Geological Society of America research grant. The authors wish to thank Drs. Robert Goldstein at the University of Kansas and Lynn Watney of the Kansas Geological Survey for their helpful reviews of this manuscript.

References

ABDULLAH, T.Y., 1985, Depositional facies in the Funston cycle (Lower Permian) of southwestern Kansas. In Watney, W. L., Walton, A. W., and Doveton, J. H. (eds.) Core studies in Kansas; sedimentology and diagenesis of economically important rock strata in Kansas. Kansas Geological Survey, Subsurface Geology Series 6, p. 161-171.

BAARS, D.L., 1990, Permian chronostratigraphy in Kansas. Geology 18, p. 687-690

BARRY R.G., AND CHORLEY, R.J., 2009, Atmosphere, Weather, and Climate, 9th Edition: Routledge, New York, 516 p.

BLAKEY, R.C., 2012, Early Permian Paleogeography and Geologic Evolution of North America, 2011, http://cpgeosystems.com/namP290.jpg. Checked April 2012.

BOARDMAN, D. R. II, 1999, Changes in patterns of cyclicity in Upper Carboniferous through Lower Permian (Virgilian-Sakmarian) depositional sequences in the North American Midcontinent (abs): AAPG Bulletin, vol. 83, no. 7, p. 1193.

BOARDMAN, D.R. II, and NESTELL, M.K., 2000, Outcrop-based sequence stratigraphy of the Council Grove Group of the Midcontinent, in Johnson, K.S. (ed.), Platform carbonates in the southern Midcontinent, 1996 symposium: Oklahoma Geological Survey Circular 101, p.275-306.

BUSCH, R.M., and WEST, R.R., 1987, Hierarchical genetic stratigraphy: a framework for paleoceanography: Paleoceanography, v. 2, p. 141-164.

COUNTS, J.W., and HASIOTIS, S. T., 2009., Neoichnological experiments documenting burrowing behaviors and traces of the masked chafer beetle (Coleoptera: Scarabaeidae: Cyclocephala sp.): Behavioral significance of extant soil-dwelling insects to understanding backfilled trace fossils in the continental realm: PALAIOS, v. 24, p. 75-92.

COUNTS, J.W., and HASIOTIS, S.T., in review, Paleoecological and paleobiological implications of Naktodemasis krausi: A new ichnospecies from the lower Permian of Kansas. Submitted to PALAIOS July 2012.

CROWN, P.H., and HOFFMAN, D.W., 1970, Relationship between water table levels and type of mottles in four Ontario gleysols: Canadian Journal of Soil Science, v. 50, p. 453-455.

CUNNINGHAM, C.R., 1989, Genetic stratigraphy, depositional environments, and vertebrate paleontology of the Speiser Shale (Gearyan stage, lower Permian series) in northern Kansas: unpublished master's thesis, Kansas State University, Manhattan, Kansas, 205 p.

DRIESSEN, P., DECKERS, J., SPAARRGAREN, O., and NACHTERGALE, F., eds., 2001, Lecture notes on the major soils of the world: FAO World Soil Resources Reports, v. 94, 337 p.

DUBOIS, M.K., GOLDSTEIN, R.H., and HASIOTIS, S.T., in press, Climate-controlled aggradation and cyclicity of continental loessic siliciclastic sediments in Asselian–Sakmarian cyclothems, Permian, Hugoton embayment, USA: Sedimentology, v. 59, p. 1782-1816.

ELIAS, M.K., 1937, Depth of deposition of the Big Blue (late Paleozoic) sediments in Kansas: Geological Society of America, Bulletin 48, p. 403-432.

FELDMAN, H.R., FRANSEEN, E.K., JOECKEL, R.M., and HECKEL, P.H., 2005, Impact of longer-term modest climate shifts on architecture of high-frequency sequences (cyclothems), Pennsylvanian of midcontinent USA: Journal of Sedimentary Research, v. 75, p. 350-368.

FOLK, R.L., 1951, A comparison chart for visual percentage estimation: Journal of Sedimentary Research, v. 21, p. 32-33.

GARNER, D.L., and TURCOTTE, D.L., 1984, The thermal and mechanical evolution of the Anadarko Basin: Tectonophysics, v. 107, p. 1-24.

GOODWIN, P. W., and ANDERSON, E.J., 1985, Punctuated aggradational cycles – general hypothesis of episodic stratigraphic accumulation: Journal of Geology, v. 93, p. 515-533.

HASIOTIS, S.T., and PLATT, B.F., 2012, Exploring the sedimentary, pedogenic, and hydrologic factors that control the occurrence and role of bioturbation in soil formation and horizonation in continental deposits: An integrative approach: The Sedimentary Record, v. 10., p. 4-9.

HASIOTIS, S.T., REILLY, M., AMOS, K., LANG, S., KENNEDY, D., TODD, J.A., MICHEL, E., and PLATT, B.F., 2012, Actualistic studies of the spatial and temporal distribution of terrestrial and aquatic organism traces in continental environments to differentiate lacustrine from fluvial, eolian, and marine deposits in the geologic record, in O. W. Baganz, Y. Bartov, K. Bohacs, and D. Nummedal, eds., Lacustrine sandstone reservoirs and hydrocarbon systems: AAPG Memoir 95, p. 1 – 55.

HECKEL, P. H., 1977, Origin of Phosphatic black shale facies in Pennsylvanian cyclothems of Midcontinent North America: AAPG Bulletin, v. 61, p. 1045-1068

HECKEL, P.H., 1984, Changing concepts of midcontinent Pennsylvanian cyclothems, North America, Southern Illinois University Press, Neuviaeme Congress International de Stratigraphie et de Geologie du Carbonifere, vol.3, p. 535-553.

HECKEL, P.H., 1986, Sea level curve for Pennsylvanian eustatic marine transgressive-regressive depositional cycles along Midcontinent outcrop belt: Geology, v 14, p 330-334

HEMBREE, D. I., MARTIN, L. D., and HASIOTIS, S. T., 2004, Amphibian burrows and ephemeral ponds of the Lower Permian Speiser Shale, Kansas:evidence for seasonality in the mid-continent. Paleogeography, Paleoclimatology, Paleoecology 203: 1-2, p.127-152.

HEMBREE, D.I., HASIOTIS, S.T., and MARTIN, L.D., 2005, *Torridorefugium eskridgensis* (new ichnogenus and ichnospecies): amphibian aestivation burrows from the lower Permian Speiser Shale of Kansas: Journal of Paleontology, v. 79, p. 583-593.

JENNY, H., 1941, Factors of soil formation: a system of quantitative pedology: Dover Publications, New York, 191 p.

JOHNSON, K.S., 1989, Geologic evolution of the Anadarko Basin: *in* Johnson K.S., ed., Anadarko Basin Symposium. Circular 90, Oklahoma Geological Survey , Norman, p. 3-12.

KESSLER, L.P., SOREGHAN, G.S. and WACKER, H.J., 2001, Equatorial aridity in western Pangaea: lower Permian loessite and dolomitic paleosols in northeastern New Mexico, U.S.A.: Journal of Sedimentary Research, v. 71, p. 817–832.

KRAUS, M.J., 1999, Paleosols in clastic sedimentary rocks: their geologic applications: Earth Science Reviews, v. 47, p. 41-70.

KRAUSS M.J., AND HASIOTIS S.T., 2006, Significance of different modes of rhizolith preservation to interpreting paleoenvironmental and paleohydrologic settings: examples from Paleogene paleosols, Bighorn Basin, Wyoming, U.S.A.: Journal of Sedimentary Research, v. 76, p. 633-636.

LANE, N.G., 1964. Paleoecology of the Council Grove Group (Lower Permian) in Kansas, based on microfossil assemblages. Kansas Geological Survey Bulletin 170: pt. 5, p. 3-23.

MARION, G.M., 1989, Correlation between long-term pedogenic $CaCO_3$ formation rate and modern precipitation in deserts of the American Southwest: Quaternary Research, v. 32, p. 291-295.

MAZZULLO, S. J., 1998, Stratigraphic architecture of Lower Permian, cyclic carbonate reservoirs (Chase Group) in the Mid-Continent U.S.A., based on outcrop studies: American Association of Petroleum Geologist Bulletin, v. 82, p. 464-483.

MAZZULLO, S. J., Teal, C.S, and Burtnett, C.A., 1995, Facies and stratigraphic analysis of cyclothemic strata in the Chase Group (Permian, Wolfcampian), south-central Kansas, *in* Hyne, N..J., ed., Sequence Stratigraphy of the Mid-Continent: Tulsa Geological Society Special Publication 4, Tulsa. p. 217-248.

MICHELI, E., SCHAD, P., SPAARGAREN, O., DENT, D., and NACHTERGAELE, F., 2006, World reference base for soil resources 2006: World Soil Resources Reports No. 103, FAO, Rome, 145 p.

MILLER, K. B, 1994, Tuttle Creek Lake spillway exposure: cycle patterns and paleosol profiles: Kansas Geological Survey Open–File Report 94-23, 26 p.

MILLER, K. B., and WEST, R. R., 1993, Reevaluation of Wolfcampian cyclothems in northeastern Kansas; significance of subaerial exposure and flooding surfaces: Kansas Geological Survey Bulletin 235, p. 1-26.

MILLER, K. B. and R. R. WEST, 1998, Identification of Sequence Boundaries within Cyclic Strata of the Lower Permian of Kansas, USA: Problems and Alternatives: Journal of Geology, v. 106, p. 119-132.

MILLER, K. B., T. J. MCCAHON, and R. R. WEST, 1996, Lower Permian (Wolfcampian) Paleosol-Bearing Cycles of the U. S. Midcontinent: Evidence of Climatic Cyclicity: Journal of Sedimentary Research, v. A66, p. 71-84.

MOORE, R.C., 1931, Pennsylvanian cycles in the northern Mid-Continent region: Illinois Geological Survey Bulletin 60, p. 247-257.

MOORE, R.C., 1936, Stratigraphic classification of Pennsylvanian rocks of Kansas: Kansas Geological Survey Bulletin 22, 256 p.

MUDGE, M. R., and YOCHELSON, E. L., 1962, Stratigraphy and Paleontology of the uppermost Pennsylvanian and lowermost Permian rocks in Kansas. U. S. Geological Survey Professional Paper 323, 213 p.

OLSZEWSKI, T. D. and M. E. PATZKOWSKY, 2003, From Cyclothems to sequences: the record of eustacy and climate on an icehouse epeiric platform (Pennsylvanian-Permian, North American Midcontinent): Journal of Sedimentary Research, vol. 73, no. 1, p.15-30.

PARK, C.C., 1997, The Environment: Principles and Applications: Routledge, New York, 577 p.

PEEL, M.C., FINLAYSON, B.L., and MCMAHON, T.A., 2007, Updated world map of the Köppen-Geiger climate classification: Hydrology and Earth System Science, v. 11, p. 1633-1644.

PERLMUTTER, M.A., and DE AZAMBUJA FILHO, N.C., 2007, Cyclostratigraphy, in Koutsoukos, E.A.M., ed., Topics in Geobiology Volume 23: Applied Stratigraphy: Springer, Dordrecht, The Netherlands, p. 302-338.

PONNAMPERUMA, F.N., 1972, The chemistry of submerged soils, *in* Brady, N.C., ed., Advances in Agronomy, Volume 24:Academic Press, New York, p. 29-96.

POTTER, D. A., 1983, Effect of soil moisture on oviposition, water absorption, and survival of Southern Masked Chafer (Coleoptera: Scarabaeidae) eggs: Environmental Entomology, v. 12, p. 1223-1227.

POTTER, D.A., and GORDON, F.C., 1984, Susceptibility of *Cyclocephala immaculate* (Coleoptera: Scarabaeidae) eggs and immature to heat and drought in turfgrass: Environmental Entomology, v. 13, p. 794-799.

PRATHER, B.E., 1985, An Upper Pennsylvanian desert paleosol in the D-zone of the Lansing-

Kansas City Groups, Hitchcock County, Nebraska: Journal of Sedimentary Petrology, v. 55, p. 213-221.

PUCKETTE, G.R., D.R. BOARDMAN, II, and Z. AL-SHAIEB, 1995, Evidence for sea-level fluctuation and stratigraphic sequences in the Council Grove Group (Lower Permian) Hugoton Embayment, southern Mid continent, in Hyne, N.J., ed.: Tulsa Geological Society Special Publication no. 4, p. 269-290.

RANKEY, E. C., 1997, Relations between relative changes in sea level and climate shifts; Pennsylvanian-Permian mixed carbonate-siliciclastic strata, Western United States. GSA Bulletin 109:9, p. 1089-1100.

RANKEY, E.C., and FARR, M.R., 1997, Preserved pedogenic mineral magnetic signature, pedogenesis, and paleoclimate change: Pennsylvanian Roca Shale (Virgilian, Asselian), central Kansas, USA: Sedimentary Geology, v. 114, p. 11-32.

RASCOE, B. JR and ADLER, F.J. (1983) Permo-carboniferous hydrocarbon accumulations, Midcontinent, USA. Am. Assoc. Pet. Geol. Bull., 67, 979–1001.

RIIS, L., ESBJERG, P., and BELLOTTI A.C., 2005, Influence of Temperature and Soil Moisture on Some Population Growth Parameters of *Cyrtomenus bergi* (Hemiptera: Cynidae): Florida Entomologist, v. 88, p. 11-22.

REEVES, C.C., JR,. 1976, Caliche: Origin, Classification, Morphology and Uses. Lubbock, Texas: Estacado Books, Lubbock, Texas, 233 p.

RETALLACK, G.J., 1994, The environmental factor approach to the interpretation of paleosols, *in* R.Amundson, J. Harden and M. Singer, eds., Factors in soil formation - a fiftieth anniversary perspective. Special Publication of the Soil Science Society of America, Madison, 33, 31-64.

RETALLACK, G.J., 1999 Depth to pedogenic carbonate horizon as a paleoprecipitation indicator?: Comment: Geology, v. 28, p. 572.

RETALLACK, G.J., 2001, Soils of the Past, 2nd ed. New York, Blackwell Science. ISBN 0-632-05376-3

ROYER, D.L., 1999, Depth to pedogenic carbonate horizon as paleoprecipitation indicator?: Geology, v. 27, p. 1123-1126.

SCHULZE, H-P., 1985, Marine to Onshore Vertebrates in the Lower Permian of Kansas and their Paleoenvironmental Implications: University of Kansas Paleontological Contributions, Paper 113, p. 1-18.

SCOTESE, C.R., PALEOMAP Project, updated 2002, http://www.scotese.com/newpage5.htm. Checked April 2012.

SCHENK, P.E.,, 1967, Facies and phases of the Altamont Limestone and megacyclothem (Pennsylvanian), Iowa to Oklahoma: Geological Society of America, Bulletin, v. 78, p. 1369-1384.

SHELDON N.D., and TABOR, N.J., 2009, Quantitative paleoenvironmental and paleoclimatic reconstruction using paleosols: Earth-Science Reviews, v. 95, p. 1-52.

SMITH, J.J., and HASIOTIS, S.T., 2008, Traces and burrowing behaviors of the cicada nymph *Cicadetta calliope*: Neoichnology and paleoecological significance of extant soil-dwelling insects: PALAIOS, v. 23, p. 503–513.

SOREGHAN, G.S., 1994, The impact of glacioclimatic change on Pennsylvanian cyclostratigraphy, *in* Embry, A.E., Beauchamp, B., and Glass, D.J., eds., Pangea: Global Environments and Resources: Canadian Society of Petroleum Geologists Memoir 17, p.523–543.

SOREGHAN, G.S., 1997, Walther's law, climate change, and Upper Paleozoic cyclostratigraphy in the Ancestral Rocky Mountains: Journal of Sedimentary Research, v. 67, p. 1001–1004.

SOREGHAN, M.J., SOREGHAN, G.S. and HAMILTON, M.A., 2002, Paleowinds inferred from detrital-zircon geochronology of upper Paleozoic loessites, western equatorial Pangea: Geology, v. 30, p. 695–698.

SORENSON, R.P., 2005, A dynamic model for the Permian panhandle and Hugoton fields, western Anadarko basin: American Association of Petroleum Geologists Bulletin, v. 89, p. 921-938.

TOLK, J.A., 2003, Soils, Permanent Wilting Points, *in* Stewart, B.A., Howell, T.A., and Trimble, S.W., eds., Encyclopedia of Water Science: Marcel Deckker Inc., New York, p. 927-929.

TREWARTHA, G.T., 1982, The Earth's Problem Climates: University of Wisconsin Press, Madison, WI, 371 p.

VESPRASKAS, M.J., RICHARDSON, J.L., TANDARICH, J.P., and TEETS, S.J., 1999, Dynamics of hydric soil formation across the edge of a created deep marsh: Wetlands, v. 19, p. 78-89.

VESPRASKAS, M.J., 2004, Redoximorphic features for identifying aquic conditions: North Carolina Agricultural Research Service, Technical Bulletin 301, 33p.

VESSBY, K., 2001, Habitat and weather affect reproduction and size of the dung beetle *Aphodius fossor*: Ecological Entomology, v. 26, p. 430-435.

VILLANI, M.G., and WRIGHT, R.J., 1990, Environmental influences on soil macroarthropod behavior in agricultural systems: Annual Review of Entomology, v. 35, p. 249-269.

WANLESS, H.R., and SHEPARD, F.P., 1936, Sea level and climatic changes related to late Paleozoic cycles, Geological Society of America Bulletin, v. 47, p. 1177-1206.

WANLESS, H.R., and WELLER, J.M., 1932, Correlation and extent of Pennsylvanian cyclothems, Geological Society of America Bulletin v. 43, no. 4, p. 1009-1016.

WARD, D., 2009, The Biology of Deserts, Oxford University Press, New York, 304 p.

WEST, R. R., AND BUSCH, R. M., 1985, Sixth-order transgressive-regressive units in the Wewoka Formation (Anna Shale member) of Oklahoma, *in* Watney, W.L., Kaesler, R.L., and Newell, K.D., eds., Recent Interpretation of Late Paleozoic Cyclothems, Proceedings of the 3d Annual Meeting and Field Conference, Midcontinent Section: Society of Economic Paleontologists and Mineralogists, p. 155–170.

WEST, R.R., MILLER, K.B., and WATNEY, W.L., 2010, The Permian System in Kansas: Kansas Geological Survey Bulletin 257, 82 p.

WILLIS, E. R., and ROTH, L.M.,1962, Soil and moisture relations of *Scaptocoris divergins* Troeschner (Hemiptera: Cynidae): Annals of the Entomological Society of America, v. 55, p. 21–32.

YOULE, J.C., WATNEY, W.L., and LAMBERT, L.L., 1994, Stratal hierarchy and sequence stratigraphy--Middle Pennsylvanian, southwestern Kansas, U.S.A. *in* Klein, G.D., ed., Pangea: Paleoclimate, tectonics, and sedimentation during accretion, zenith, and breakup of a supercontinent: Geological Society of America Special Paper 288, p. 267-285.

CHAPTER THREE. PALEOECOLOGICAL AND PALEOBIOLOGICAL IMPLICATIONS OF *NAKTODEMASIS KRAUSI*: A NEW ICHNOSPECIES FROM THE LOWER PERMIAN OF KANSAS

ABSTRACT

Paleosols in core from the Lower Permian (Wolfcampian) Council Grove Group of western Kansas reveal an assemblage of meniscate backfilled burrows that have been left in open nomenclature. Burrows are similar, but not identical, to *Naktodemasis bowni* Smith et al. 2008, and hence are placed in the newly erected ichnospecies *Naktodemasis krausi* Counts and Hasiotis. *N. krausi* differs from other meniscate backfilled ichnogenera by its tightly spaced, slightly asymmetrical, texturally homogeneous, packeted menisci, and its lack of a constructed lining. *Naktodemasis krausi* is distinguished from *N. bowni* by differences in packeting of menisci—the alignment of the central axes of adjacent packets in *N. krausi* is uniform compared to *N. bowni*, in which the axes of the packets are offset at an angle to adjacent packets. The diameter of the packets in *N. krausi* is also more uniform compared to the packets of *N. bowni*, which can vary greatly over the length of the burrow. Traces are visible in paleosols due to differential redoximorphic coloration between burrows and host sediment, and were likely formed in a subaerial environment with seasonally fluctuating soil moisture and ground water table. *N. krausi* are found only in incipient and well-developed paleosols in continental deposits. We hypothesize that the Permian trace fossils are the result of the feeding and locomotion activities of insect larvae most similar to that of the Coleoptera, based on similarities to traces made by extant insects. This occurrence of *Naktodemasis* is the oldest documented occurrence of the ichnogenus, and roughly coincides with the earliest known Coleopteran body fossils. Given

the environmental tolerances of modern Coleopteran larvae, the presence of such traces indicates a narrow range of soil moisture conditions and the presence of adequate vegetation and organic matter.

Introduction

This paper documents an occurrence of adhesive meniscate burrows (AMB) in Lower Permian (Wolfcampian) deposits from the subsurface Anadarko basin of western Kansas. Distinctive trace fossil morphologies indicate that these burrows belong to a new ichnospecies, erected here as *Naktodemasis krausi*.

Meniscate burrows have been thought historically to be the work of sediment-ingesting organisms in subaqueous environments (e.g., Ekdale et al., 1984; Frey et al., 1984; Squires and Advocate, 1984; Bromley, 1996; Genise et al., 2004; Buatois and Mángano, 2004, 2007; Bromley et al., 2007). Recent and ongoing research, however, has shown that terrestrial organisms can also produce such burrow morphologies in subaerial environments (e.g., Smith et. al., 2008; Smith and Hasiotis, 2008; Counts and Hasiotis, 2009). The trace fossils described herein are hypothesized to have been produced subaerially in incipient to well-developed paleosols. The stratigraphic distribution, association with rhizoliths and other paleopedogenic features, and similar burrow morphology to extant burrows produced by modern terrestrial insect larvae provide evidence for this hypothesis.

AMB are widely distributed in continental deposits across North America in Triassic to present-day deposits (e.g., Bown and Kraus, 1983; Hasiotis and Dubiel, 1994; Hasiotis, 2002; Jacobs and Mason 2004; Hembree and Hasiotis 2008; Smith et al., 2008). The ichnospecies

Naktodemasis bowni (Smith et al., 2008) was erected to provide an ichnotaxonomic framework for these burrows. Recently, AMB have been identified in Lower Permian continental strata (Counts and Hasiotis, 2009; Dubois et al., 2012). These Lower Permian burrows described here should be included within the ichnogenus *Naktodemasis,* but are a separate and distinct ichnospecies, and represent the earliest known occurrence of this ichnotaxon.

Background

The Lower Permian Council Grove Group consists of numerous alternating marine and continental deposits, or cyclothems. Stratigraphic units within the Council Grove Group are traceable across Kansas, outcropping near Manhattan and shallowly dipping to 640–960 m (~2,000–3,000 ft) below the surface near the border between Kansas and Colorado (Fig. 2). Trace fossils described in this study occur in the Easly Creek, Blue Rapids, and Speiser shales in the uppermost Council Grove Group (Fig. 2). Similar trace fossils are found in the Hooser Shale within the Council Grove Group and in the overlying Chase Group.

The cores in which AMB are found were taken from the northern Hugoton extension of the Anadarko Basin, a complex asymmetric foreland basin formed during the Pennsylvanian Ouachita-Marathon orogeny and associated formation of the supercontinent Pangaea (Johnson, 1989; Dubois et al., 2012). The Hugoton embayment is a northern extension of the Anadarko Basin, consisting of a shallow, south-dipping ramp bounded on the north, west, and east by structural highs. Current structural dip is much greater than the original dip at the time of deposition. Deposits within the basin are part of the Hugoton-Panoma gas field, the largest gas field in North America (Dubois et al., 2007). By Permian time, the basin had been filled with over 6,000 m (18,000 ft) of sediment, though subsidence and deposition of both marine and continental deposits continued throughout the Permian (Johnson, 1989). Mesozoic and later deposits are largely eroded from the basin.

Permian deposits in the basin are characterized by alternating marine and continental deposits that change facies and thicken basinward, recording eustatic sea-level changes likely related to Milankovitch cycles. Iron-stained continental siltstones and fine-grained sandstones (i.e., redbeds) are major components of these cyclic sediments and have been hypothesized as paleosols (e.g., Boardman and Nestell, 2000).

Trace fossils described here were found in core taken from the northern part of the Hugoton embayment (Fig. 1). Although only five cores are discussed in this study, the presence of identical traces in each one indicates that these trace fossils occur over a broad spatial area. Formations in which these trace fossils are found are laterally continuous across Kansas and may be correlated over across hundreds of kilometers (Hattin, 1957; Puckette et al., 1995; West et al., 2012).

The five cores examined were selected to form a roughly northwest–southeast transect perpendicular to the strike of the paleoshelf (Fig. 1)—each successive core southward is deeper in the basin than the previous. Predictably, basinward cores contain a higher proportion of marine deposits than those to the northwest, and consequently, cores to the northwest are dominated by continental redbeds (Dubois et al., 2003).

Methodology

The five cores studied (Cross H Cattle; API 15-075-20543, May Beaty E2; API 15-093-20134, D. Alexander 2; API 15-067-20338, Stuart 3-34; API 15-067-21415, and Prater Gas Unit

A-2; API 15-175-20250) are housed at the Kansas Geological Survey in Lawrence, Kansas. The slabbed face of the cores used in this study is approximately 9.5 cm in diameter.

Cores were slabbed vertically and relevant formations identified. Cut faces of the slabbed cores were examined for trace fossils, and trace fossil density was estimated and recorded every 15 cm using Folk's (1951) visual estimation chart for the percentage of space occupied by AMB. Trace fossil depth and orientation was noted, and trace fossils were described in detail, measured with calipers (Appendix 2 and 3), and digitally photographed or scanned on a flatbed scanner. Other indicators of soil formation (e.g., rhizoliths, redoximorphic coloration patterns, and presence of carbonate nodules) were also measured, but will be reported in a separate paper. Some intervals were compared to the ichnofabric indices developed by Droser and Bottjer (1986) to assess the degree of sedimentary bed disruption.

Several sections containing the best-preserved trace fossils were selected for thin-section analysis. Large-format thin sections (5 x 7.6 cm; 2" x 3") were made from the thicker portion of the core in order to preserve one set of cut faces for later viewing, and were impregnated with blue epoxy to increase the visibility of porosity within the strata. Photomicrographs and laser scans were taken of the thin sections.

Trace Fossils

Distribution

AMB are found only in continental clastic deposits composed of fine- to very fine-grained sandstones and siltstones with a substantial clay component. Trace fossils rarely crosscut into subjacent limestone. Trace fossils are visible on core faces as transverse, oblique, and longitudinal cross-sections. Terrigenous sediments are often iron-stained and highly oxidized with occasional, discrete zones of gleying (i.e., grey or green zones of reduced iron). Certain intervals also contain numerous pedogenic features, such as rhizoliths, cutans, peds, and caliche nodules (Fig. 20). Distinct pedogenic horizons uncommon, which suggests that most soil formation was incipient to cumulic in nature.

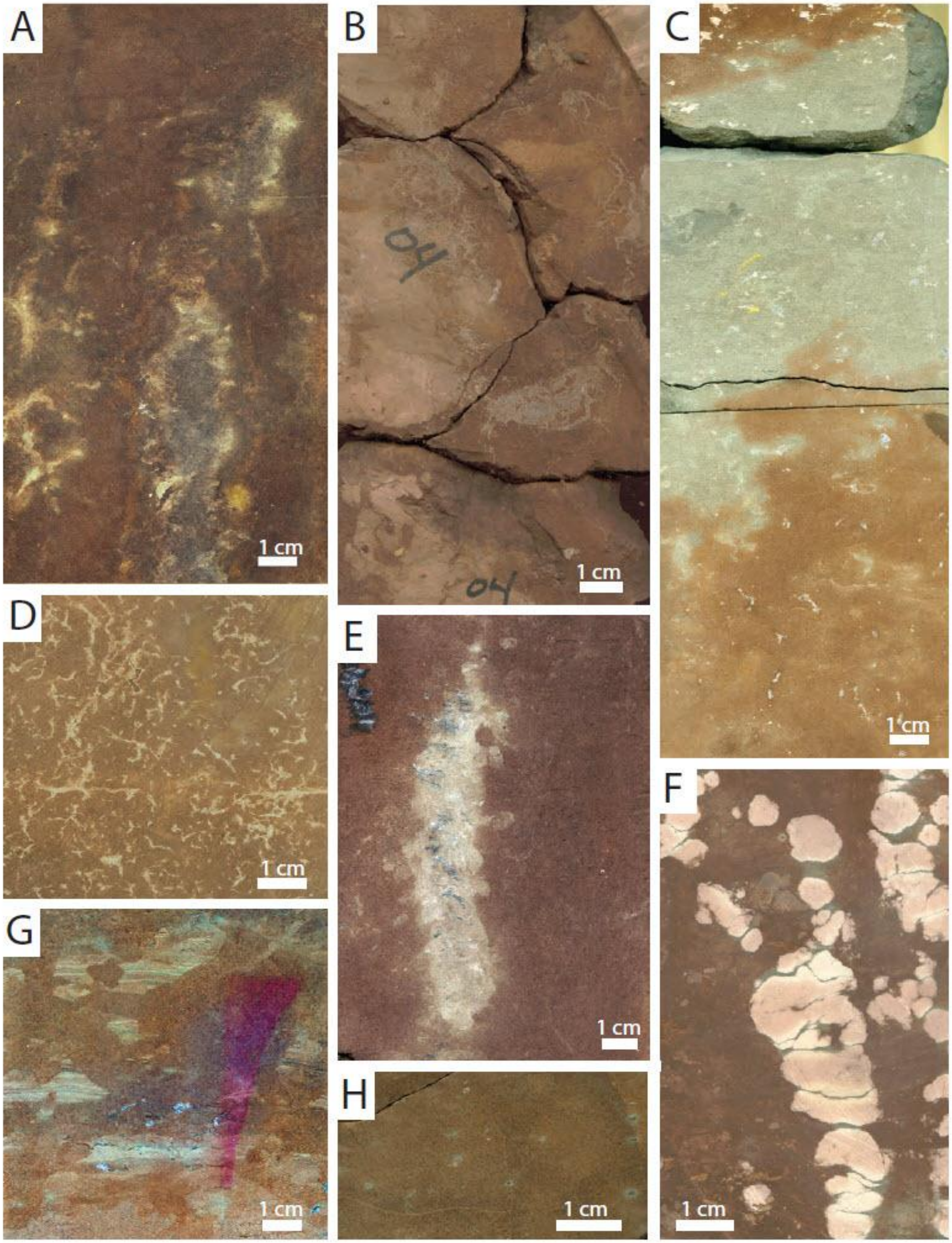
A
1 cm
B
04
04
1 cm
C
1 cm
D
1 cm
E
1 cm
F
1 cm
G
1 cm
H
1 cm

Figure 20. Indicators of soil formation and soil development seen in core. A) Rhizoliths with gleyed haloes and purple interiors. Cross H Cattle core, 787 m (2582’). B) Breakage of core along clay-rich cutans, outlining soil structure (peds). Prater core, 946 m (3104’). C) Discrete zone of gleying, indicating water saturation, within surrounding oxidized sediment. Cross H Cattle core, 824 m (2704’). D) Oxidized paleosol with fine, dense rhizoliths throughout interval. May Beaty E 2 core, 829 m (2723’). E) Gleyed rhizohalo with visible burrows. Cross H Cattle core, 791 m (2596’). F) Accumulations of caliche (soil carbonate) nodules, a definitive indicator of subaerial exposure. Stuart 3-34 core, 909 m (2982’). G) Discrete remnants of original horizontal laminations disrupted by later burrowing. Stuart 3-34 core, 859 m (2820’). H) Millimeter-scale rhizoliths with dark organic cores and gleyed halos. D Alexander core, 905 m (2970’)

Discrete trace fossils are often visible only within and around the margins of gleyed zones, which typically surround rhizoliths or form mottled grey-green intervals. Much of the core intervals are homogeneous red siltstone. In the majority of these homogeneous intervals, closer inspection of the core and thin sections reveals a very faint red on red mottling, indicative of thorough bioturbation by AMB (ichnofabric index of 5–6). In other in intervals of core, subtle gleying accentuates outlines of AMB in otherwise uniformly colored sediment (e.g., Fig. 20E).

Trace Fossil Morphology

AMB are multidirectional, unbranched, unlined, cylindrical burrows filled with a series of variably sized, packeted, crescent-shaped backfill. The alignment of the central axes of adjacent packets in is uniform. The diameter of the packets is also uniform and varies little over the length of the burrow.

Orientation—Trace fossils are oriented in all directions, ranging from vertical to horizontal. The vast majority of observed burrows, however, are horizontal to subhorizontal (Figure 21).

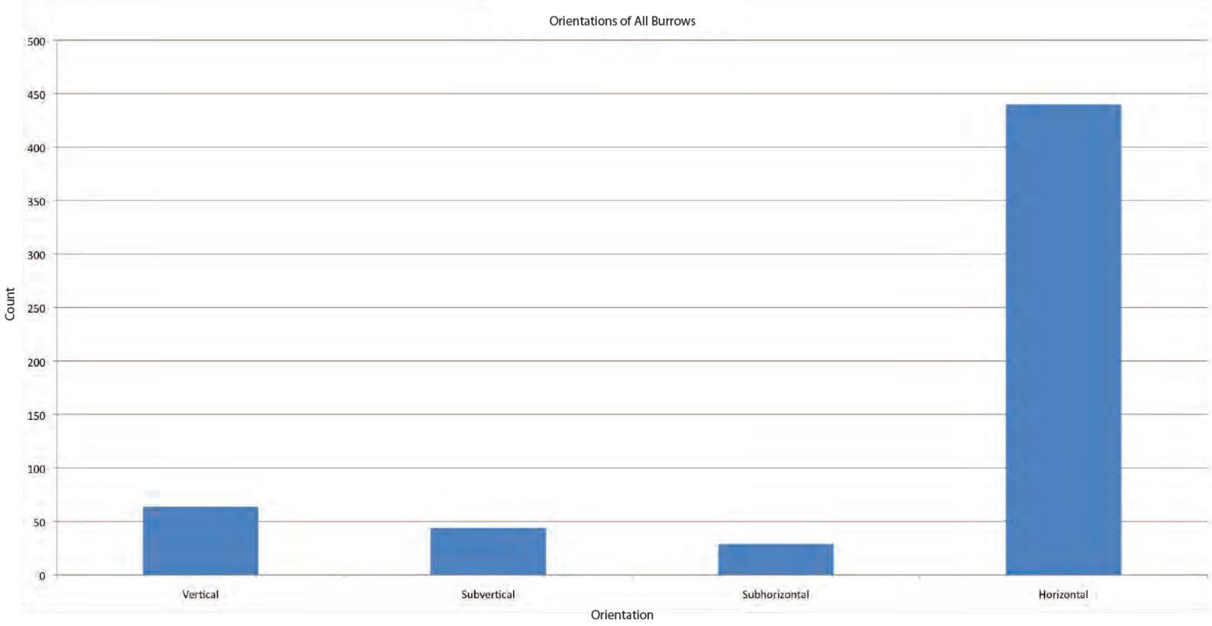

Figure 21. Orientations of all burrows. The vast majority of burrows were viewed as transverse sections and therefore classified as horizontal

Shape—Burrows are circular to elliptical in cross section. The burrows themselves are cylindrical to elliptically cylindrical in three dimensions, based on views of single burrows intersecting the slabbed core face and core tops. Burrows do not branch and often crosscut one another to produce pseudobranching, which is uncommon. Burrow axes are often highly sinuous in three dimensions, preventing most individual burrows from being traced over significant distances due to the two-dimensional nature of core. Occasionally, burrows will intersect the core face and contain relatively straight sections up to several centimeters. Change in burrow direction can appear as both curvilinear and rectilinear, which is likely an artifact of the cut face.

Size—Burrow diameters range from 0.085 to 1.06 cm (Figure 22). Burrow size is remarkably consistent across both core and formation (Figures 23–24), and across all burrow orientations (Figures 25–26). Mean burrow diameter of all burrows studied was 0.41 cm. Length of burrows is more difficult to quantify as individual burrows cannot be traced over significant distances. The longest burrow measured was 12.5 cm, which is likely much shorter than the true length of many burrows.

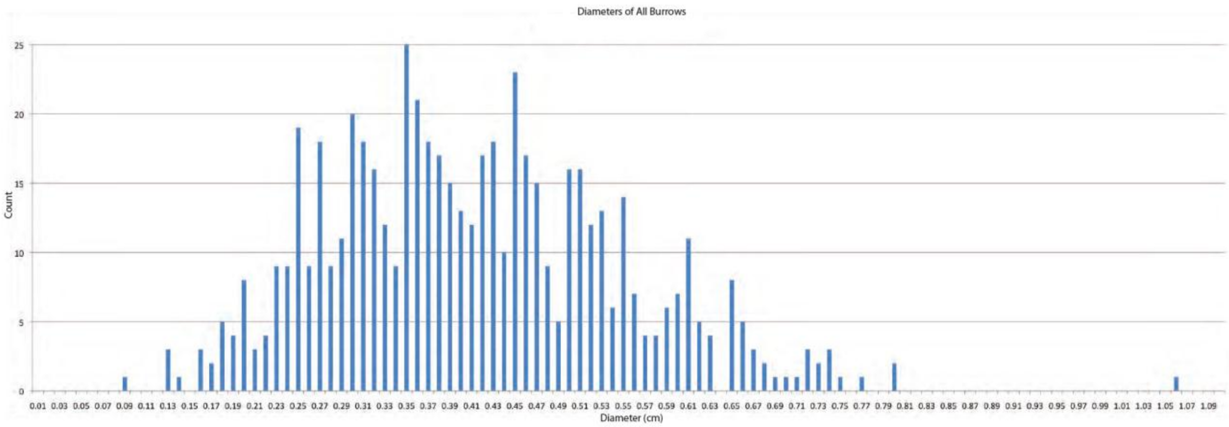

Figure 22. Measured diameter of 591 burrows on core slab faces. Diameter of each discrete burrow was measured using calipers to the nearest 1/100 cm

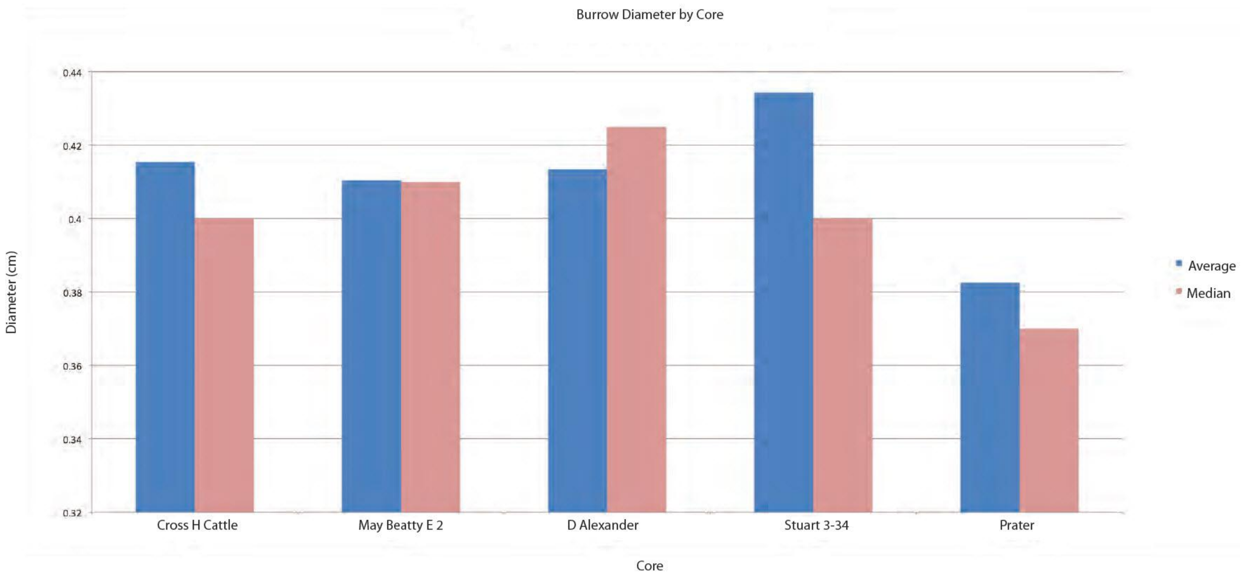

Figure 23. Comparison of average and median burrow diameters by core. Both average and median values vary by less than 0.06 cm over the entire transect, which covers approximately 50 miles.

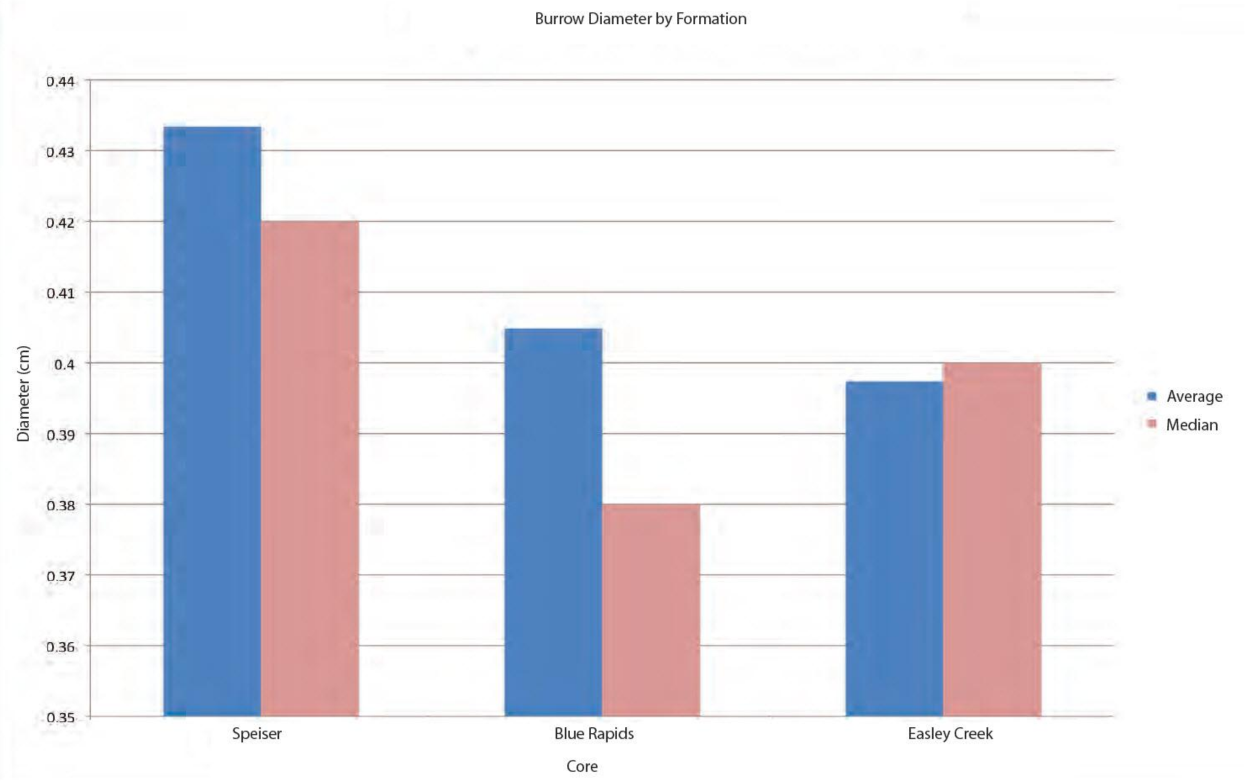

Figure 24. Comparison of average and median burrow diameters by formation. Both average and median values vary by less than 0.04 cm over the entire stratigraphic range studied.

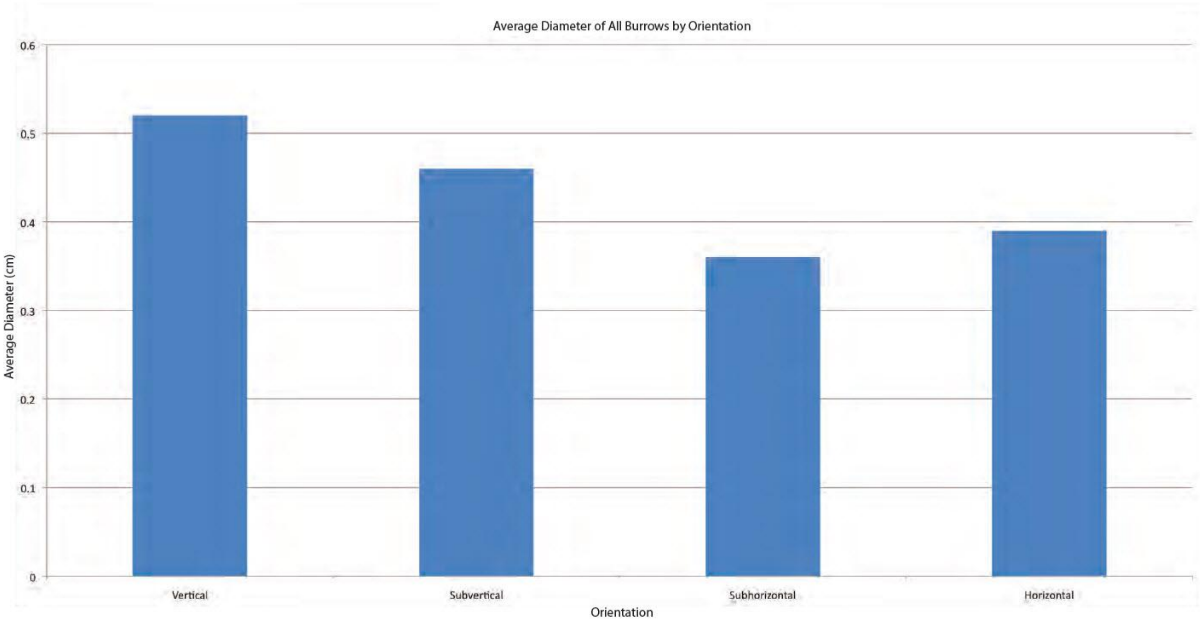

Figure 25. Comparison of average burrow diameter by orientation. Vertical and subvertical burrows were generally larger by approximately 0.1 cm

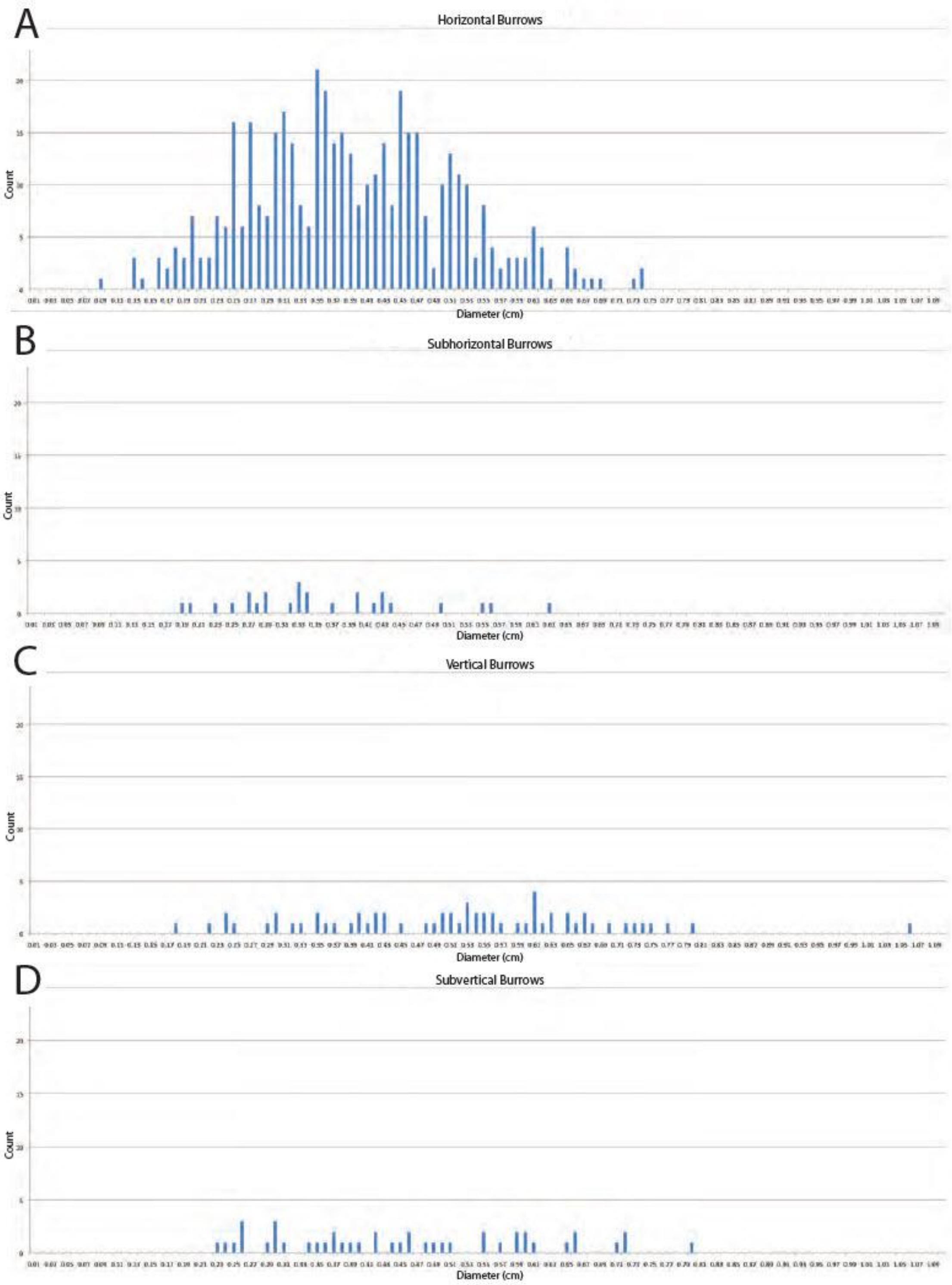

Figure 26. Distribution of burrow diameters by orientation. Burrow diameters of all orientations fall within the same approximate range

Fill—Trace fossils, where visible in longitudinal cross section, show either homogeneous or meniscate fill. The fill of many burrows consists of a series of alternating dark- and light-colored, crescent-shaped (menisci) sediment packages, which are mm-scale in thickness. Menisci are often contained within a series of larger packets, with a single packet containing several smaller, individual menisci. Packets are visible but usually not offset from the adjacent packet—the alignment of the central axes of adjacent packets is uniform (Fig. 27–28). Neither meniscate-filled nor homogeneous burrow fills show evidence of a predominant grain orientation in thin section (Fig. 29). Color of the fill was likely determined by local redoximorphic conditions within the microenvironment associated with the burrow, as well as varying quantities of organic matter within the burrow fill and between individual menisci.

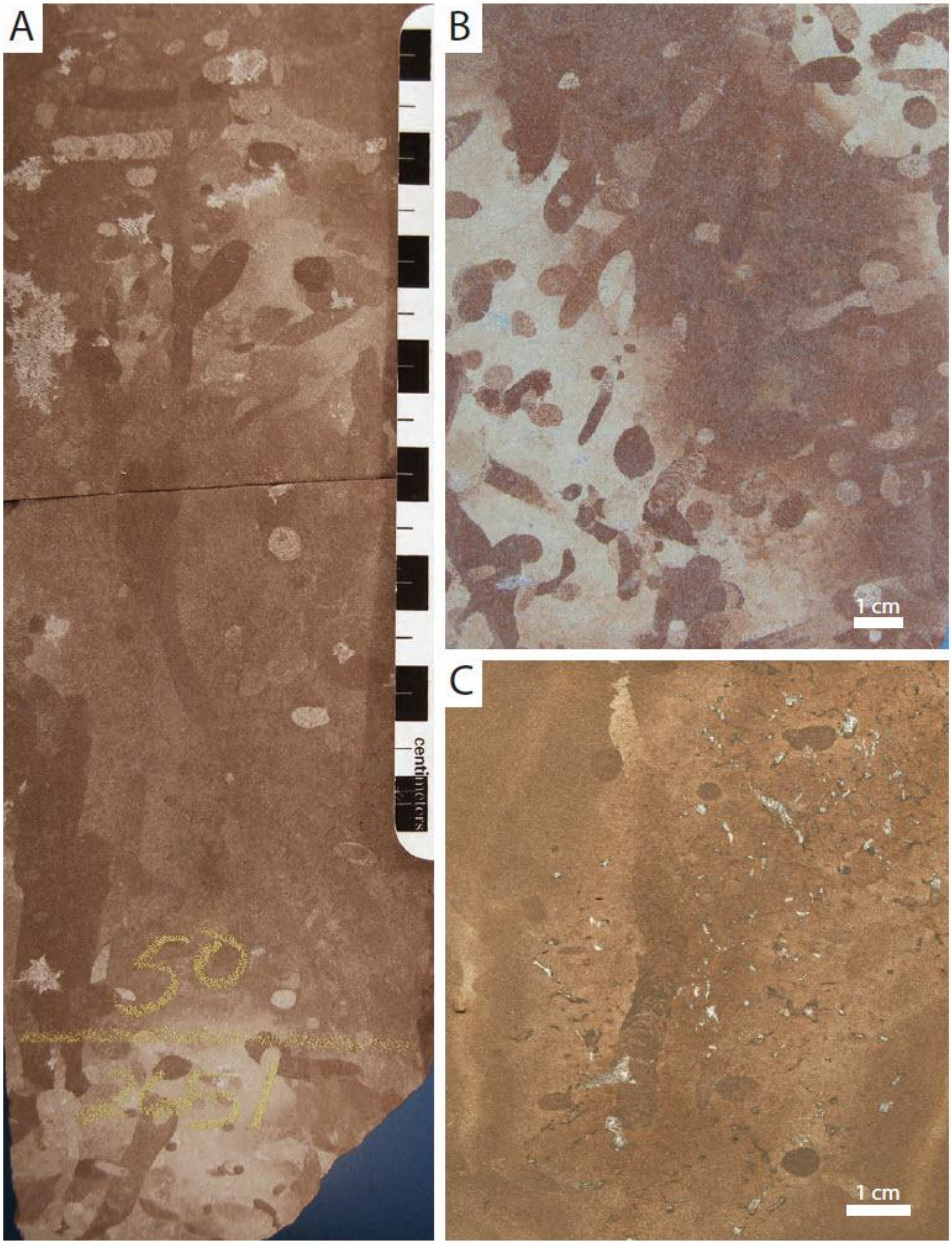
A
centimeters
50
2651
B
1 cm
C
1 cm

Figure 27. Wider views of burrows in Cross H Cattle core. A-B) High densities of visible burrows in mottled very fine-grained sandstone 808 m (2650-2651’). B) Discrete burrows visible within rooting zone. 828 m (2716’)

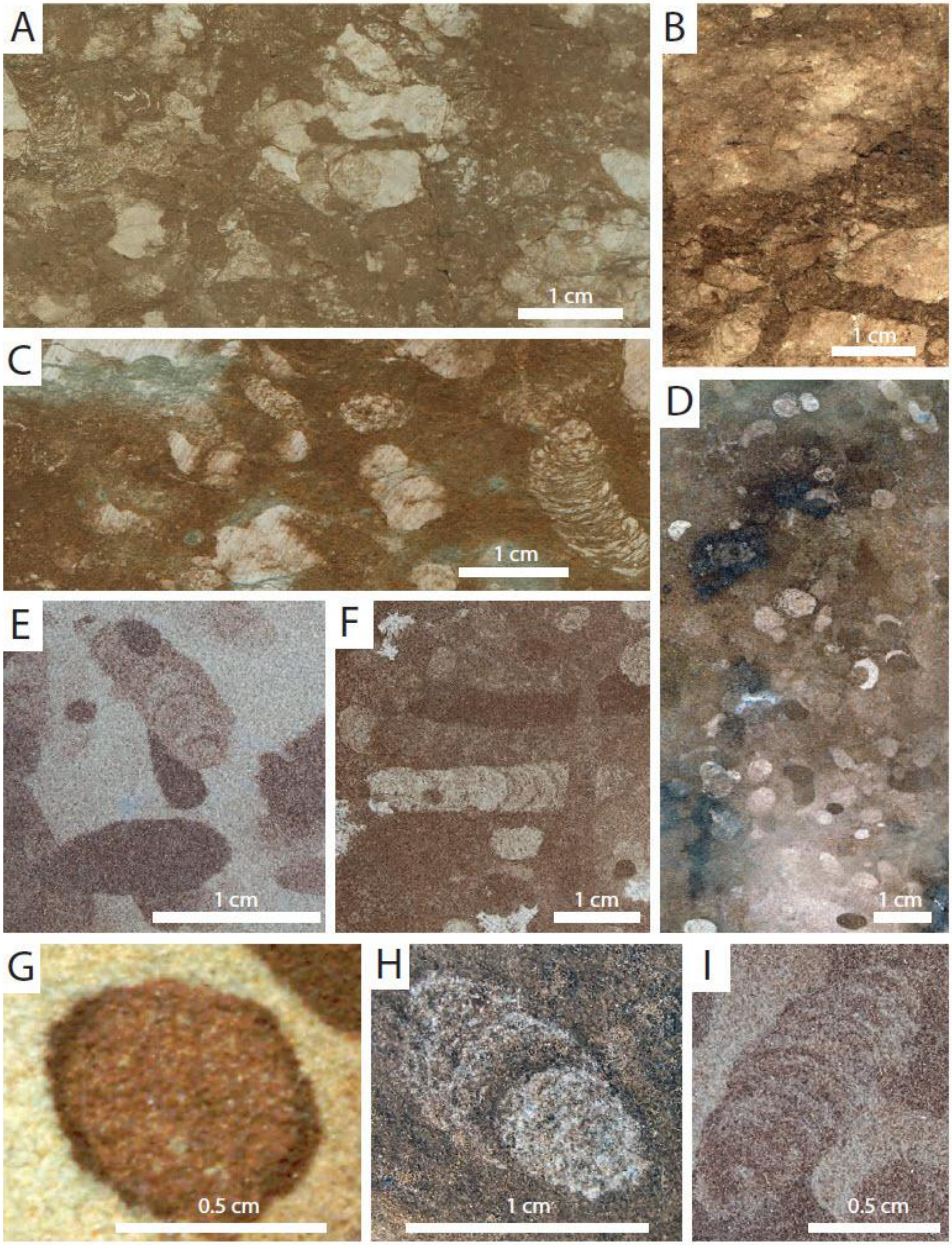
A
1 cm
B
1 cm
C
1 cm
D
1 cm
E
1 cm
F
1 cm
G
0.5 cm
H
1 cm
I
0.5 cm

Figure 28. Burrow close-ups. A-B) Burrows cutting carbonate nodules, indicating early formation of soil carbonate. Prater core, 903 m (2963’). C) Burrows containing carbonate within burrow fill. Note differential amounts of carbonate between individual menisci. May Beaty E 2 core, 831 m (2727’). D) Contrast-enhanced view of densely burrowed interval showing predominately horizontal orientation of burrows. Cross H Cattle core, 831 m (2728’). E-F) Close up of individual burrow showing crosscutting of burrows and packeting of menisci. Cross H Cattle core, 808 m (2650-51’). G) Cross-section of vertical burrow showing asymmetric nature of menisci. Cross H Cattle core 808 M (2650’). H-I) Individual burrows showing nature of menisci and differing patterns of redoximorphic coloration between menisci. Cross H Cattle core 808 m (2652’)

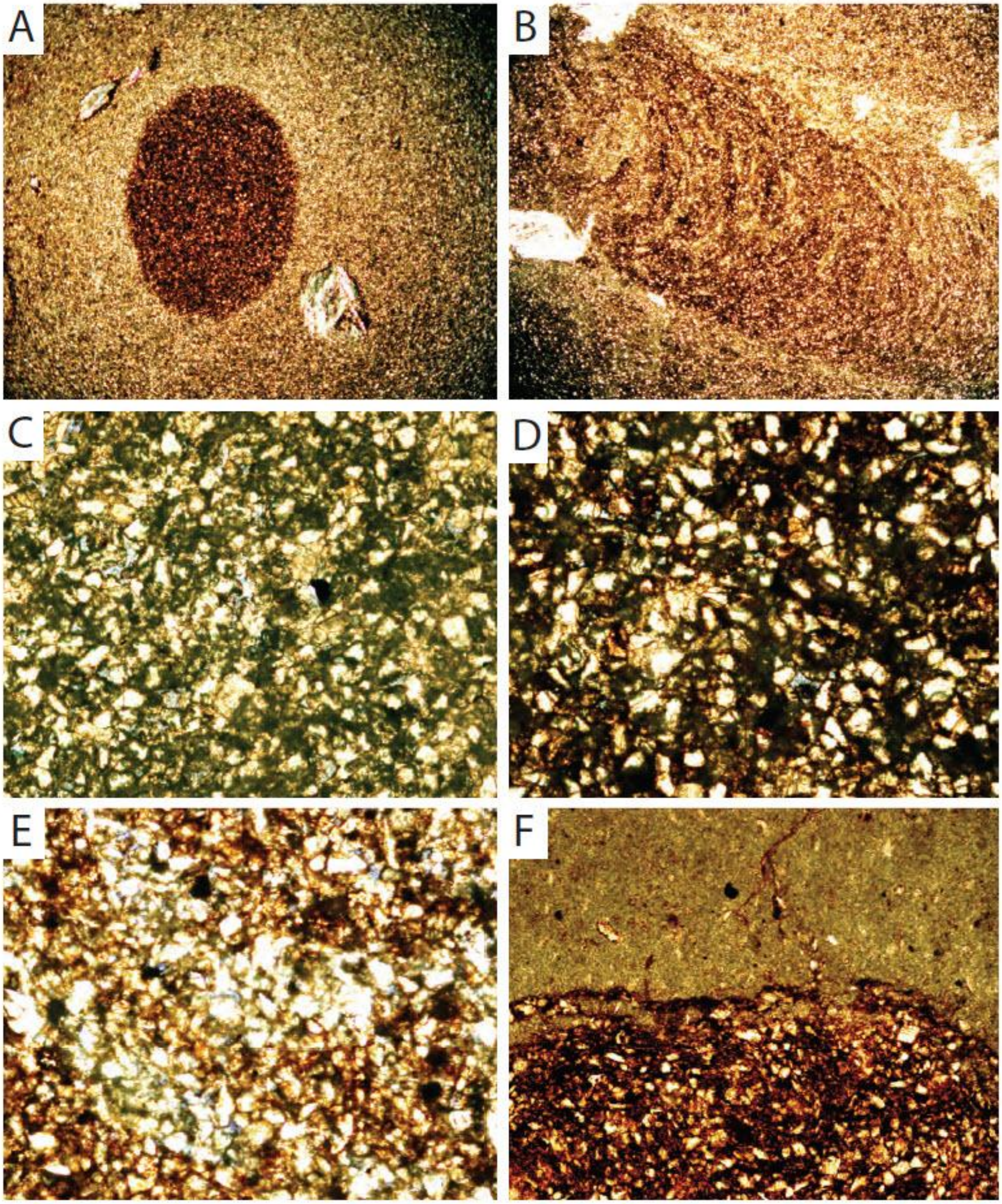

Figure 29. Thin sections of burrows. A) Transverse view of oxidized burrow, Cross H Cattle core, 1X, 827 m (2716’). B) Oblique view of meniscate-filled burrow, Cross H Cattle core, 1x, 792 m (2600’) C) Matrix sediment outside burrow fill, 10X, Cross H Cattle 808 m (2651.5’). D)

Interior of burrow fill, 10x, Cross H Cattle 808 m (2651.5’). E) Close up of menisci within burrow fill, 10X. F) Burrow margin adjacent to caliche nodule, 10X, Prater 947 m (3108’)

Linings—Burrows are mostly unlined. Rarely, a circular burrow cross-section will appear to have a thin veneer of darker or lighter sediment less than 1 mm thick surrounding an inner core. This is simply the result of the cut face of the core intersecting multiple menisci or packets of menisci. Close examination of thin sections and hand specimens reveals no evidence of either a mantle, a deliberately constructed burrow wall or a lining of any type.

Morphologic variability

Variations occur in size, orientation, presence or absence of menisci, and amount of menisci packeting in the burrows. Much of the variation between burrows is in the preservation. The majority of burrows, for instance, do not show visible meniscate backfill. Most burrows are only visible as transverse sections and, thus, backfill would most likely not be visible even if present. In addition, a lack of differing redoximorphic coloration between menisci may cause burrow fills to appear homogeneous, which explains the lack of menisci in some transversely cut burrows.

Comparison with other ichnotaxa

The distinguishing characteristics of most taxonomically valid meniscate trace fossils are summarized in Table 3. The Permian burrows described here are obviously distinct from many previously described ichnotaxa, and more subtly distinct from others.

Burrow or Ichnotaxon	Illustration	Diagnosis
Masked Chafer larvae burrows (modern)	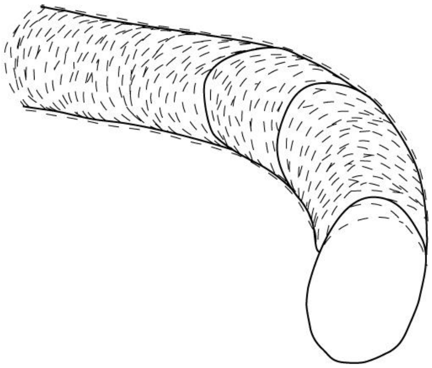	Cylindrical, straight to highly tortuous, variably oriented unbranched burrows with meniscate backfill and thin, discontinuous linings. Backfill sometimes contained within larger packets, but packeted backfill are often separated by long segments of continuous, unpacketed menisci. Menisci are not always symmetrical about the central axis of the burrow. Packets of menisci are slightly offset from adjacent packets, though not to the extent of *N. bowni*.
Cicada nymph burrows (modern)	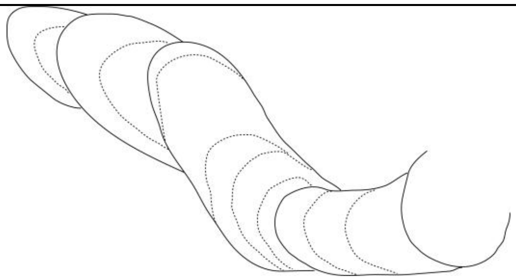	Similar diagnostic criteria to *N. bowni*; burrows composed of a nested series of distinct, ellipsoid-shaped, asymmetrical packets which contain menisci of varying curvature. Burrow margins have a tapered and widened appearance where cicadas rotate and change directions within their burrow (Smith et al., 2008).
Adult dung beetle (*Typhaeus typhoeus*) burrows (Holocene and modern)	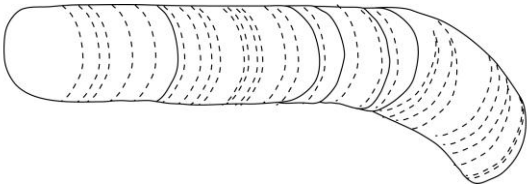	Mostly straight, vertical to horizontal burrows with diameter of roughly 14 mm, a series of menisci which are mostly symmetrical about the central burrow axis (Brussaard and Runia, 1984).

Ancorichnus ancorichnus Heinburg 1974	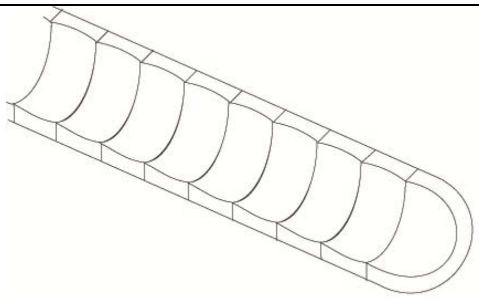	Cylindrical, weakly sinuous subhorizontal to horizontal burrow containing a central meniscate fill and a visibly structured mantle (Frey et al., 1984).
Laminites kaitiensis Ghent and Henderson, 1966	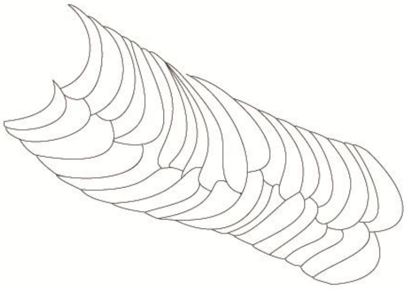	Unlined, unbranched, gently meandering burrows composed of thin, 1.5–3 mm thick, texturally homogeneous backfills successively light and dark in color. Backfills concave, biconcave (bow-shaped), or comma-shaped with the thicker part touching or overlapping along the medial axis of the burrow.
Naktodemasis bowni Smith et al., 2008	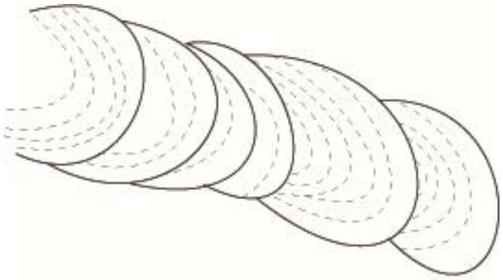	Sinuous, variably oriented, unbranched, unlined burrows composed of a nested series of distinct, ellipsoid-shaped, asymmetrical packets. Packets asymmetrically oriented around the burrow axis and offset from one another. Packets contain thin, indistinct, and tightly spaced meniscate fill. Menisci are subparallel to the bounding packet, unpelleted and texturally homogeneous with each other, discontinuous, and difficult to trace. Short burrow sections may be composed only of unbound menisci. Burrow wall is mostly smooth or with slight annulae and correspond with ellipsoidal packets.

Scoyenia gracilis White 1929	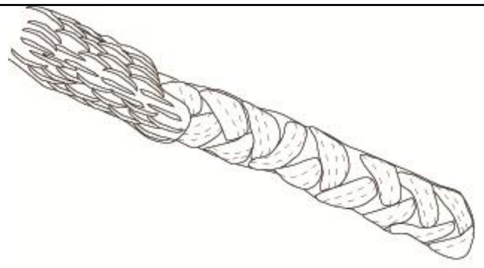	Straight to curved, unbranched, horizontal to variably oriented burrows with chevron-shaped to arcuate backfill of homogeneous or heterogeneous lithologies Burrows may be unlined or with thin clay linings and burrow surfaces are ornamented with convex, mostly parallel, short longitudinal striae (Frey et al., 1984).
Beaconites barretti Bradshaw, 1981	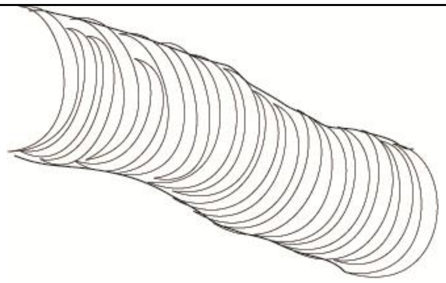	Straight to variably meandering, unbranched, unwalled, meniscate backfilled burrow. Menisci are commonly hemispherical or deeply arcuate, tightly packed or stacked, forming noncompartmentalized backfill or thin meniscate segments.
Taenidium cameronensis (Brady, 1947)	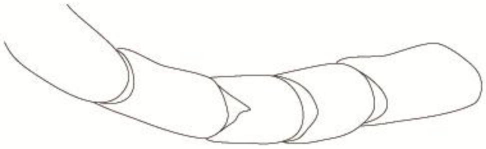	Unwalled meniscate burrows, secondary successive branching and intersection may be present. Meniscate packets usually longer than wide, with the deeply concave meniscate interfaces resulting in a nested appearance (D'Alessandro and Bromley, 1987).
Taenidium satanassi D'Alessandro and Bromley, 1987		Weakly arcuate menisci in sinuous to nearly straight burrows, the fill consisting of meniscate backfill, each containing two types of sediment of more or less equal thickness; backfill considerably shorter than wide. Darker parts of each backfill segment are

		composed of fecal pellets.
Taenidium serpentinum Heer, 1877	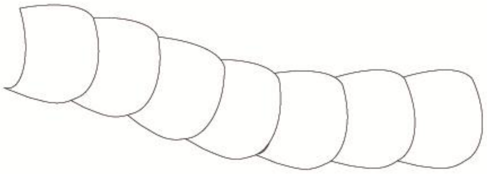	Well-spaced menisci about equal to or slightly less than burrow width. External molds may show slight annulation corresponding to menisci, or fine transverse wrinkling. Secondary successive branching and intersections occur. Boundary sharp and lacks lining (Keighley and Pickerill, 1994).

Table 3: Diagnostic criteria of meniscate backfilled burrows. Illustrations modified from Smith et al. (2008) and Smith and Hasiotis (2008)

Ancorichnus Heinburg, 1974, is a horizontal to subhorizontal meniscate burrow that contains a mantle—a zone along the exterior boundary of the burrow that is disturbed but distinct from the burrow core and produced passively as a function of the burrowing mechanism. Permian AMBs occur in all orientations and none of them are mantled, indicating a fundamental difference in the way that they were created.

Scoyenia White, 1929, is characterized by tightly spaced, longitudinal striations with 360^{o} coverage of the burrow surface; internally the burrow fill is composed of tightly packed, chevron-shaped backfill. Although Permian AMBs are not preserved in three-dimensional relief, burrow cross sections show no evidence of clay linings nor striations. Permian AMB also have crescent-shaped rather than chevron-shaped backfill, reflecting a substantially different body shape and behavior of the tracemaker.

The description of *Laminites* Ghent and Henderson, 1966, an uncommon backfilled trace, also does not adequately characterize Permian AMB. Backfill in *Laminites* are not continuous across the diameter of the burrow, and backfill thickness relative to burrow diameter is much greater in *Laminites* than in Permian AMBs.

Taenidium Heer, 1877, is reserved for meniscate burrows that are unlined. *Taenidium* is more similar to the Permian AMBs than any of the other backfilled burrows described here, but it, too, fails to adequately categorize the Permian AMBs. All ichnospecies of *Taenidium* are inconsistent with Permian AMBs on the basis of internal morphology, menisci composition, and pattern of menisci construction. The fill of *T. satanassi* is composed of relatively thick menisci whose sediment is internally graded. The backfill of *T. cameronensis* and *T. serpentinum* are much thicker relative to the size of the burrow—a lower length-to-width ratio, where length is measured perpendicular to the long axis of the burrow—than observed in the menisci of AMB. None of the *Taenidium* ichnospecies are equivalent to the Permian AMBs.

The differences between *Beaconites* and *Taenidium* are still the subject of some degree of ichnotaxonomic confusion, although the morphologic features that distinguish both burrow morphologies is distinct (Smith et al., 2008). *Beaconites antarcticus*, *B. capronus*, and *B. coronus* have been inconsistently described by various authors as being unlined, lined, or walled. Keighley and Pickerill (1994) attempted to resolve the taxonomic confusion by firmly defining *Beaconites* as a smoothly walled ichnotaxa. *Beaconites barretti* was described and included in the genus by Bradshaw (1981), but the lining of Bradshaw's specimens was formed solely by the merging of menisci near the burrow margin. For this reason, Keighley and Pickerill moved *Beaconites barretti* Bradshaw, 1981, to *Taenidium barretti* (Bradshaw, 1981). This taxonomic change has not been fully accepted, however—*Beaconites barretti* is still in use by some workers (e.g., Buatois and Mangano, 2004; Morrissey and Braddy, 2004; Morrissey et al., 2004; Smith et al., 2008). Adding to the confusion, *Taenidium barretti* is also used in recent studies (e.g., Melchor et al. 2002; Kim et al., 2005; Minter et al., 2007; Melchor et al., 2006). Other ichnospecies of *Beaconites* (e.g., *B. antarcticus*, *B. capronus,* and *B. coronus*) remain within the genus because they are lined and, thus, are still considered valid by Keighley and Pickerill. *Beaconites,* as currently defined, is therefore inconsistent with Permian AMB. Regardless of the taxonomic problems, the diagnosis of *Taenidium barretti* as emended by Keighley and Pickerill (1994) or of *Beaconites barretti* as originally stated by Bradshaw (1981, see Table 1) excludes the Permian AMB described here. Although many aspects of Permian burrows are similar to *Beaconites* or *Taenidium barretti*, (e.g., both lack a lining, and menisci are generally arcuate and tightly stacked) the overall pattern of meniscate backfilling in Permian AMBs differ substantially. Backfill in *Taenidium* or *Beaconites* are "non-compartmentalized" or are ambiguously described as "thin meniscate segments" (Keighley and Pickerill, 1994), as opposed to the packeted bundles of menisci in AMBs.

The distinct morphology of the Permian AMBs, therefore, represents a significant difference in the behavior of the tracemaker compared to those behaviors that produced *Ancorichnus, Beaconites, Laminites,* and *Taenidium*. Permian AMBs share most similar morphological features with the recently erected ichnogenus *Naktodemasis* Smith et al. 2008. Slight differences between Permian AMBs and the type species of *Naktodemasis* (*N. bowni*) are considered to be species-level ichnotaxobases and hence, Permian AMBs are placed in the newly erected ichnotaxon *Naktodemasis krausi*.

Discussion

Recent neoichnological studies have investigated both the burrowing mechanisms and the tracemakers responsible for the formation of meniscate burrows in subaerially exposed sediments (e.g., Smith and Hasiotis, 2008; Counts and Hasiotis, 2009). Backfilled burrows produced by extant insect larvae (masked chafer beetles) and insect nymphs (cicadas) show remarkable similarities to AMBs found in paleosols formed in continental deposits since the Triassic. Studies with extant organisms suggest that AMB tracemakers likely had similar burrowing methods to these modern insect larvae and nymphs, with specialized body plans adapted for digging and a subterranean lifestyle. The differences in burrow morphology that distinguish the various ichnospecies of backfilled burrows (i.e., packeted vs. unpacketed menisci) can, therefore, be highly significant in reconstructing the behaviors and morphology of ancient organisms from trace fossils. The Permian AMBs described here are very similar morphologically to the modern traces produced by scarabaeid larvae described by Counts and Hasiotis (2009), although taphonomic and diagenetic overprinting of fossil burrows prevents an exact comparison. Both scarabaeid burrows and AMBs, however, are unlined, unbranched, and variably oriented sinuous burrow systems that contain thin, arcuate menisci in packets that are only slightly offset from adjacent packets. If the modern scarabaeid burrows were to pass through the taphonomic and diagenetic window, they would likely appear identical to the Permian burrows described herein. The Permian AMBs, therefore, were likely made by an organism with similar anatomy and burrowing mechanism to scarabaeid larvae.

Modern holometabolous insects, including scarabaeids, go through complete metamorphosis in their life cycle, beginning with eggs and followed by larval, pupal, and adult stages. Although soil-dwelling beetles have a variable life span, many species go through a one-year life cycle. Eggs are laid underground by adults in late summer, which quickly hatch into C-shaped grubs (larvae) that remain underground until they form an ellipsoidal cell, pupate, and then escape to the surface as adult beetles. The vast majority of their life cycle is thus spent in the subsurface vadose zone as rhizophagous or detritiphagous larvae. The Permian AMB assemblages described here are consistent with this type of burrow system—they are found in association with rhizoliths, often to the point where all that remains of the former root trace is a gleyed halo and a mass of burrows. Permian AMBs also have very high length to width ratios. By extrapolating burrow lengths found in the experimental work of Counts and Hasiotis (2009), individual burrows can be inferred to have reached lengths of tens of meters over the course of a single larvae's lifetime. Bioturbation in the Council Grove Group was thus a function of a permanently established population rather than a temporary colonization of exposed sediments. Although no body fossils are found in association with these deposits, the earliest beetles are found in the Late Pennsylvanian of Illinois (Bethoux, 2009), and are also known from the Early Permian of Europe (Kuklova-Peck and Willman, 1990). Beetles, or insects with a similar holometabolous life cycle, may thus have been well-established in the midcontinent of North America by Council Grove time.

The conclusions reached by Smith and Hasiotis (2008) and Counts and Hasiotis (2009) dispel the idea purported by some authors that meniscate burrows are produced only in subaqueous environments, and their presence in paleosols is the result of overprinting from subsequent inundation (e.g., Buatois and Magano, 2002; 2004; 2007; Genise 2004; Genise et al., 2004; Bromley et al., 2007). In the occurrences of Permian AMBs described herein, the burrows are found only in pedogenically modified, iron-stained, muddy siltstone, very fine-grained sandstone, and fine-grained sandstone, all of which are found in close association with rhizoliths and rhizohalos. The formations in the Council Grove Group containing these burrows have been previously interpreted as pedogenically modified eolian deposits (e.g., Dubois et al., 2012), an interpretation that is also supported here. Stratigraphically adjacent limestone contains few discrete trace fossils, and most that are present are clearly marine in origin (e.g., *Zoophycos*). AMBs are present only in the upper portions of limestone as a result of downward burrowing from the overlying clastic deposits in which occurred soil development. The distribution of AMB and pedogenic features provides strong evidence that the AMB and rhizoliths were made contemporaneously with soil formation under subaerial conditions.

Paleoenvironmental Implications and Significance

Paleosols of the Hugoton embayment were formed proximal to the shallow epicontinental seas that covered much of southwestern North America in the Early Permian, based on paleogeographic reconstructions and stratigraphic proximity to fully marine units (Rascoe and Adler, 1983; Boardman and Nestell 2000; Dubois et al., 2012). The lack of primary sedimentary structures indicates that pedogenic development and bioturbation was extensive enough to obliterate primary sedimentary fabrics, but the lack of distinct soil horizonation indicates that landscape aggradation produced composite and cumulic soil profiles (e.g., Kraus, 1999). Given that bioturbation was ubiquitous and spatially extensive throughout the Easly Creek, Blue Rapids, and Speiser shales, burrowing and plant growth played an important role in forming these incipient paleosols and promoting their preservation by stabilizing the land surface.

The Permian AMBs and the associated paleopedogenic features indicate a very specific range of environmental conditions during the time of pedogenesis and burrow construction. Moisture requirements of soil-dwelling insect larvae and nymphs are highly dependent on soil moisture and temperature, which are a product of regional climate and seasonal weather patterns.

Many infaunal insect larvae have a soft integument are known to be susceptible to low soil moisture levels. Masked chafer larvae, specifically, have increased mortality rates at soil moisture levels that deviate from a range of 18% to 27% (Potter, 1983; Potter and Gordon, 1984). Villani and Wright (1990) reported experimental data that showed that multiple species of scarab beetle larvae will move stratigraphically within a soil in order to avoid dry soils. Dung beetles in the holarctic region of Europe (approx. 60 degrees N latitude) were shown to have an increased positive response to moisture in dung pats with respect to pat preference, reproduction, and overall size (Vessby, 2001). Riis et al. (2005) found that tropical soil bugs (Hemiptera: Cydnidae) had highest population growth at soils with a moisture content of 33% (field capacity) to 44% (wet, but not fully saturated), with the lowest survival at soil moisture levels less than 25.5% (wilting point) in loamy clay soils. Willis and Roth (1962) also experimented with tropical soil bugs, and found that optimum survival occurred at soil moistures of 14 to 37% by weight in a mixture of 40% sand, 41% silt, and 19% clay. Field capacity and optimum soil moisture is likely variable between species and at different grain sizes, as grain size controls the capillarity of the soil and its' ability to hold water. However, multiple independent experiments show that highest survival of a number of different species occurs at a reasonably consistent range of moisture levels. All of these studies demonstrate that infaunal insects cannot survive for extended periods of time in extremely arid conditions. Permian climates, therefore, were likely not desert-like or arid for extended amounts of time, as evidenced by the number of burrows and their widespread distribution.

Soil-dwelling insect larvae are also unable to survive in fully saturated conditions. Gleying, however, is a common feature of Council Grove Group paleosols and implies that soils were saturated at least part of the time—such conditions would be fatal to the proposed tracemakers. Most fossorial insects and larvae are likely less susceptible to oversaturation than dessication—Villani et al.(1999) noted that some grubs are able to create an air pocket around their bodies in order to breathe during periods of flooding. Soil drainage was likely variable, as reflected by stratigraphic variations in gleying and redoximorphic coloration. Tracemakers likely survived in the vadose zone below the perched water table. The presence of rhizoliths also indicates a range of environmental conditions that were wet enough for consistent plant growth.

These observations support the conclusions of Miller et al. (1996), that the Early Permian paleoclimate in Kansas was seasonal or monsoonal, with a distinct wet and dry season. Soils were likely saturated during the wet season, forming reduced intervals, while oxidation took place during the drier, but still moist, periods. Other recent work (Dubois et al., 2012) emphasizes the stabilizing role that plant growth and bioturbation have had on these subaerial sediments, and favors a more arid paleoclimate interpretation. Based the numerous modern analogs discussed here, we favor a climate reconstruction that includes seasonal variations in moisture but does not reach fully arid conditions.

Conclusions

This study documents the earliest known occurrence of the ichnogenus *Naktodemasis*, as well as introducing a new morphologic variant, named herein as *N. krausi*. This new ichnospecies represents a behavioral difference from the type species, *N. bowni*, and is also likely produced during subaerial conditions by soil-dwelling insect larvae. This occurrence of *N. krausi* further confirms the ubiquity of continental meniscate backfilled burrows in the fossil record. Their abundance in the studied core indicates a repeated recolonization of Council Grove Group paleosols by the same organism over Milankovitch-scale time periods. Extant organisms that produce similar burrow structures are constrained to a limited range of environmental conditions, which are in agreement with those previously hypothesized for the Early Permian of Kansas.

Systematic Ichnology

NAKTODEMASIS KRAUSI ichnospecies nov.

Diagnosis.—Same as for type ichnospecies (*Naktodemasis bowni*; see Smith et al. 2008), except that the alignment of the central axes of adjacent packets and the diameter of packets is uniform and consistent compared to *N. bowni*, in which the axes of the packets are offset at an angle to adjacent packets and the diameter is more variable over the length of the burrow.

Etymology.—For Dr. Mary J. Kraus, who, along with Dr. Tom M. Bown, who described the first specimens of the ichnogenus as adhesive meniscate burrows (Bown and Kraus, 1983).

Types.—Holotype, KUMIP number to be determined (Fig. 28F)

Type stratum.—Lower Permian Speiser Shale, Council Grove Group

Type locality.—Cross H Cattle well, Hamilton County, Kansas, USA (lat. -101.6464517, long. 37.9105826).

Repository.—Division of Invertebrate Paleontology, Museum of Natural History and Biodiversity Research Center, University of Kansas, Lawrence, Kansas, United States of America.

Description.—*Naktodemasis krausi* is present in large numbers in paleosols in the Lower Permian Council Grove and Chase groups in the subsurface of western Kansas. Although complete trace fossils are not visible due to the nature of core exposure, burrows seen in cross section are characterized by a tortuous, vertical to horizontal in orientation, unbranching axis containing variably asymmetrical, crescent-shaped, meniscate backfill within a series of discrete packets. The central axes of successive packets are uniformly aligned. The diameter of packets is uniform throughout the length of the burrow. Burrows may contain a thin (sub-millimeter scale) discontinuous lining. Trace fossils and their internal structure are visible due to differential redoximorphic coloration between discrete burrows and the surrounding sediment.

Remarks.—*N. krausi* is interpreted as the combined deposit feeding and locomotion trace fossil of terrestrial insect adults or larvae. Traces are found in association with rhizoliths and rhizohalos in Permian sediments, which is consistent with rhizophagus or detritiphagus organisms. Trace fossils are similar to burrows made by extant larvae of the masked chafer beetle (Coleoptera, Scarabaeoidea, Scarabaeidae), and share similarities with the burrows of cicada larvae. Although these organisms have very different body plans, their burrowing mechanism is very similar. Both organisms accomplish burrowing by moving a single closed cell forward using a dig-rotate-fill sequence, described in Smith and Hasiotis (2008) and in Counts and Hasiotis (2009). Rotation within the cell disturbs sediment on the wall of the chamber, and creates a thin lining where the organism's body comes into contact with the cell. The tracemaker responsible for *N. krausi* likely used a similar burrowing mechanism based on the similarity in burrow morphologies of the Permian burrows and extant beetle larvae. *N. bowni* is likely analogous to cicada nymph backfilled burrows described in Smith and Hasiotis (2008).

References

BETHOUX, O. 2009, The earliest beetle identified: Journal of Paleontology, v. 83, p. 931-937.

BOARDMAN, D.R. and NESTELL, M.K., 2000, Outcrop-based sequence stratigraphy of the Council Grove Group of the Midcontinent, in: Johnson, K.S. ed., Platform Carbonates in the

Southern Midcontinent, 1996 Symposium: Oklahoma Geological Survey Circular 101, p. 275-306.

BOWN, T. M., and KRAUS, M.J.,1983, Ichnofossils of the alluvial Willwood Formation (Lower Eocene), Bighorn basin, northwestern Wyoming, U.S.A.: Palaeogeography, Palaeoclimatology, Palaeoecology, v. 43, p. 95–128.

BRADSHAW, M. A., 1981, Paleoenvironmental interpretations and systematics of Devonian trace fossils from the Taylor Group (Lower Beacon Supergroup), Antarctica: New Zealand Journal of Geology and Geophysics, v. 24, p. 615–652.

BROMLEY, R.G., 1996, Trace Fossils: Biology, Taphonomy and Applications: 2nd ed., Chapman & Hall, London, 361 p.

BROMLEY, R.G., BUATOIS, L.A., GENISE, J.F., LABANDEIRA, C.C., MANGANO, M.G., MELCHOR, R., SCHLIRF, M., and UCHMAN, A., 2007, Discussion of the paper ‘‘Reconnaissance of the Upper Jurassic Morrison Formation ichnofossils, Rocky Mountain Region, U.S.A.: Paleoenvironmental, stratigraphic, and paleoclimatic significance of terrestrial and freshwater ichnocoenoses’’ by Stephen T. Hasiotis: Sedimentary Geology, v. 200, p. 141–150.

BUATOIS, L.A., and MANGANO, G., 2002, Trace-fossil analysis of lacustrine facies and basins: Palaeogeography, Palaeoclimatology, Palaeoecology, v. 140, p. 367–382.

BUATOIS, L.A., and MANGANO, M.G., 2004, Animal-substrate interactions in freshwater environments; applications of ichnology in facies and sequence stratigraphic analysis of fluvio-lacustrine successions, in McIlroy, D., ed., The Application of Ichnology to Paleoenvironmental and Stratigraphic Analysis: Geological Society, London, Special Publications, v. 228, p. 311–333.

BUATOIS, L.A., and MANGANO, M.G., 2007, Invertebrate ichnology of continental freshwater environments, in Miller, W., ed., Trace Fossils: Concepts, Problems, Prospects: Elsevier, Oxford, UK, 637 p.

COUNTS, J.W., and HASIOTIS, S. T., 2009., Neoichnological experiments documenting burrowing behaviors and traces of the masked chafer beetle (Coleoptera: Scarabaeidae: Cyclocephala sp.): Behavioral significance of extant soil-dwelling insects to understanding backfilled trace fossils in the continental realm: PALAIOS, v. 24, p. 75-92.

DROSER, M.L. and BOTTJER, D.J. 1986. A semiquantitative field classification of ichnofabric. Joumal of Sedimentary Petrology, v. 56, p. 558-559.

DUBOIS, M.K., BYRNES, A.P., BHATTACHARYA, S., BOHLING, G.C., DOVETON, J.H., and BARBA, R.E., Hugoton Asset Management Project (HAMP): Hugoton Geomodel Final Report, 2006, updated April 9, 2007, http://www.kgs.ku.edu/PRS/publication/2007/OFR07_06. Checked May 15 2011.

DUBOIS, M.K., BYRNES, A.P., BOHLING, G.C., SEALS, S.C., and DOVETON, J.H., Statistically-based lithofacies predictions for 3-D reservoir modeling: An example from the Panoma (Council Grove) field, Hugoton embayment, southwest Kansas: Kansas Geological Survey Open-File Report 2003-30, updated 2003, http://www.kgs.ku.edu/PRS/publication/2003/ofr2003-30/index.html. Checked May 15th 2011.

DUBOIS, M.K., and GOLDSTEIN, R.H., 2005, Accommodation model for Wolfcamp (Permian) redbeds at the updip margin of North America’s largest onshore gas field: Kansas Geological Survey Open File Report no. 2005-25, http://www.kgs.ku.edu/PRS/AAPG2005/2005-25/index.html. Checked May 15 2011.

DUBOIS, M.K., GOLDSTEIN, R.H., and HASIOTIS, S.T., 2012, Climate controlled aggradation and cyclicity of continental loessic siliciclastic sediments in Asselian–Sakmarian cyclothems, Permian, Hugoton embayment USA: Sedimentology, in press.

EKDALE, A.A., BROMLEY, R.G., and PEMBERTON, S.G., 1984, Ichnology: The use of trace fossils in sedimentology and stratigraphy: SEPM (Society for Sedimentary Geology) Short Course no. 15, p. 1–317.

FOLK, R.L., 1951, A comparison chart for visual percentage estimation: Journal of Sedimentary Research, v. 21, p. 32-33.

FREY, R.W., PEMBERTON, S.G., and FAGERSTROM, J.A., 1984, Morphological, ethological, and environmental significance of the ichnogenera Scoyenia and Ancorichnus: Journal of Paleontology, v. 58, p. 511–528.

GENISE, J.F., and BOWN, T.M., 1994, New Miocene scarabeid and hymenopterous nests and Early Miocene (Santacrucian) paleoenvironments, Patagonian Argentina: Ichnos, v. 3, p. 107–117.

GENISE, J. F., 2004, Ichnotaxonomy and ichnostratigraphy of chambered trace fossils in paleosols attributed to coleopterans, ants, and termites, in D. McIlroy, ed., The Application of ichnology to paleoenvironmental and stratigraphic analysis: Geological Society (London) Special Publications 228, p. 419–453.

GENISE, J. F., BELLOSI, E.S. and GONZALEZ, M. G., 2004, An approach to the description and interpretation of ichnofabrics in paleosols, in D. McIlroy, ed., The application of ichnology to paleoenvironmental and stratigraphic analysis: Geological Society (London) Special Publication 228, p. 355–382.

HASIOTIS, S. T., 2002, Continental Trace Fossils: SEPM (Society for Sedimentary Geology) Short Course Notes no. 51, Society for Sedimentary Geology, Tulsa, Oklahoma, 134 p.

HASIOTIS, S. T., and DUBIEL, R. F., 1994, Ichnofossil tiering in Triassic alluvial paleosols: Implications for Pangean continental rocks and paleoclimate, in Embry, A.F., Beauchamp, B., and Glass, D., eds., Pangea: Global environments and resources: Canadian Society of Petroleum Geologists Memoir 17, p. 311–317.

HEMBREE, D.I., and HASIOTIS, S.T., 2008. Miocene vertebrate and invertebrate burrows defining compound paleosols in the Pawnee Creek Formation, Colorado, USA: Palaeogeography, Palaeoclimatology, Palaeoecology, v. 270, p. 349-365.

HATTIN, D.E., 1957, Depositional environment of the Wreford Megacyclothem (Lower Permian) of Kansas: Kan. Geol. Surv., Bull. 124, 150 p.

JACOBS, P.M. and MASON, J.A., 2004. Paleopedology of soils in thick Holocene loess, Nebraska, USA: Revista Mexicana de Ciencias Geologicas, v. 21, p. 54–70.

JOHNSON, K.S., 1989, Geologic evolution of the Anadarko basin, in K. S. Johnson, ed., Anadarko basin symposium: Oklahoma Geological Survey Circular 90, p. 3-12.

KEIGHLEY, D.G., and PICKERILL, R., 1994, The ichnogenus Beaconites and its distinction from Ancorichnus and Taenidium: Palaeontology, v. 37, p. 305–337.

KIM, J.Y., KEIGHLEY, D.G., PICKERILL, R.K., HWANG W., and KIM, K.S., 2005, Trace fossils from marginal lacustrine deposits of the Cretaceous Jinju Formation, southern coast of Korea: Palaeogeography, Palaeoclimatology, Palaeoecology, v. 218, p. 105-124.

KRAUS, M. J., 1999, Paleosols in clastic sedimentary rocks: Their geologic applications: Earth Science Review, v. 47, p. 41–70.

KUKALOVA-PECK, J, and WILLMANN, R.,1990, Lower Permian “mecopteroid-like” insects from central Europe (Insecta, Endopterygota): Canadian Journal of Earth Science, v. 27, p. 459-468.

MELCHOR, R.N., BEDATOU, E., DE VALAIS, S., and GENISE, J.F., 2006, Lithofacies distribution of invertebrate and vertebrate trace-fossil assemblages in an Early Mesozoic ephemeral fluvio-lacustrine system from Argentina: Implications for the Scoyenia ichnofacies: Palaeogeography, Palaeoclimatology, Palaeoecology, v. 239, p. 253-285.

MELCHOR, R.N., GENISE, J.F., and MIQUEL, S.E., 2002, Ichnology, Sedimentology and Paleontology of Eocene Calcareous Paleosols From a Palustrine Sequence, Argentina: Palaios, v. 17, p. 16 - 35.

MILLER, K.B., MCCAHON, T.J., AND WEST, R.R., 1996, Lower Permian (Wolfcampian) paleosol-bearing cycles of the US midcontinent: evidence of climatic cyclicity: Journal of Sedimentary Research, v. 66, p. 71–84.

MINTER, N.J., KRAINER, K., LUCAS, S.G., BRADDY S.J., and HUNT, A.P., 2007, Palaeoecology of an Early Permian playa lake trace fossil assemblage from Castle Peak, Texas, USA: Palaeogeography, Palaeoclimatology, Palaeoecology, v. 246, p. 390-423.

MORRISSEY, L.B., and BRADDY, S.J., 2004, Terrestrial trace fossils from the Lower Old Red Sandstone, southwest Wales: Geological Journal, v. 39, p. 315–366.

MORRISSEY, L.B., BRADDY, S.J., BENNETT J.P., MARRIOTT, S.B., and TARRANT, P.R., 2004, Fish trails from the Lower Old Red Sandstone of Tredomen Quarry, Powys, southeast Wales: Geological Journal, v. 39, p. 337–358.

POTTER, D. A., 1983, Effect of soil moisture on oviposition, water absorption, and survival of Southern Masked Chafer (Coleoptera: Scarabaeidae) eggs: Environmental Entomology,

v. 12, p. 1223-1227.

POTTER, D.A., and GORDON, F.C., 1984, Susceptibility of *Cyclocephala immaculate* (Coleoptera: Scarabaeidae) eggs and immature to heat and drought in turfgrass: Environmental Entomology, v. 13, p. 794-799.

PUCKETTE, G.R., D.R. BOARDMAN, II, and Z. AL-SHAIEB, 1995, Evidence for sea-level fluctuation and stratigraphic sequences in the Council Grove Group (Lower Permian) Hugoton Embayment, southern Mid continent, in Hyne, N.J., ed.: Tulsa Geological Society Special Publication no. 4, p. 269-290.

RASCOE, B. JR and ADLER, F.J. (1983) Permo-carboniferous hydrocarbon accumulations, Midcontinent, USA. Am. Assoc. Pet. Geol. Bull., 67, 979–1001.

RIIS, L., ESBJERG, P., and BELLOTTI A.C., 2005, Influence of Temperature and Soil Moisture on Some Population Growth Parameters of *Cyrtomenus bergi* (Hemiptera: Cynidae): Florida Entomologist, v. 88, p. 11-22.

SMITH, J.J., and HASIOTIS, S.T., 2008, Traces and burrowing behaviors of the cicada nymph *Cicadetta calliope*: Neoichnology and paleoecological significance of extant soil-dwelling insects: PALAIOS, v. 23, p. 503–513.

SMITH, J.J., HASIOTIS, S.T., WOODY, D.T., and KRAUS, M.J., 2008, *Naktodemasis bowni*: New ichnogenus and ichnospecies for adhesive meniscate burrows (AMB), and paleoenvironmental implications, Paleogene Willwood Formation, Bighorn Basin, Wyoming: Journal of Paleontology, v. 82, p. 267–278.

SQUIRES, R.L., and ADVOCATE, D.M., 1984, Meniscate burrows from Miocene lacustrine-fluvial deposits, Diligencia Formation, Orocopia Mountains, southern California: Journal of Paleontology, v. 58, p. 593–597.

VESSBY, K., 2001, Habitat and weather affect reproduction and size of the dung beetle *Aphodius fossor*: Ecological Entomology, v. 26, p. 430-435.

VILLANI, M.G., and WRIGHT, R.J., 1990, Environmental influences on soil macroarthropod behavior in agricultural systems: Annual Review of Entomology, v. 35, p. 249-269.

VILLANI, M.G., ALLEE, L.L., DIAZ, A., and ROBBINS, P.S., 1999, Adaptive strategies of edaphic arthropods: Annual Review of Entomology, v. 44, p. 233-256.

WEST, R.R., MILLER, K.B., and WATNEY, W.L., 2012, The Permian System in Kansas: Kansas Geological Survey Bulletin 257, 88 p.

WILLIS, E. R., and ROTH, L.M.,1962, Soil and moisture relations of *Scaptocoris divergins* Troeschner (Hemiptera: Cynidae): Annals of the Entomological Society of America, v. 55, p. 21–32.

CHAPTER FOUR. NEOICHNOLOGICAL EXPERIMENTS WITH MASKED CHAFER BEETLES (COLEOPTERA: SCARABAEIDAE): IMPLICATIONS FOR BACKFILLED CONTINENTAL TRACE FOSSILS

Published as:

COUNTS, J.W., and HASIOTIS, S. T., 2009., Neoichnological experiments documenting burrowing behaviors and traces of the masked chafer beetle (Coleoptera: Scarabaeidae: *Cyclocephala* sp.): Implications for backfilled continental trace fossils: PALAIOS, v. 24, p. 75-92.

Abstract

Laboratory experiments conducted with larvae and adults of the northern or southern masked chafer beetle (Scarabaeidae: *Cyclocephala lurida* or *C. borealis*) tested hypotheses that beetle larvae construct meniscate, backfilled burrows, and that they are distinct from backfilled burrows constructed by marine organisms. Beetle larvae were placed in narrow enclosures with laminated moist, fine- to medium-grained sand and allowed to burrow for several weeks. Beetle larvae did not create open burrow systems, but instead excavated a single open cell approximately twice their body width and roughly equal to their body length. Burrowing was accomplished by scraping sediment with the head and mandibles, consolidating excavated sediment into a ball, rotating 180° with the ball to the back of the cell, and packing the ball onto the posterior end of the cell. The beetle larvae produced vertical to horizontal traces that were straight to tortuous and composed of discrete packets of meniscate backfill. Adult chafer beetles moved through the media using a sand-swimming motion, i.e., passing sand around their bodies with the legs. Traces produced by adults are characterized by straighter axes and mixed passive and active fill resulting from sediment collapse and sediment transported backwards. When vertical, adult burrows contain chevron-shaped fill. Traces produced by these beetles are similar to adhesive meniscate burrows (AMB) found in many ancient continental deposits as old as the Permian, and can be assigned to *Naktodemasis* isp. We propose that *Naktodemasis* with this kind of burrow morphology were soil-dwelling insect larvae that used burrowing mechanisms similar to chafer beetle larvae. These experiments demonstrate that this kind of burrow morphology is terrestrial in origin, and that previous interpretations suggesting they are subaqueous in origin need to be reevaluated.

Introduction

The ability of insect larvae, nymphs, and adults to construct meniscate, backfilled burrows in terrestrial settings is currently a subject of controversy. Backfilled burrows are thought traditionally to have only been produced primarily through deposit feeding, in which organisms ingest sediment and pass it through their bodies, filling the burrow at the posterior end (e.g., Ekdale et al., 1984; Frey et al., 1984; Bromley, 1996). Many backfilled burrows in continental strata, dating back to the late Paleozoic, are thought to have been produced in lacustrine and fluvial deposits by worms or aquatic arthropods (e.g., Frey et al., 1984; Squires and Advocate, 1984; Savrda et al., 2000; Genise et al., 2004; Buatois and Mángano, 2004, 2007;

Bromley et al., 2007). Other research, however, demonstrates that these types of burrows were made in subaerial terrestrial environments (e.g., Willis and Roth, 1962; O'Geen and Busacca, 2001; Smith and Hasiotis, 2008), and were frequent components of ancient paleosols (e.g., Bown and Kraus, 1983; Hasiotis and Dubiel, 1994; Retallack, 2001a, 2001b; Genise et al., 2004; Smith et al., 2008). The earliest meniscate, backfilled burrows have been reported from the Ordovician (Retallack, 2001a).

Studies concentrating on understanding the traces and tracemaking behavior of modern burrowing beetles are rare. Modern burrows of other species of scarab beetles have been described by McColloch et al. (1928), Lengerken (1954), Halffter and Edmonds (1982), Brussaard (1983), Brussaard and Runia (1984), and Hanski and Cambefort (1991), among others.

This paper documents the burrows and burrowing mechanism of modern masked chafer-beetle larvae and adults (Fig. 30) (Coleoptera: Scarabaeidae: Dynastinae: *Cyclocephala lurida* or *C. borealis*). Neither the method by which grubs excavate sediment and fill their burrows nor burrow morphology of the larva or adult beetles has been described previously. We show that meniscate backfilled burrows are produced by modern masked chafer-beetle larvae in subaerial settings and that the morphology of these modern burrows is comparable to fossil backfilled burrows found in paleosols. Thus, the similar morphology of extant and fossil burrows indicates that ancient backfilled burrows were constructed by organisms with body plans and behaviors similar to modern insect larvae. Traces produced by beetle larvae and adults are compared to examples of morphologically similar trace fossils in ancient paleosols. These findings will aid in the interpretation of ancient environments, hydrologic conditions, and climatic settings of continental deposits, as well as marine deposits modified by pedogenic processes.

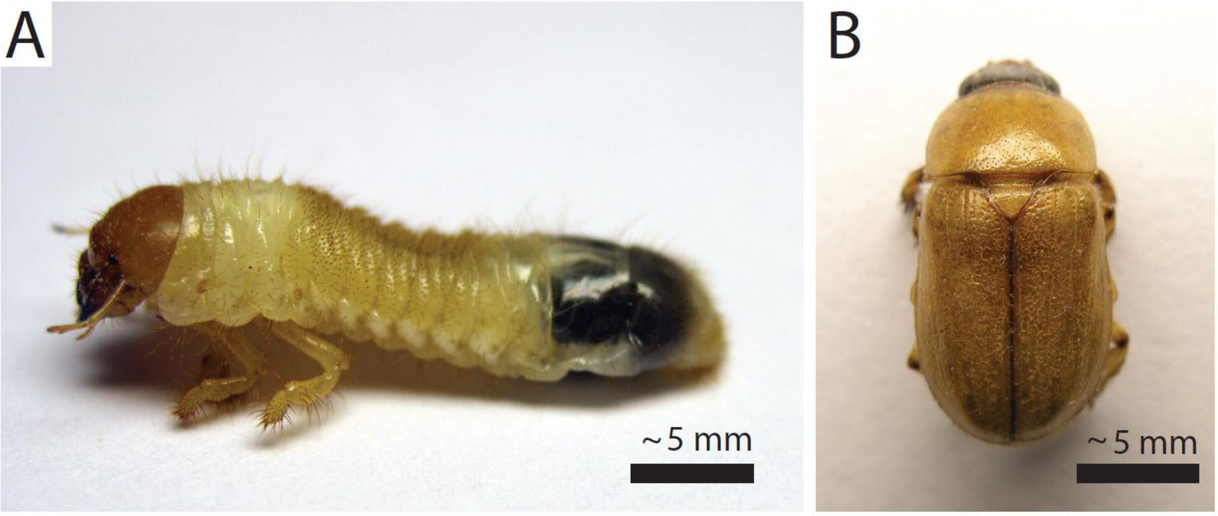

Figure 30. Insects used in the study. A) Masked chafer larvae. B) Masked chafer adult

Background

The earliest known beetle-like fossils are Early Permian (Kukalová-Peck and Willmann, 1990) and beetles (Insecta: Coleoptera) were well established by the Middle Triassic (Rasnitsyn and Quicke, 2002; Grimaldi and Engel, 2005). The oldest body fossils attributed to Scarabaeoidea are from the Late Jurassic, the oldest Scarabaeidae are Early Cretaceous, and the earliest fossils from the subfamily Dynastinae are found in the Eocene (Krell, 2000, 2006).

True scarab beetles belong to the family Scarabaeidae and the order Coleoptera. Over 30,000 species are known within this family and are found on every continent except Antarctica. The Scarabaeidae include some of the largest known insects—the rhinoceros and Goliath beetles—and also include the more familiar scarab, dung, and June beetles. The biology and ecology of scarabs vary considerably among genera (Crowson, 1981).

There are at least five species of *Cyclocephala* in Kansas (Bauernfeind, 2001), all of which have similar life cycles and environmental tolerances. These beetles have a one-year life cycle, divided into adult and larval stages. Eggs are laid within the soil in early to mid-summer and hatch into larvae soon after. The larvae, which are soft-bodied, white grubs (Fig. 30A), go through three growth stages (instars). Each stage is successively larger than the previous, although there is little change in body morphology between these initial stages (Richter, 1966). Larvae remain in the soil the rest of the year, burrowing deeper during winter months to avoid freezing. As temperatures rise in the spring, larvae return closer to the surface to feed, then pupate in May or June to become adult beetles (Fig. 30B) (Potter, 1998; Vittum et al., 1999; Rogers and Potter, 2002).

Potter and Gordon (1984) conducted field experiments to test the susceptibility of masked chafer grubs to heat and drought in turfgrass. In nonirrigated plots with 8%–15% soil moisture, only 1.7% of grubs survived, whereas irrigated plots, with soil moisture of 18%–27%, resulted in a 56.7% grub survival rate. Masked chafer eggs also showed decreased survival with hotter temperatures and drier conditions. These results are similar to those obtained for moisture experiments with soil bugs (Hemiptera: Cydnidae), which showed survival of nymphs in 7%–37% soil moisture with the greatest survivability under moisture levels of 14%–37% (Willis and Roth, 1962).

Larvae of the northern and southern masked chafer, *Cyclocephala lurida* and *C. borealis*, have been the subject of much research, due to their prevalence in cultivated lawns and agricultural areas (see references in Vittum et al., 1999). Grubs are considered pests and have considerable economic impact because they feed on the roots of herbaceous plants. Most research has focused on habitat preference, distribution, and means of control (Potter, 1998; Vittum et al., 1999; Bauernfeind, 2001; Merchant et al. 2004). Burrowing mechanism and burrow characteristics are of little interest to agronomists and thus remain relatively unknown.

Masked chafers prefer vegetated habitats including open lawns, gardens, and cultivated areas as well as grasslands and forest floors with underbrush growth. Larvae feed on living plant roots, especially grasses, and disseminated soil organic matter, making them facultative deposit feeders. Chafers are prey species for many types of animals; their eggs are frequently eaten by ants and other beetles, and the grubs are prey of such vertebrates as armadillos and birds, as well as being parasitized by tiphiid wasps (Vittum et al., 1999; Zenger and Gibb, 2001).

Materials and Methods

Chafer larvae were collected from two locations—an open, mulch-covered area in a suburban lawn, and a proximal floodplain characterized by mixed grasses and forbs between the Kansas River and an artificial levee. Soil trenches were hand dug by members of the University of Kansas IchnoBioGeoScience research group. Larvae were found predominately in humic A horizons that are high in organic matter with dense roots. All larvae found in both field sites were in their third instar when collected. They were transported to the laboratory, and kept alive in terraria containing the moist soil from which they were collected. Although soil moisture was not directly measured in the field, periodic rewetting kept moisture levels in terraria at approximately the same level as field moisture (see below). Grubs (Fig. 30) were identified to either the northern or southern masked chafer by rastral hair patterns (Vittum et al. 1999).

Three experimental containers were constructed in the laboratory to observe beetle burrowing behavior (Table 1). The thickness of sediment laminae was varied between experiments in order to determine how burrow morphology is expressed in different lamina thicknesses (thick, thin, or no laminae). Sediment composition was also altered in each experiment to test whether the amount of organic matter (none, discrete layers of organic-rich sediment, or uniformly distributed organic-rich sediment) in the sediment had an effect on burrow morphology.

The first enclosure consisted of a rectangular aquarium 16 cm high, 25 cm long, and 15 cm wide (Fig. 31). Corrugated cardboard was placed upright inside the aquarium, parallel to the aquarium walls and at distances of 7 and 15 mm from the glass sides. The interior of the aquarium not used for burrowing was filled with a mixture of sand and silt, and the space between the cardboard and the glass used for burrowing was filled with colored sand. At the start of the experiment, beetle larvae were placed atop the colored sand, where they were forced to burrow in the narrow space between the cardboard and the glass.

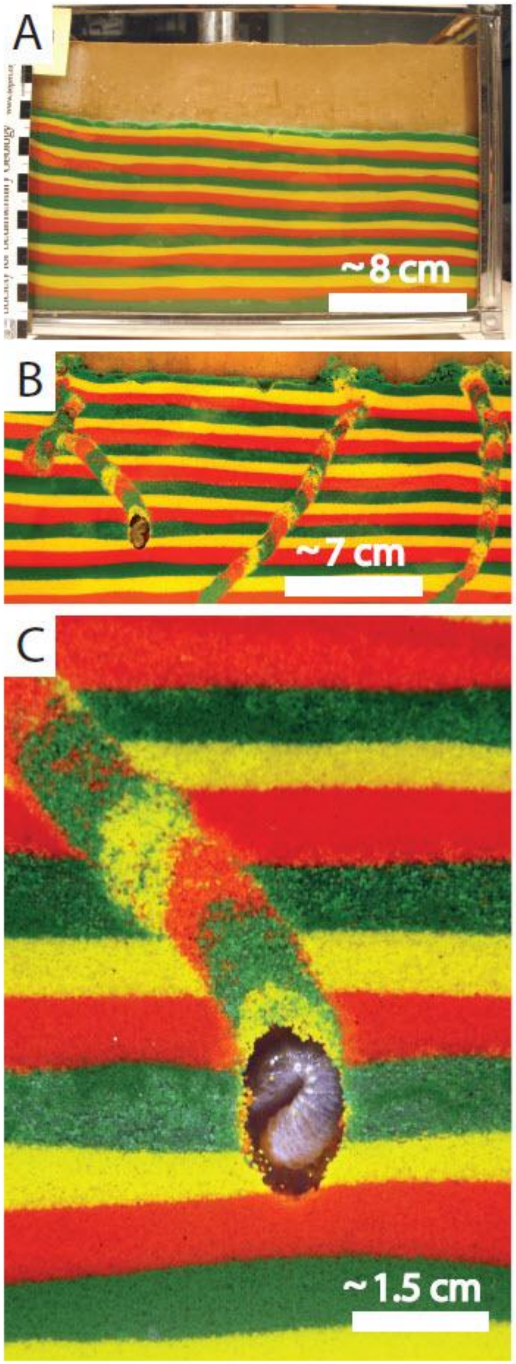

Figure 31. Traces produced in Experiment 1. A) Initial setup before introduction of grubs. B) Bioturbation after ~2 hours. C) Close up of larval burrow

Experiment	Enclosure length	Enclosure height	Width of burrowing space	Sediment type	Lamina thickness
1	15 cm and 25 cm	16 cm	7 mm and 15 mm (two sides of aquarium used)	Medium- to fine-grained, artificially colored, yellow, orange, and green sand, no organic matter	Mostly 5 mm; widest 10 mm
2	38.5 cm	34 cm	6 mm	Medium- to fine-grained, artificially colored, yellow, orange, and green sand, with discrete layers of natural, poorly sorted, organic-rich sediment	1–10 mm, most laminae 2–3 mm thick
3	38.5 cm	34 cm	6 mm	Natural, poorly sorted, organic-rich sand from Kansas River sandbars	No laminae

Table 4: Enclosure parameters used in experiments 1–3

Two additional enclosures were created for experiments 2 and 3—these were constructed using a three-sided wood frame with inset slots cut into the wood to hold two panes of glass (Figs. 32–35). Glass panes 34 cm high, 38.5 cm long, and 0.3 cm thick were placed in the slots, separated by a space of 0.6 cm. This space had to be narrow enough to force the grubs to burrow adjacent to the glass pane in order to observe the burrowing process and resulting burrows (Fig. 36). The glass-wood contact was sealed on the outside using weather-stripping putty, although the seal was left incomplete at the bottom to allow water drainage. Prior to the start of this set of experiments, adult beetles were placed in similar enclosures and media to test whether the insects would burrow in a laboratory setting (Fig. 37). The methods and materials described herein were used in the test experiments and allowed the observation and description of the beetle burrowing activity.

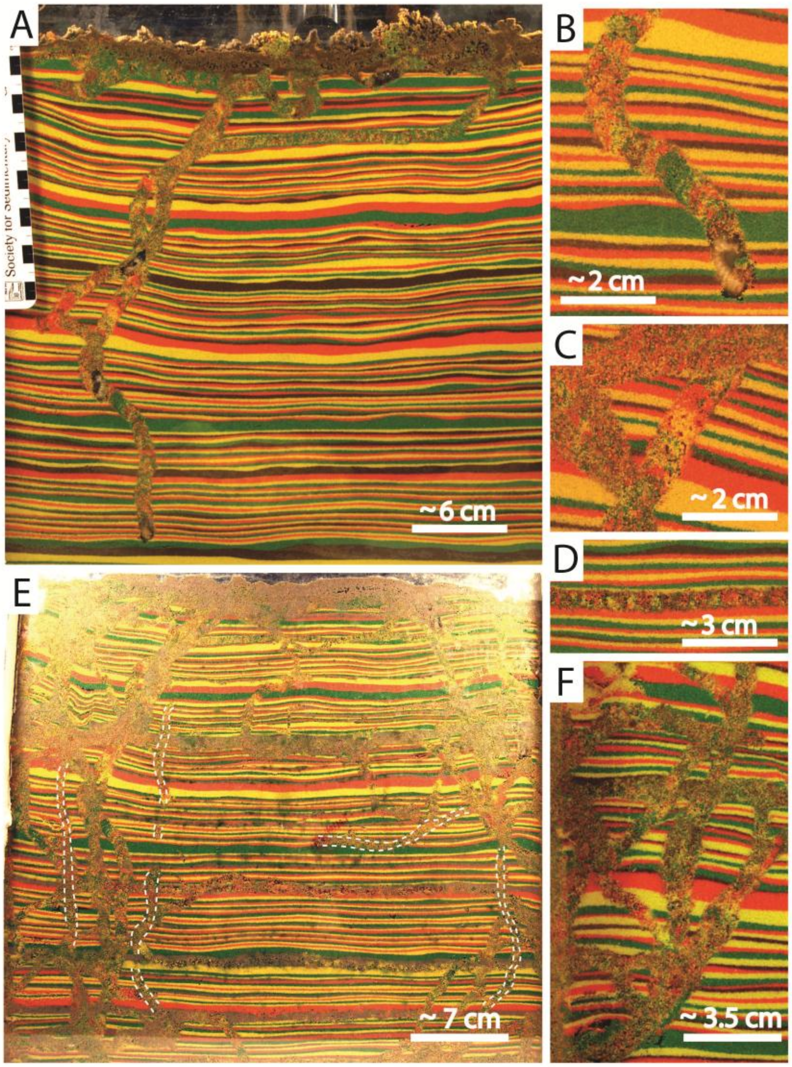

Figure 32. Larval traces produced in Experiment 2. A) Experiment 2 shortly after introduction of grubs. B) Close up of larval burrow showing meniscate backfill and thin lining. C) Close up of larval burrow showing higher porosity within burrow fill. D) Close up of horizontal larval burrow showing exploitation of organic-rich layer. E) Photograph of entire enclosure at the end of the experiment. Adult beetle burrows traced in white. F) Larval burrow complex showing extensive reburrowing and interconnected traces

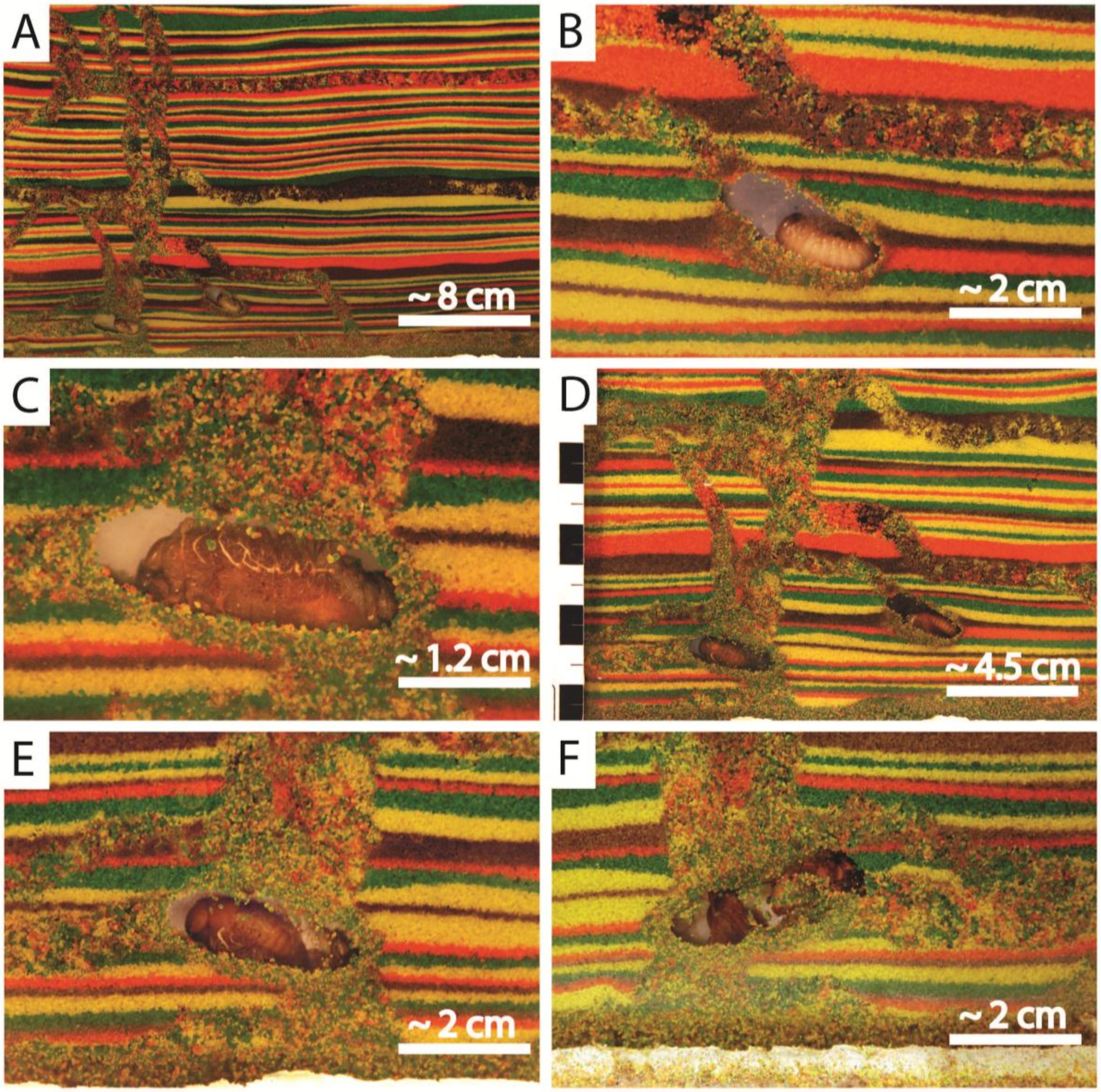

Figure 33. Pupation chambers produced in Experiment 2. A) Overview of experiment 2 showing position of pupation chambers near bottom of enclosure. B) Close up of masked chafer larva during construction of pupation chamber. C) Close up of pupae approximately two weeks after onset of pupation. D–E) Pupae in chambers, showing thick lining surrounding chamber. F) Pupal chamber, showing initial excavation by adult beetle a few days after hatching.

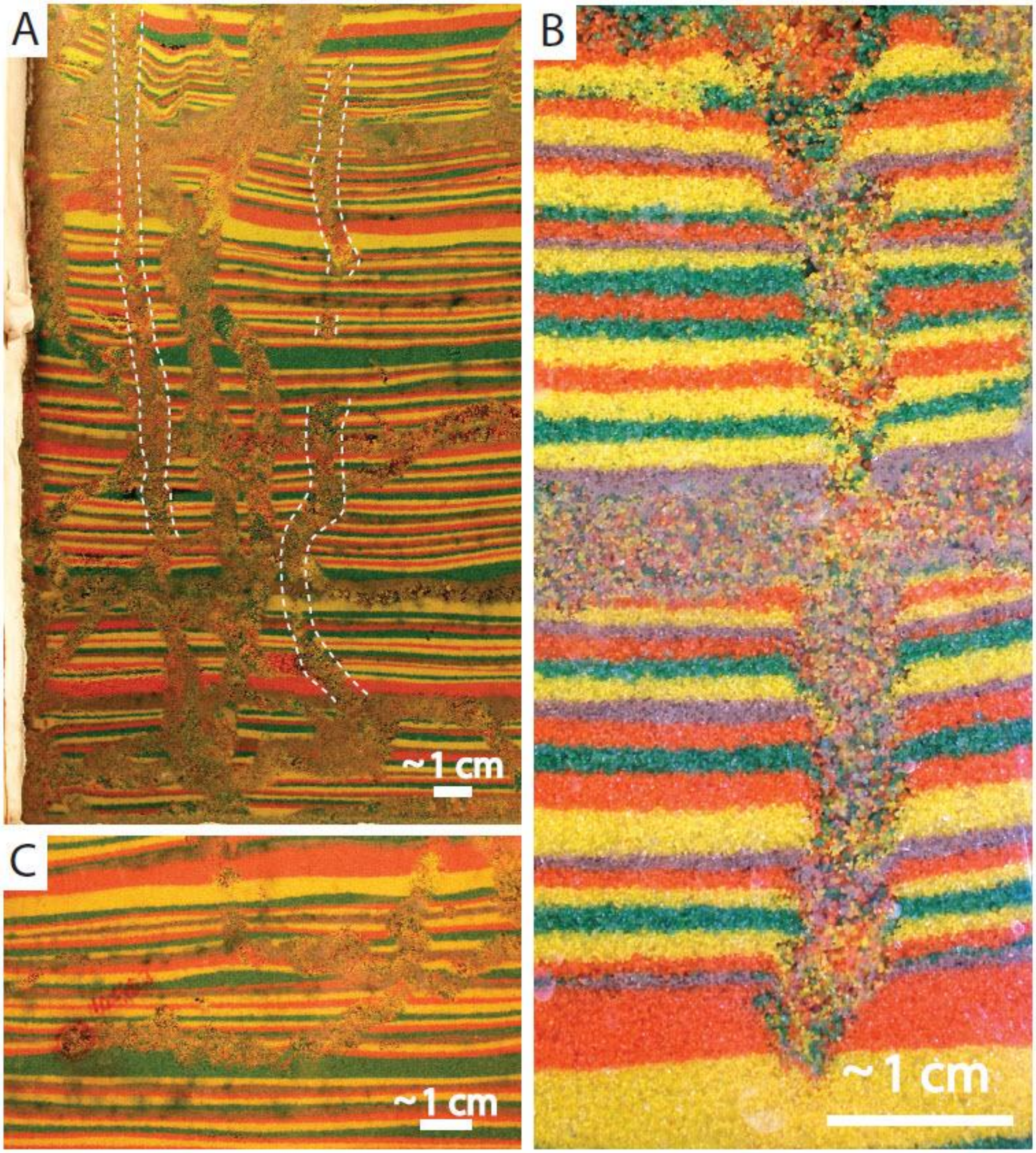

Figure 34. Adult beetle traces produced in Experiment 2. A) Burrow complex showing adult beetle trace (dashed lines). B) Close up of adult beetle trace, showing downward-pointing V-shaped fill. C) Irregular horizontal burrow of adult beetle

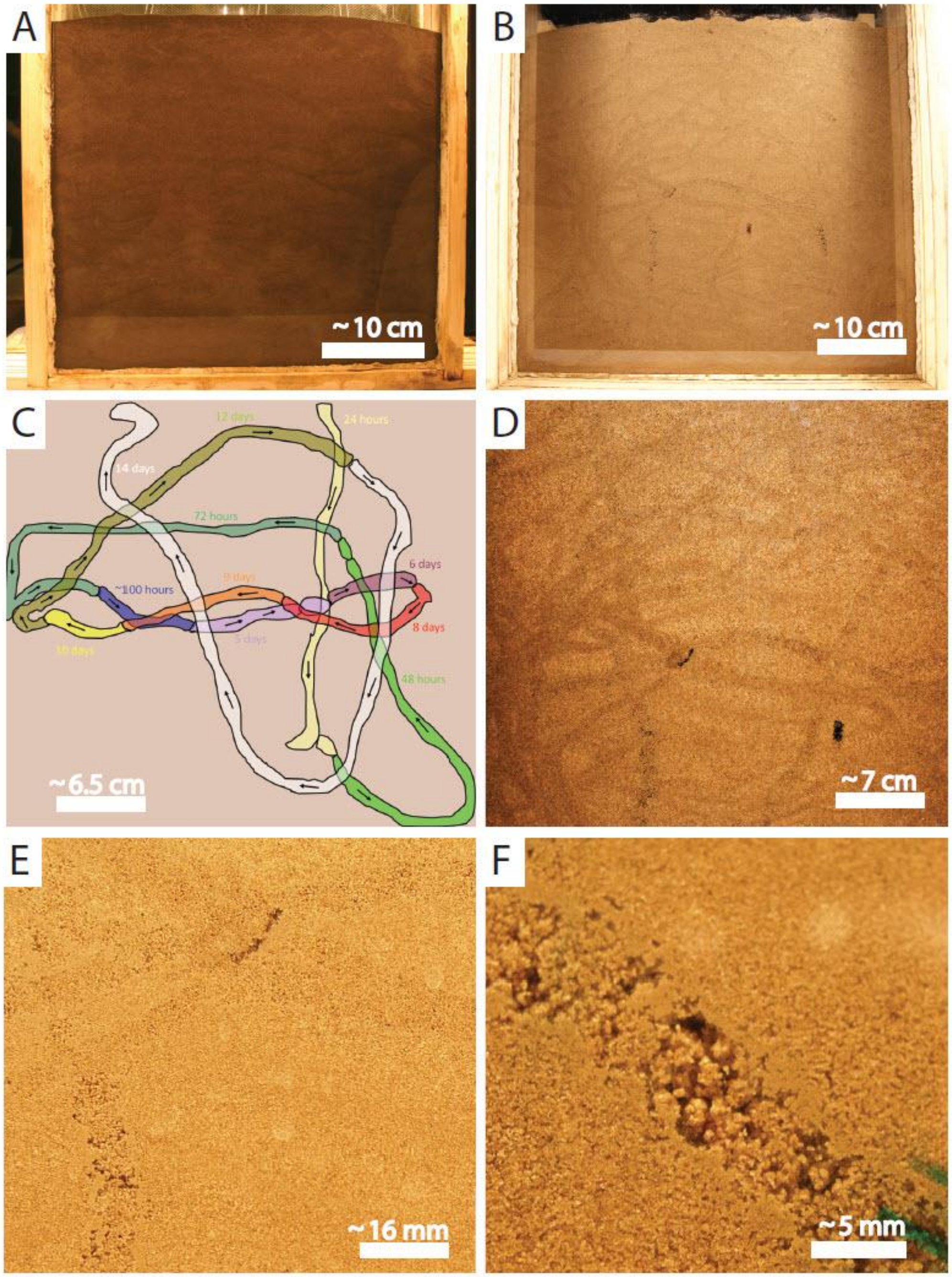

Figure 35. Traces produced in Experiment 3. A) Initial setup before introduction of grubs. B) Photograph of entire enclosure at end of experiment. C) Outline of burrows and burrow timing for first two weeks of experiment. D) Contrast-enhanced close up of burrow network. E–F) Close up of larval burrows showing increased porosity within fill of burrow

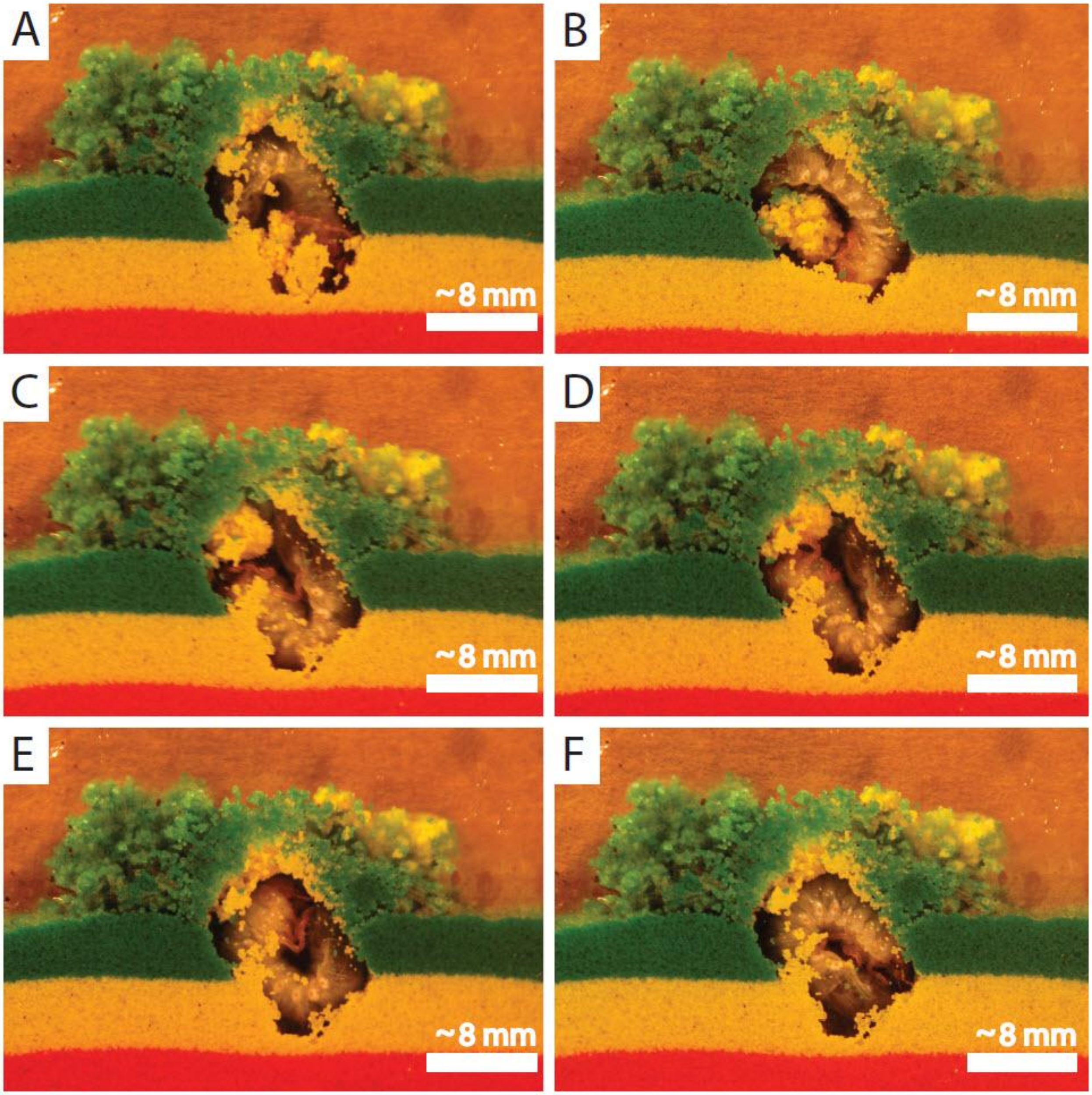

Figure 36. Steps in burrowing mechanism used by masked chafer larvae. A) Excavation of sediment at anterior end of cell. B) Consolidation of sediment into a ball held close to abdomen. C) Transport of sediment to posterior end of cell. D) Continued transport and compaction of sediment ball with legs. E) Step 5: Compression of sediment with head and formation of meniscate backfill. F) Continued rotation and restart of burrowing process

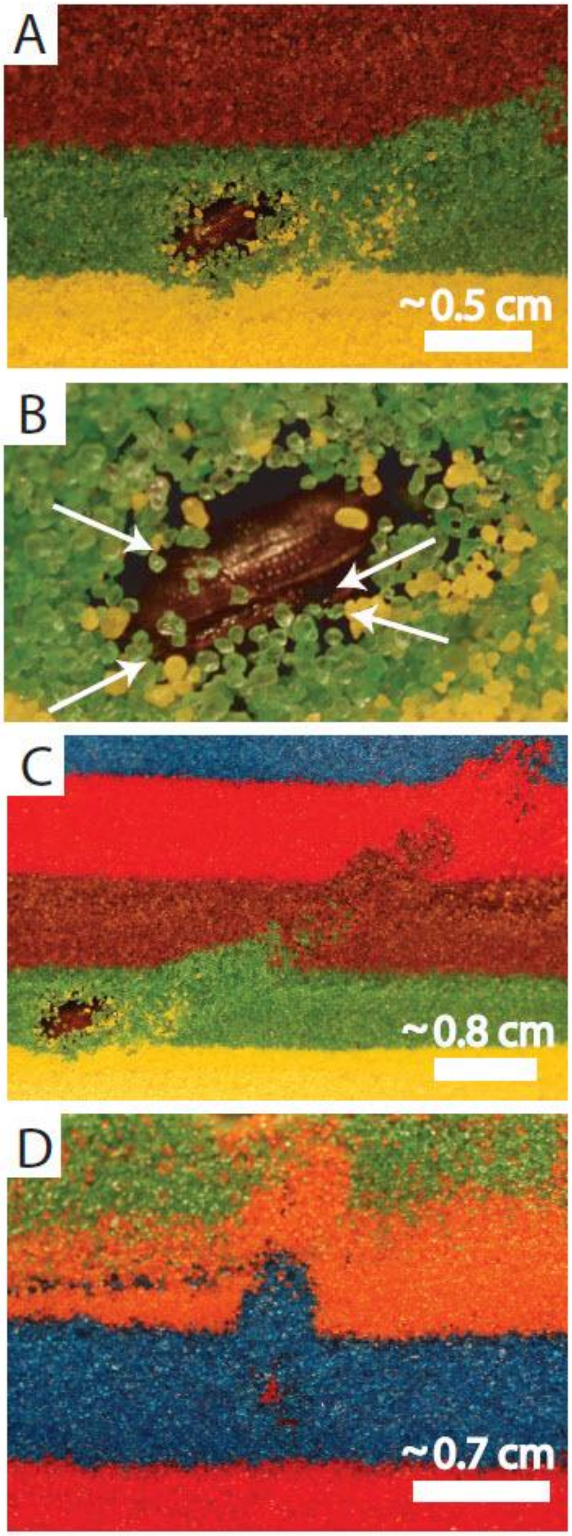

Figure 37. Adult masked chafer beetle burrows produced in preliminary experiments to test the viability of enclosures. A) Adult beetle during locomotion. Position of legs indicated by arrows. B) Adult beetle and trace produced during locomotion. Direction of movement is toward the lower left corner. C) Adult beetle trace showing backfill morphology. Direction of movement is toward the bottom.

In experiment 1 the burrowing medium consisted of medium- (0.25–0.5 mm) to fine-grained (0.125–0.25 mm), artificially colored yellow, orange, and green sand. Each sand layer was individually poured into the enclosure, producing planar laminae with sharp horizontal boundaries between layers. Colored sand laminae in experiment 1 were ~0.5 cm thick. Three grubs were placed between the cardboard partition and the glass on each side of the enclosure. No organic matter existed within the sand.

The enclosure for experiment 2 was primarily also filled with artificially colored sand, although in this experiment, 24 discrete layers of natural sediment with a higher organic matter content collected from sandbars along the Kansas River were interspersed between the colored layers (Figs. 32–34). Laminae ranged from 0.1–1.0 cm thick. Five grubs were placed in the enclosure, although only two survived for a significant time. The cause of death of these grubs is unknown, and no evidence of parasitism or infection was observed.

The enclosure for experiment 3 (Fig. 35) was filled only with organic-rich, natural sand from the Kansas River in order to create a more natural habitat and observe the effect of increased organic matter on burrowing behavior. This sand was poorly sorted and contained a higher percentage of clay and organic matter. The filling process produced faint, irregular layers created by settling of finer grained material while pouring. Three grubs were used in experiment 3, but one died shortly after the experiment began.

Sediments in all experiments were poured dry into each enclosure. The sediments were then wetted thoroughly until the entire enclosure was saturated. Water movement consolidated the sediment. Moisture content was determined by wetting a sand sample using the same method as that used to moisten the enclosures. The sample was weighed both dry and wet, and water content was then calculated as a weight percentage. The initial saturated moisture content for each experiment was ~15% water weight.

Beetle larvae were placed into the enclosures on the sediment surface immediately after the sediments were saturated. To prevent desiccation of the grubs, the sediment during each experimental run was remoistened periodically by spraying the upper surface until a wetting front developed and began to move downward through the sediment. At no time was the sediment completely resaturated. Once enclosures were set up, burrowing activity was photographed and videotaped every few minutes within the first four hours, decreasing in frequency throughout the duration of each experiment.

In order to test the similarity between modern beetle traces produced in experiments 1–3 and ancient backfilled trace fossils, trace fossils found in core taken in the Hugoton-Panoma gas field in southwestern Kansas were examined.   Trace fossils used for comparison were found in the Speiser, Blue Rapids, and Easly Creek Shales, which form the continental portions of three asymmetric cyclothems in the upper portion of the Lower Permian Council Grove Group.   Core used for comparison—Cross H Cattle, May Beaty E 2, D Alexander, Stuart 3-34, and Prater—are stored at the Kansas Geological Survey in Lawrence, Kansas, and can be accessed on line (www.kgs.ku.edu /PRS/petroDB.html).

Results

Burrowing Mechanism of Larvae

In all experiments, the larvae began to burrow as the moisture content lessened and the sediment became drier. Initial penetration into the media created loose, granular piles of sediment on the surface (Fig. 36). Masked chafer grubs create an elliptical, open cell and actively move it forward by excavating sediment from the front end of the cell and depositing it at the back. This process can be divided into five steps: (1) excavation, (2) consolidation, (3) rotation, (4) transport of sediment, and (5) packing (Fig. 36; see video in Supplementary Data).

Excavation (1).—Sediment is excavated through a scraping motion of the larva's mandibles and head at the anterior end of the burrow. Rather than holding sediment in the mouth, the open mandibles and head are used as a scraper and shovel, respectively, moving them toward the center of the body and immediately passing sediment to the first pair of limbs (Fig. 36A).

Consolidation (2).—As each successive measure of excavated sediment is passed to the limbs, the grub uses its legs and body to consolidate the sediment into a ball. As the sediment package grows larger, the grub's body forms a C shape around the package. Sediment is compressed until it is large enough to fill the space between the anterior and posterior ends of the abdomen and the cell wall (Fig. 36B).

Rotation and Transport of Sediment (3–4).—Using contractions of the body, the grub braces itself against the cell wall and rotates toward the ventral side of the abdomen until the head is at the posterior end of the chamber. Concurrently, the grub pushes the sediment ball to the back of the chamber with the head, limbs, and the front portion of the body (Fig. 36C–D). The first two pairs of legs are also used to push the sediment ball to the rear of the cell where it is compacted into the cell wall with the head and third pair of legs. The posterior of the abdomen is used to brace the grub during sediment packing. The dorsal side of the grub's abdomen is in continuous contact with the wall of the cell during the entire rotation process, often disturbing sediment along the cell wall.

Packing (5).—Once the sediment ball is at the back of the chamber, it is compacted against the wall with the legs and sclerotized head, the only hard parts of the grub's body. The ball of sediment is pushed against the back wall several times in all directions to fully compact it (Fig. 36E). This also has the effect of disrupting and compacting previously backfilled sediment and sediment grains immediately outside of the cell margin. The process is then repeated as the grub rotates to the front of the cell (Fig. 36F) and continues to excavate sediment, repeating steps 1–5.

Biogenic Structures of Larvae

Burrowing in experiment 1 resulted in well-developed traces. Traces were generally vertical to subvertical and relatively straight, although abrupt changes in burrowing direction occasionally produced tortuous burrow axes. The smaller size of enclosures used in the initial experiment prevented the development of spatially extensive burrow networks (Fig. 31B–C). Since sediment laminae in this experimental setup were much thicker than the amount of sediment transported in a single excavation session, individual meniscate backfill patterns were more difficult to observe. They were mostly visible near boundaries between layers of colored sand.

Grubs produced more extensive traces in experiment 2 due to the larger size of the enclosure (Fig. 32A–F). Meniscate backfill was also more visible in this experiment due to the thinner sediment laminae; these were narrower than the amount of sediment excavated by the grub in each burrowing session, resulting in a mixture of colors within each backfill packet. Some of the natural sand layers used in experiment 2 were preferentially burrowed, resulting in horizontal traces extending across the length of the enclosure (Fig. 32D). These layers were preferentially burrowed presumably due to their higher organic matter content, which was exploited as a food source. The majority of bioturbation was around the edges of the enclosure, reflecting the movement of the organism laterally until it reached the enclosure wall (Fig. 32E–F).

In experiment 3, the lack of contrast within the sediment prevented most backfill from being visible, even though the same burrowing process was used by the grubs (Fig. 35B–E). Burrows are traceable, however, due to their granular nature and higher porosity relative to the surrounding sediment (Fig. 35E–F). Although sediment is packed into the back of the burrow by the organism, void spaces are created between individual sediment packets. By the end of this experiment, the majority of sediment in the enclosure had been reworked by the grubs, creating burrows totaling several meters in length.

Burrow Size and Shape.—Burrow width was ~0.75 cm and remained consistent throughout the length of the burrow. Some burrows reached nearly 2 m in length (Fig. 35B–D), as the larvae continued to burrow, feeding on organic matter and likely searching for areas with higher organic matter. The length-width relationship leads to very high length-to-width ratio—>267:1. Burrow width is ~2 times the width of the grub's body. The burrow must be wide enough for the grub to curl into a C shape and hold sediment between the anterior and posterior parts of the abdomen, as well as to rotate 360º in the cell. Burrow diameters were likely circular; however, due to the nature of enclosures we were unable to determine whether burrows were precisely circular or slightly elliptical in cross section. Burrow length was controlled mostly by the size of the enclosure and the duration of burrowing experiment. In two cases, the grubs lived long enough to pupate and emerge as adults (see section on adult beetles). True branching was not observed in any of the experiments. Numerous false branches were produced as burrows intersected previously constructed burrows, or when a grub partially reburrowed a pre-existing backfilled burrow and deviated from the original course.

Orientation.—All burrows observed in these experiments had highly variable orientations, ranging from completely vertical to completely horizontal. Axes ranged from straight to highly tortuous. In some places, burrows were characterized by abrupt, angular changes in direction.

Fill.—Arcuate, densely packed meniscate backfill was created by the compaction of individual sediment balls, which were usually compacted to a thickness of 0.5–1 mm. Graded menisci were not observed. Each ball of sediment was not always placed at the center of the posterior end of the cell nor was it evenly packed against the back wall. This created shuffled or slightly asymmetric menisci in some areas. Pellets were not observed in any of the burrows, although cohesion of soil particles in experiment 3 led to a granular texture in some burrow fills.

Linings.—A thin (< 1 mm), discontinuous zone of disturbed sediment was visible along the exterior burrow margin. This was produced by the animal bracing itself against the chamber wall during excavation of sediment, rotation to the back of the cell, and packing the sediment onto the cell wall. This activity resulted in a passive, discontinuous sediment lining along the margins of the cell, which was visible in the resulting backfilled burrow.

Pupation Chambers.—Several weeks into the experiment, each surviving grub created a chamber (Fig. 33A) near the bottom of the enclosure in which to pupate. The larvae rotated and wiggled in all directions to emulate an ellipsoid to enlarge the locomotion cell. This behavior also caused the cell to be elongated. The larva primarily used its head and secondarily used its appendages to rework the sediment, and used the head and the tip of the abdomen to compact the sediment to form a lining of variable thickness. The pupation chambers were ~3.4 cm long and ~1.7 cm wide. The open pupation chamber was ~3 cm long and ~1 cm wide. A lining ~0.2–0.4 cm thick surrounded the open chamber (Fig. 33B–E). Vittum et al. (1999) report that pupation chamber linings are cemented by a secretion from the grub. Sediment composing the lining is also compacted due to grubs moving within their cell for an extended period of time. Adult beetles emerged from one of the terminal ends of the long dimension of the cocoons two weeks later and stayed within their subterranean chambers for several days (Fig. 33F). Exit burrows produced by the adults differed significantly from the burrowing traces made by the larvae (see section on adult burrows).

Burrowing Mechanism—Adults

Two adult masked chafer beetles emerged from pupae in experiment 2. Rather than using the excavation techniques exhibited by the larvae, the adults used a swimming-like behavior, pushing sediment around their bodies with their limbs as they moved through the sediment. It was more difficult to observe the burrowing mechanism used by the adults because they did not create a large, open cell. It appears that the adult beetles used their mandibles and head to chew into and loosen the sediment in front of them, while using a subtle side-to-side motion with their appendages. Excavated sediment was removed with the first pair of legs and passed backwards to the second and third pair of legs—essentially moving material backwards while the beetle moved forward. The second and third set of legs could be seen bracing against and moving along the margins of the burrow, particularly when the adult was against the glass. As the adult beetle moved forward, sediment also passively filled the previous occupied space by collapsing behind the beetle; thus, the fill is both passive and actively produced but does not closely resemble the backfill pattern of the larvae.

An identical burrowing mechanism by adult beetles was observed in preliminary burrowing experiments using the same types of colored sediment to test the viability of the enclosures (Fig. 37).

After the adult beetles exited the chambers, they did not immediately go to the surface in the enclosure. Instead they burrowed in multiple directions within the media. Adult beetles, however, spent much less time within the sediment compared to the larvae. After initially burrowing upward, the adults changed directions and burrowed downward and horizontally. This type of burrowing mechanism resulted in less disruption of sediment and a smaller diameter, less conspicuous trace.

Biogenic Structures—Adults

Overall burrow morphology of adult beetle traces was significantly different than the larval traces due to the substantially different burrowing mechanism, body plan, and behavior of adult beetles (Fig. 34). Adult beetles used in preliminary burrowing trials also produced burrows similar to those observed here (Fig. 37).

Size and Shape.—Burrow diameter ranged from ~0.3–0.5 cm and was generally narrower than those produced by larvae, even though adult body size was equal to or wider than the body size of the grubs. Smaller diameters were primarily the result of the different burrowing mechanism of the adults. Burrow axes of adult beetle traces also moved away from the glass so that only partial diameters were visible—this also resulted in discontinuous traces. Burrow diameters were likely circular; however, due to the nature of enclosures we were unable to determine whether burrows were precisely circular or slightly elliptical in cross section. Length of adult traces was also much less than that of larvae.

Orientation.—Adult burrows are vertically oriented more often than larval burrows; however, adults were observed to burrow horizontally and laterally in all directions. For example, the first-emerged adult produced a burrow consisting of a single loop from the pupation chamber to just below the surface, followed by downward movement toward the center of the enclosure. This beetle then moved laterally for several centimeters whereupon it died. The second-emerged beetle slowly burrowed upward and exited the sediment after a few days, producing a subvertical, slightly sinuous burrow.

Fill.—Vertical to subvertical burrows produced by upward-moving adult beetles contained downward-pointing, chevron-shaped fill (Fig. 34A–B), which was the result of sediment collapse rather than active backfilling. Horizontal burrows contained indistinct, poorly organized fill structures (Fig. 34C), resulting in a higher porosity zone of sediment disruption compared to surrounding media.

Linings.—No linings were observed in any of the adult burrows during these and preliminary experiments with adult chafer beetles. Instead, the burrow margins appear to be more irregular compared to the larval traces (Figs. 2–4, 6).

Trace Fossils in Core

Western Kansas core were examined for trace fossils analogous to the burrow morphology produced by masked chafer beetles. Core was found to contain a low-diversity, high-abundance assemblage of meniscate backfilled traces. These trace fossils (Fig. 38) are associated with intervals that commonly contain rhizoliths, redoximorphic features, and zones of gleying—all characteristics of paleosols. Features of these burrows include packeted meniscate backfill, thin discontinuous linings, and unbranched, highly sinuous axes. Burrow diameters are variable and range from 0.09–1.06 cm. Meniscate backfill and packeting of menisci are visible in many burrows. Visibility of backfill is largely dependent on redoximorphic coloration and the proximity to zones of gleying; burrows near or within light-colored areas stand out in contrast to the surrounding matrix.

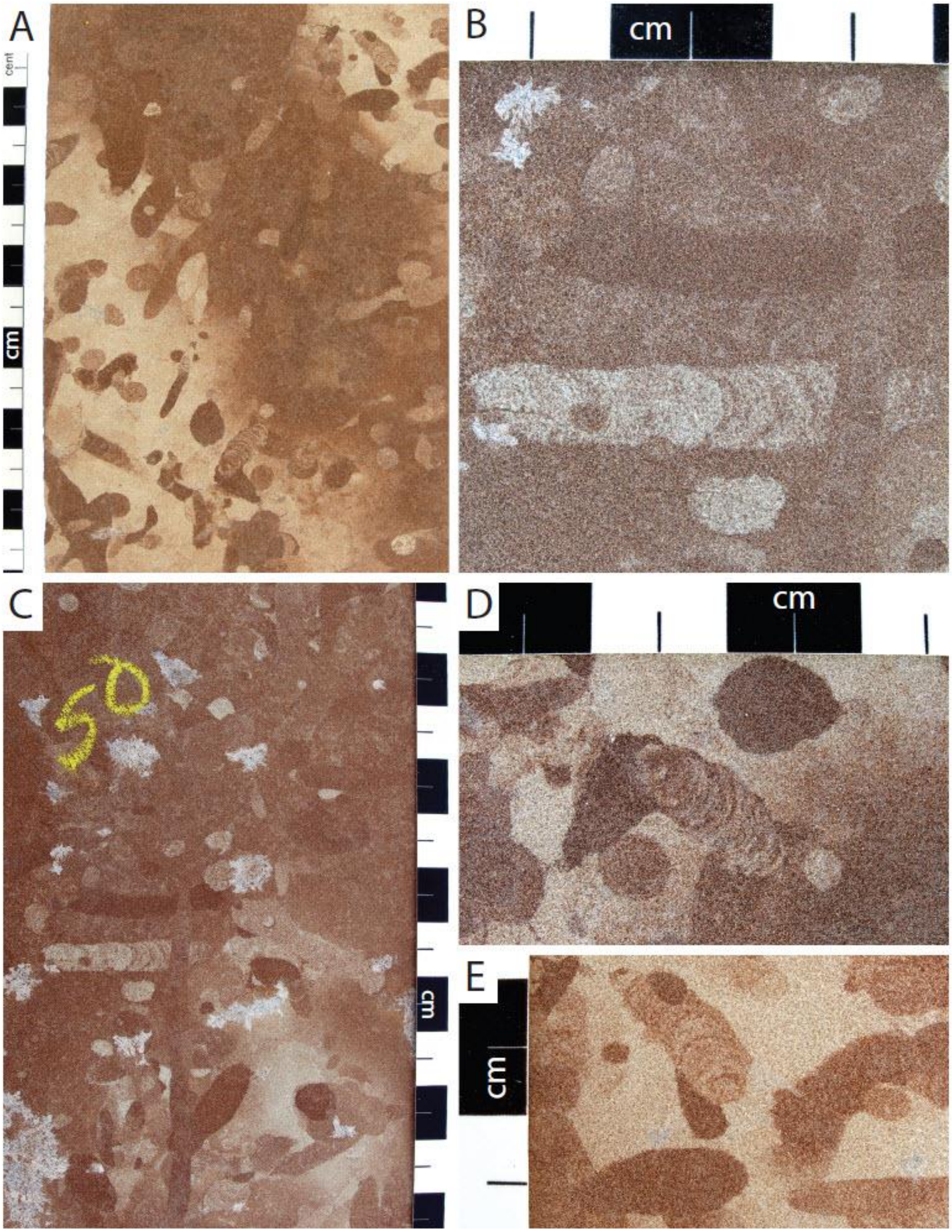
A
cent
cm
B
cm
C
50
cm
D
cm
E
cm

Figure 38. Trace fossils from Lower Permian Council Grove Group seen in core. A) Core surface showing high density of burrows in silt matrix. B) Close up of individual burrows showing meniscate backfill. C) Core surface showing high-density of burrows, composite burrows, and cross-cutting relationships. D–E) Close ups of individual burrows

Discussion

Masked chafer beetles produce different types of traces as larvae and adults. Backfilled meniscate burrows and walled ellipsoidal chambers are produced by the larvae, while adults produce poorly organized backfilled burrows. Trace morphology is controlled by the burrowing mechanism and behavior of the particular stage in the life history of the beetle. The behaviors of larvae and adults are an indication of their respective body morphologies.

Our results show that masked chafer larval burrows display highly organized, tightly spaced, shuffled meniscate backfill that form as the grub actively packs sediment into the rear of its locomotion cell. The larvae have several morphologic adaptations that make its unique burrowing mechanism possible. The sclerotized head and mandibles (see Fig. 30; Supplemental data) serve as a shoveling apparatus with which the grub excavates sediment. The long, C-shaped, soft abdomen of the grub allows it to change its shape readily during excavation, rotation, and transport of the sediment package. The grub uses the posterior of the abdomen to maintain its position in the cell while excavating with its head and mandibles. The position of the legs near the front of the body allows the grub to consolidate sediment into a ball between the anterior and posterior of the abdomen, which is held by the third pair of legs. The continuous contact of the grub’s body with the cell wall during the entire burrowing process can be referred to as a form of thigmotactic behavior, i.e., an organism's response to continuous contact with a solid surface (e.g., Hasiotis, 2003). The larval body plan is thus ideally suited for a fossorial lifestyle.

Masked chafer adult beetle traces did not form the distinct arcuate backfill seen in larval traces, due to their swimming type of locomotion behavior. Poorly organized backfill and irregular burrow margins are formed because the adult does not create a large open cell in which to physically carry excavated material from the front and pack it into the rear of the cell. Swimming-like locomotion allows the sediment to collapse behind the beetle as it moves forward. Since sediment grains were simply transported around the beetle's body by the legs, the resulting burrows may lack a high degree of organization (Fig. 37).

In more compact sediment, adult beetles would likely form an irregularly shaped, elongate cell that is slightly longer than its body. The backfill would be poorly organized because the body plan of an adult beetle prevents it from using an excavation-forward, rotation-packing method similar to that of the larvae. Excavated sediment would still be transported around the body of beetle by the legs and would likely produce a granular or vuggy fill. The resultant burrow would not have been open to the soil or sediment surface. This kind of burrow morphology would be recognized as having sharp, irregular walls with or without scratch marks depending on media firmness and grain size, and granular to vuggy fill.

Masked chafer larvae contribute to bioturbation and soil formation much more than adults. Throughout the larval stage, grubs are continually moving through the sediment. Adult beetles, however, spend most of their life above ground, and female adults usually burrow only 2–4 cm below the soil surface to deposit eggs (Potter, 1983). Adult beetle traces, therefore, are much less extensive than those of larvae. The burrowing mechanism of larvae also physically disturbs the soil more than that of adults—the swimming-like mechanism of adults results in little net movement of soil particles, while larvae actively transport sediment within their burrow.

The three experiments demonstrated that the introduction of larvae at the surface of the experiments had no adverse effect or bias on the burrow morphology or burrowing behavior of the larvae. In natural settings adults lay eggs belowground where the larvae hatch and begin to burrow. Placement of the larvae at the surface did not introduce any bias with respect to the depth of burial and amount of sediment compaction, which would have been introduced if the larvae had been artificially buried. All three experiments also showed that the larvae used the same burrowing mechanism and produced the same burrow morphologies regardless of the laminae thickness, sediment composition, or organic content.

Other Modern Meniscate Burrows and Burrowing Mechanisms

Studies describing modern terrestrial meniscate burrows are relatively uncommon (e.g., Willis and Roth, 1962; Ratcliffe and Fagerstrom, 1980; Brussaard, 1983; Brussaard and Runia, 1984; Brussaard, 1985; O'Geen and Busacca, 2001; Smith and Hasiotis, 2008). Ratcliffe and Fagerstrom (1980) illustrated many modern terrestrial traces and their tracemakers, but did not describe meniscate burrow patterns or burrowing mechanisms. O'Geen and Busacca (2001) described crescentic filled burrows interpreted to have been produced by cicadas, but did not observe or describe their burrowing methods. Modern masked chafer pupation chambers have been well illustrated and summarized by Vittum et al (1999). Brussaard and Runia (1984) and Brussaard (1985) briefly described the morphology of dung beetle burrows. Studies documenting the burrowing mechanisms that produce backfilled meniscate burrows are nearly nonexistent with the exception of Brussaard (1983) and Smith and Hasiotis (2008).

*Dung Beetles (*Typhaeus typhoeus).—Brussaard (1983) conducted experiments similar to those used in our study with actively reproducing dung beetles (*Typhaeus typhoeus*), and described their burrowing mechanism as well as burrow morphology. Together, adult male and female beetles of *T. typhoeus* excavate burrows for reproduction; these are composed of a vertical shaft with several horizontal chambers constructed and filled at different times and depths during excavation. The female lays an egg at the end of the horizontal chamber after copulation and then backfills the end part of the chamber with soil to form a separate egg chamber; no menisci are produced. The remaining portion of the horizontal chamber is backfilled with dung to form a dung sausage. Dung is compacted into the chamber by the female with her head and thorax, intermittently turning around her body length axis to apply equal force to different points of the dung to produce a meniscate backfilled pattern. We interpret the wording in Brussaard (1983) to mean that the female remains oriented in the same direction and rotates about the long axis of the body. The dung sausage is then sealed with sand scraped from the walls from the open shaft several centimeters above the end of the dung sausage. The larvae, after hatching, burrows into the dung using a somersaulting motion, which was not described in detail. The larva, through three instars of growth, eats its way through the dung sausage multiple times, backfilling the space behind it with its own excrement; the exact behavior and burrowing mechanism during this stage was not detailed. The pupation chamber is constructed in the original position of the egg chamber, where a void is created and the chamber wall is plastered with the larva's excrement. The newly hatched adult remains in the chamber for a few days to a few weeks, after which time the adult usually exits to the surface by excavating their own exit burrow. The adult excavates upward, scraping sand from above, turning around, and packing it the pupation chamber or dung sausage, although the turning process was not elucidated. This produces an 8-cm-long corridor (i.e., elongate cell or chamber) that moves upward with the adult beetle until it reaches the ground surface; it emerges to begin the lifecycle again. No cell length-to-body length ratios for the dung beetle larvae or adults were reported by Brussaard (1983).

The burrowing process of adult dung beetles is distinctly different from that exhibited by adult masked chafer beetles. Dung beetles used combined male-female excavation to construct their reproductive burrow system, whereas the newly hatched adult dung beetle uses some form of excavation, turning, and packing to produce a vertical exit burrow. The final exit burrow morphology is analogous to the trace fossil *Skolithos*, which is an open vertical tube. Adult masked chafer beetles burrow into and out of the soil using only a swimming motion and do not produce an open cell (i.e., void space) that moves in unison with the individual. No open cell or vertical burrow was been observed with the adult masked chafer beetles.

Dung beetle larvae use a somersaulting behavior to produce a backfilled burrow similar to the masked chafer beetle larvae; however, a dung beetle larva only produces a backfilled burrow within its dung sausage. The extent of this burrowing behavior differs greatly from that of masked chafer beetle larvae, which can produce meniscate backfilled burrows that are several meters long. The burrows of masked chafer beetle larvae, therefore, have a greater chance of preservation and a greater effect on pedoturbation and the rhizosphere compared to the burrows of dung beetle larvae.

The morphology of pupation chambers of dung beetle and masked chafer beetle larvae appears to be similar in size and shape, although the construction methods of the pupation chambers appear to differ. Dung beetle larvae have a chamber lining of excrement, whereas masked chafer beetle larvae have a thickened chamber wall of sand and body secretions produced by the larvae. Adult dung beetles actively backfill their pupation chambers with sediment removed during construction of a vertical exit corridor that eventually becomes an open vertical burrow at the surface. Pupation chambers of masked chafer beetle larvae are not actively filled.

*Prairie Cicada (*Cicadetta calliope*).*—Meniscate burrows and burrowing mechanisms of prairie cicada nymphs of *Cicadetta calliope* Walker 1850 (Hemiptera: Cicadidae) were observed by Smith and Hasiotis (2008) in unsaturated sediments in laboratory experiments. The experimental design was similar to that described here.

The burrowing mechanism of cicada nymphs consists of an excavation-rotation-packing process similar to that of masked chafer larvae. Like the masked chafer larvae, a nymph maintains an open cell as it moves through the sediment, excavating material from the front, forward rolling to reverse direction, and then packing the sediment ball onto the rear of the cell. The cicada nymph appeared to always use a forward roll to change direction in the cell, even when excavating upside down. Rather than using the head and mandibles, the cicada nymph almost exclusively used its large forelimbs to penetrate sediment, pull it towards the head, and consolidate it into a ball held against the ventroanterior portion of the thorax just below the head. Simultaneously, hindlimbs were used to brace the nymph against the cell wall. Alternating thrusts of the left and right forelegs were used to pack the sediment ball at the rear of the burrow.

The morphology of the cicada nymph burrows also shares many similarities with burrows constructed by masked chafer larvae. Packeting of menisci is more evident in cicada burrows, reflecting periods of inactivity followed by a return to burrowing with a slight change in direction. Cicada nymph burrows are larger in diameter and more irregular, as a result of the larger body size and the particular style of forward rotation of the tracemaker. The cell length-to-body length ratio for cicada nymphs was larger than that for the masked chafer larvae. Overall burrow length in the cicada experiments was shorter owing to the smaller size of the enclosures, which led to lower length-to-width ratios. Fifth instar cicadas constructed open emergence burrows, which were not constructed by masked chafer larvae or adults (see Smith and Hasiotis, 2008, for a full description). These burrows are also analogous to *Skolithos*, and may be similar in morphology to the vertical exit burrows of adult dung beetles.

Preservation Potential

Burrows of masked chafer beetles have an excellent chance of being preserved in the fossil record, despite potential overprinting by pedogenesis. Masked chafers as well as other types of scarabaeid beetles are extremely common in certain habitats, reaching densities as high as 40 grubs per 0.1 m^2 in turfgrass (Potter and Gordon, 1984; Dalthorp et al., 2000). As important components of soil biota and pedogenesis (Hole, 1981; Hasiotis, 2007; Hasiotis et al., 2007), masked chafer larvae and adults have the ability to significantly bioturbate upper soil horizons in all stages of their life cycle. Most grub activity takes place within the soil root zones (e.g., Potter, 1983; Potter and Gordon, 1984; Potter et al., 1996; Vittum et al., 1999), which include the A and upper B horizons. Deeper burrows produced by grubs during overwintering or during the dry season are less susceptible to reworking by soil biota and other pedogenic processes, including future generations of masked chafers.

Larval burrows far outnumber burrows made by adults or pupae. At least 80% of the chafer beetle life cycle is spent beneath the sediment surface as a larva (Vittum et al., 1999). Winter mortality rates of larvae may be as high as 50% (Vittum et al., 1999), and mortality rates of both eggs and larvae dramatically increase during times of drought (Potter, 1983; Potter and Gordon, 1984). Fewer grubs thus survive to adulthood and larval populations are likely to exceed adult populations. The behavior of larvae also produces more extensive burrows compared to adults because larvae feed underground and continually move in search of new food sources. Higher adult to larvae burrow ratios in a given area would, therefore, indicate favorable moisture and temperature conditions for masked chafer survival, and theoretically could be used as climate, rainfall, or soil-moisture proxies.

In general, backfilled burrows rarely are observed in modern soils. Burrow-fill material like that observed in these experiments is unaltered during the burrowing process and compositionally and texturally identical to the surrounding soil matrix, with the exception of masticated plant material and feces included in the backfill. The burrowing mechanism of larvae disturbs the soil to a greater extent when compared to adults. Adult beetle traces may be less conspicuous in the field owing to their lower abundance, smaller size, and lack of significant sediment disruption. In some cases in the laboratory experiments, porosity and permeability were variable in the burrow fill, which may have enhanced burrow preservation and visibility. Since larval burrows are constructed in three dimensions, it is unlikely that the entire length of a single burrow would be visible in a given exposure. Length-to-width ratios, therefore, could not be accurately determined.

Meniscate backfill burrows are visible in many continental trace fossils due to redoximorphic coloration produced by differences in organic matter content between individual menisci (Hasiotis and Bown, 1992; Hasiotis et al., 1993, Retallack, 2001b). Larval and adult burrows may be highlighted by preferential gleying—the redistribution of Fe and Mn in the soil profile in the presence of organic matter due to water-table fluctuations (e.g., Schwertmann, 1993; Vepraskas, 1999)—to produce mottles of various colors. These mottles would highlight individual backfill and overall backfill patterns similar to the production of mottles in association with rhizoliths (Kraus and Hasiotis, 2006). In natural settings, masked chafer larvae would leave fecal pellets in their burrow as they ingested disseminated organic matter and fed on plant roots. This would lead to organic-rich and organic-poor parts of the burrow fill, and would increase the visibility of menisci and menisci packets through redoximorphic coloration. Such patterns in meniscate backfilled burrows have been observed in the Upper Triassic Chinle Formation, Upper Jurassic Morrison Formation, Paleogene Willwood Formation, and Miocene alluvial deposits in Spain (e.g., Hasiotis et al., 1993; Hasiotis and Dubiel, 1994; Hasiotis, 2002, 2004). If chafer burrows are preserved in the geologic record, the thin linings along the exterior burrow margins may or may not be visible because they are extremely thin and discontinuous, usually only a few sediment grains wide. Visibility of linings would be dependent on diagenetic enhancement.

Pupation chambers may have a high preservation potential; however, a beetle larva can only pupate once and results in a single chamber per grub. This activity pales in comparison to the amount of bioturbation produced during the adult stage and, particularly, during the larval stage. Cell linings of pupation chambers are relatively thick and are reported to be reinforced by the larvae through some type of secretion (Vittum et al., 1999). The cell is more likely to remain open for an extended period of time, which increases its chance of being preserved as an open void. Pupation cells may also be filled with sediment washed down through the higher-porosity exit burrow left by the adult, producing passively filled, ellipsoidal molds and casts, which are common trace fossils (see section on Ellipsoidal Trace Fossils). The larval exuvia, shed within the cell, further increase the concentration of organic matter and may contribute to increased preservation during diagenesis.

Fossil Record of Meniscate Backfilled Burrows

Several features of chafer larval burrows distinguish them from previously described meniscate traces (Table 3). Chafer larval burrows do not show the high density, short, longitudinal striations of *Scoyenia* or the distinct thick continuous walls of *Ancorichnus* (Frey et al. 1984; Keighley and Pickerill, 1994). *Laminites* (Ghent and Henderson, 1966) can also be excluded as an analog for chafer larval burrows because individual menisci are not continuous across the entire burrow. *Beaconites* has shuffled menisci, often composed of alternating coarse- and fine-grained sediment, which are not contained within packets (Gevers et al., 1971; Bradshaw, 1981). Backfill in chafer larval burrows does not show size sorting or textural differences and thus, is not analogous to *Beaconites*. Ichnospecies of *Taenidium* as recognized by D'Alessandro and Bromley (1987) are morphologically inappropriate as analogs for the morphology exhibited by chafer burrows. The thick, size-sorted backfill of *T. satanassi* and the thick, symmetrical, regularly spaced backfill of *T. cameronensis* and *T. serpentinum* (D'Alessandro and Bromley, 1987; Keighley and Pickerill, 1994) are inconsistent with the thin, homogeneous, slightly asymmetric backfill and packeted menisci observed in chafer beetle larvae burrows.

Adhesive meniscate burrows (AMB), however, cannot be ruled out as analogues for chafer beetle larval burrows, based on the morphological features observed in these experiments. AMB were first described in Eocene deposits by Bown and Kraus (1981, 1983), and occur in paleosols as old as the Permian (Counts and Hasiotis, 2006, 2007). Smith et al. (2008) erected the ichnotaxon *Naktodemasis bowni* for burrows exhibiting the morphology diagnostic of AMB, which have been likened to the burrows of cicadas, other hemipterans, and beetle larvae (Smith and Hasiotis, 2008). These traces are common in paleosols, are often found in association with rhizoliths, and have previously been attributed to insect larvae (Hasiotis and Bown, 1992; Hasiotis and Dubiel, 1994; Hasiotis, 2002, 2004, 2007; Smith et al., 2008). *Naktodemasis bowni* burrows are characterized by a series of offset ellipsoid-shaped packets composed of thin menisci—a feature present but not as pronounced in the experimentally produced traces. These burrows are straight to sinuous, variably oriented, unbranched, and unlined and are described as having short sections composed of unbound menisci. Packets of menisci are visible in some, though not all, sections of chafer larvae burrows (Fig. 32); where visible, packets are longer and better organized than those described in *N. bowni*. Packeting in *N. bowni* is hypothesized to be the result of periods of resting or changes in direction between intervals of continuous movement (e.g., Hasiotis and Dubiel, 1994; Hasiotis 2002, Smith et al., 2008). Chafer larvae burrows are similar, but not identical to *N. bowni*, and trace fossils with morphologies similar to larval burrows may be classified as a new ichnospecies of *Naktodemasis*. The current study presents another burrowing mechanism that produces burrow morphologies similar to *Naktodemasis.*

Masked chafer beetle larvae burrows are also similar in morphology to meniscate backfilled burrows observed in continental deposits within the Lower Permian Council

Grove Group in the subsurface of western Kansas (Dubois and Goldstein, 2005; Counts and Hasiotis, 2006) (Fig. 38). Both masked chafer burrows and Permian burrows are characterized by packeted meniscate backfill, highly sinuous unbranched axes, and thin discontinuous linings. The burrow morphologies illustrated here from western Kansas core are the oldest documented morphology that may represent a burrowing behavior similar to that observed in extant masked chafer beetle larvae.

Adult beetle traces are not easily comparable to known trace fossils. Morphology of adult beetle egg-laying and emergence burrows may change considerably depending on the burrowing media. Their traces, therefore, may not have morphological features that are diagnostic.

Ellipsoidal Trace Fossils

Ellipsoidal cells constructed by the masked chafer larvae as pupation chambers superficially resemble passively filled ellipsoidal cells in paleosols found as early as the Triassic (e.g., Hasiotis, 2002, 2003). *Celliforma* is a slightly ellipsoidal to flask-shaped trace fossil with a spiral terminus and constriction at one end of the cell that indicates the trace is most likely produced by bees (e.g., Brown, 1934; Genise and Bown, 1994; Hasiotis, 2002, 2003). *Fictovichnus* (Johnston et al., 1996) is a small, ellipsoidal trace surrounded by a clay-rich zone and occasional passive infilling. Johnston et al. (1996) attribute *Fictovichnus* to the pupation chambers of beetles by comparing fossil specimens with specimens of modern pupation chambers (length-to-width ratio of 1.64:1). Masked chafer pupation chambers are much more elongate (length-to-width ratio of interior cell ~3:1; including lining ~2:1) than the type specimens of *Fictovichnus* (length to width ratio of 1.5:1 to 1.7:1). Considering all the morphological features, masked chafer pupation chambers do not conform to either *Celliforma* or *Fictovichnus*.

Rebuffoichnus and *Teisseirei* are similar to *Fictovichnus* in that they are ellipsoidal and may be surrounded by an actively constructed lining with a terminal emergence hole. Both are tentatively attributed to pupation chambers of Coleoptera. Genise (2004) distinguishes these ichnotaxa in that *Teisseirei* is characterized by an internal bioglyph and a depressed (i.e., ovate) cross section, whereas *Rebuffoichnus* differs by lacking an active fill and the presence of a rounded hole. These characters are not necessarily mutually exclusive, however. For example, photographs of *T. barattinia* in Genise (2004, Fig. 3b) show a terminal emergence hole, although this character has been used to distinguish *Rebuffoichnus* from other ellipsoidal traces. Regardless of the taxonomic uncertainty, the size and preservation of *Rebuffoichnus* and *Teisseirei* preclude masked chafer larvae as the potential tracemakers of these ichnotaxa. The abundance of ellipsoidal cells in the fossil record, however, does demonstrate that pupation chambers like those produced by masked chafer beetles are often preserved in the geologic record.

Implications And Significance

Paleontological Significance

Although body fossils are often used to note the first appearance of a particular taxon, the presence of diagnostic trace fossils may serve as an alternative way to identify past occurrences of an organism. The presence of traces similar to those produced by extant masked chafer larvae in Permian paleosols, for example, implies the early evolution of a comparable larval body plan and burrowing, feeding, and reproductive behaviors in certain insects at that time. The trace fossils in paleosols from the Early Permian suggest that the tracemaker had well-developed burrowing adaptations with a C-shaped, grublike larva that bore a large sclerotized head, strong biting mandibles, and well-developed legs. These features are also characteristic of the superfamily Scarabaeoidea (Grimaldi and Engel, 2005). Though it may not be possible to determine the morphology of the adult from the Permian trace fossils, it could be possible that the adult form of the tracemaker was similar in body plan to the adult masked chafer beetle. Such striking similarities in burrow morphologies, therefore, may indicate an earlier origination for the Scarabaeoidea. This possibility is supported by the fact that the earliest beetle-like fossils are Early Permian (Kukalová-Peck and Willmann, 1990), and additional evidence indicates that beetles had diversified by the Triassic (e.g., Rasnitsyn and Quicke, 2002; Grimaldi and Engel, 2005; Hunt et al., 2007).

Paleoecological Implications

Previous studies have hypothesized that backfilled burrows are made exclusively in subaqueous settings by deposit-feeding invertebrates that ingest sediments at one end and excrete sediments and waste products at the other end to produce meniscate backfill, and that it is unlikely that insects produce backfilled burrows (i.e., Frey et al., 1984; Squires and Advocate, 1984; Genise, 2004; Genise et al., 2004; Buatois and Mángano, 2004, 2007; Bromley et al., 2007). This study demonstrates conclusively that such insects as masked chafer beetle larvae produce actively backfilled burrows in terrestrial, subaerial well-drained settings without ingesting sediment or wholesale deposit feeding. Meniscate burrows may occur in a much wider range of environments than previously thought; therefore, meniscate burrows in general cannot be said to be diagnostic of any specific depositional environment.

Environments previously thought to be subaqueous fluvial, lacustrine, or marine in origin based on the presence of meniscate backfilled burrows need to be reevaluated in light of the data presented here and similar recent neoichnological research (e.g., Smith and Hasiotis, 2008).

Similarities in burrow morphology between masked chafer larvae traces, cicada nymphs (Smith and Hasiotis, 2008), and *Naktodemasis* (Smith et al., 2008) demonstrate that forms of *Naktodemasis* are likely produced by soil-dwelling insect larvae. *Naktodemasis* burrows have been found only in paleosols; therefore, they are likely to be diagnostic of subaerial exposure and soil formation. Beetle larvae, such as masked chafers, have specific moisture tolerances ranging from 18–27% (Potter, 1983; Potter and Gordon, 1984). If the tracemaker of *Naktodemasis* is an insect larva similar to that of masked chafers, the presence of *Naktodemasis* likely indicates that burrowing occurred within a limited range of soil moisture content within the vadose zone, where moisture content on average was below saturation but above the wilting point, i.e., the minimum soil moisture at which a plant wilts and cannot recover (e.g., Brady and Weil, 2002), for a particular soil. *Naktodemasis* would, therefore, also indicate the presence of adequate vegetation (i.e., rhizoliths) or organic matter within the soil because larvae need a consistent food source to survive. Since the presence of the masked chafer-like trace fossil *Naktodemasis* is indicative of soil formation, these traces may prove to be useful in recognizing paleosols as sequence boundaries and as sea-level lowstand deposits when found in combination with other pedogenic features that overprint marine deposits.

Conclusions

Masked chafer larvae burrow by creating an elliptical, open cell that is actively moved forward. The larvae excavate sediment from the front of the cell and deposit it at the back in a five step process that includes excavation, consolidation, forward rotation, transport of sediment, and packing. Sediment is excavated through a scraping motion of the larva’s mandibles and head and is moved toward the center of the body with the first pair of limbs. The legs and body consolidate the sediment into a ball, forming a C-shape around the package. The grub rotates forward until the head is at the posterior end of the chamber where the sediment ball is pushed to the back of the chamber with the head, limbs, and the front portion of the body. The legs and the head simultaneously compact the sediment ball to into the cell wall in all directions. The result of this burrowing mechanism is a series thin menisci. Packets are formed when the larvae excavate, stop to rest or feed, and restart the burrowing process again.

High length-to-width ratios and thin, slightly offset menisci characterize masked chafer larvae burrows. Meniscate backfill are mostly contained within packets that result from periods of inactivity followed by a change in burrowing direction. Larval burrows are also characterized by thin, discontinuous linings and a lack of true branching. Orientation and tortuosity are highly variable.

Masked chafer pupation chambers are elongate, ellipsoidal cells with a variably thick lining. Pupation chambers are larger and more elongate than locomotion cells, and may have an emergence hole. Pupation chambers are left open by the exiting adult beetle, and subsequently may be infilled passively through time. Traces produced by masked chafer adults do not have a clear morphological signature and may not be identifiable if taphonomically or pedogenically modified by other biotic (including larval bioturbation) and abiotic processes.

Overall morphology of masked chafer larvae burrows is similar to *Naktodemasis* (AMB; Smith et al. 2008), which are interpreted to have been produced by C-shaped insect larvae and represent locomotion and dwelling behaviors. Our results add further evidence to the hypothesis that *Naktodemasis* is exclusively formed in subaerial environments and is associated with pedogenesis (e.g., Bown and Kraus, 1983; Hasiotis and Bown, 1992; Hasiotis, 2002, 2004, 2007; Hasiotis et al., 2007; Smith et al., 2008). Given the environmental tolerances of masked chafer beetle larvae, traces similar to masked chafer burrows may also be useful for reconstructing soil-moisture levels of ancient deposits, which in turn can be used for paleoenvironmental and paleoclimatic reconstruction. The presence of such burrows also implies the presence of vegetation or another source of soil organic matter. Trace fossils with morphologies similar to those traces produced by masked chafer beetle larvae may be used to extend the geographic and stratigraphic range in the geologic record of beetle taxa with similar larval body plans. Our research suggests that this may be possible for members of the Scarabaeoidea with C-shaped larvae, well-developed appendages, and a large sclerotized head, which may have evolved as early as the Permian.

This research serves as a springboard for more experiments with masked chafer beetle larvae as well as with other tracemaking continental organisms to more fully investigate the influences that local media composition, soil moisture, and climate have on the viability and distribution of populations and the nature of their burrows with respect to those influences. The relationship between burrow morphology and organism behavior in both modern and ancient continental deposits can be better understood through the detailed study of extant tracemaking organisms. The present study highlights the need for additional neoichnologic research with burrowing organisms that live in various terrestrial as well as aquatic settings. Detailed knowledge of extant traces and their tracemakers in the continental realm can be used to recognize the presence of related taxa or behaviors in deposits where body fossils are not preserved, as well as to aid in the reconstruction of evolutionary histories. Continental trace fossils can be calibrated against similar trace morphologies produced in neoichnological studies where the physicochemical conditions of the media and the physiology of the organism are known. This will lead to more accurate paleoenvironmental, paleohydrologic, and paleoclimatic interpretations using continental trace fossils.

Acknowledgments

This research was funded by National Science Foundation grant EAR-0229300 to STH. JWC acknowledges the Geological Society of America, American Association of Petroleum Geologists R.C. Moore Memorial Grant, and University of Kansas Department of Geology Joseph M. Patterson Scholarship and Summer Field Research Award for financial and research support. We thank Ian Rowell, Jon Smith, and the University of Kansas IchnoBioGeoScience research group, and KU Paleosols and Ichnology classes for assistance with fieldwork, insect collection, and experimental setup and design. Frank Krell, an anonymous reviewer and an Associate Editor, and Coeditor Edith L. Taylor provided thoughtful and constructive editorial comments that greatly improved the clarity of the manuscript.

References

BAUERNFEIND, R.J., 2001, Distribution of *Cyclocephala* spp. (Coleoptera: Scarabaeidae) in Kansas. Environmental Entomology, v. 30, p. 899–902.

BOWN, T.M., and KRAUS, M.J., 1981, Lower Eocene alluvial paleosols (Willwood Formation, Northwest Wyoming, U.S.A.) and their significance for paleoecology, paleoclimatology, and basin analysis: Palaeogeography, Palaeoclimatology, Palaeoecology, v. 34, p. 1–30.

BOWN, T.M., and KRAUS, M.J., 1983, Ichnofossils of the alluvial Willwood Formation (lower Eocene), Bighorn Basin, northwest Wyoming, U.S.A.: Paleogeography, Paleoecology, Paleoclimatology, v. 43, p. 95–128.

BROWN, R. W., 1934, *Celliforma spirifer*, the fossil larval chambers of mining bees: Journal of the Washington Academy of Sciences, v. 24, p. 532–539.

BRADSHAW, M. A., 1981, Paleoenvironmental interpretations and systematics of Devonian trace fossils from the Taylor Group (Lower Beacon Supergroup), Antarctica: New Zealand Journal of Geology and Geophysics, v. 24, p. 615–652.

BROMLEY, R. G., 1996, Trace Fossils: Biology, Taphonomy and Applications, Second Edition: Chapman & Hall, London, 361 p.

BROMLEY, R.G., BUATOIS, L.A., GENISE, J.F., LABANDEIRA, C.C., MÁNGANO, M.G., MELCHOR, R., SCHLIRF, M., and UCHMAN, A., 2007. Discussion of the paper “Reconnaissance of the Upper Jurassic Morrison Formation ichnofossils, Rocky Mountain Region, U.S.A.: paleoenvironmental, stratigraphic, and paleoclimatic significance of terrestrial and freshwater ichnocoenoses” by Stephen T. Hasiotis. Sedimentary Geology, v. 200, p. 141–150.

BRUSSAARD, L., 1983, Reproductive behavior and development of the dung beetle *Typhaeus typhoeus* (Coleoptera, Geotrupidae): Tijdschrift voor Entomologie, v. 126, p. 203–231.

BRUSSAARD, L., 1985, Back-filling of burrows by the scarab beetles *Lethrus apterus* and *Typhaeus typhoeus* (Coleoptera: Geotrupidae): Pedobiologia, v. 28, p. 327–332.

BRUSSAARD, L. and RUNIA, L.T., 1984, Recent and ancient traces of scarab beetle activity in sandy soils of the Netherlands: Geoderma, v. 34, p. 229–250.

BUATOIS, L.A., and MÁNGANO, G.M., 2004, Animal-substrate interactions in freshwater environments; applications of ichnology in facies and sequence stratigraphic analysis of fluvio-lacustrine successions, *in* McIlroy, D., ed., The Application of Ichnology to Paleoenvironmental and Stratigraphic Analysis: Geological Society Special Publication 228, London, p. 311–333.

BUATOIS, L. A., and MÁNGANO, M. G., 2007, Invertebrate ichnology of continental freshwater environments, *in* Miller, W., Trace Fossils: Concepts, Problems, Prospects. Elsevier, Oxford, UK, 637 p.

COUNTS, J.W., and HASIOTIS, S.T., 2006, Ichnology of cyclothem deposits in the Lower Permian Council Grove Group (Kansas, USA): Geological Society of America Abstracts with Programs, v. 38, p. 435.

COUNTS, J.W. and HASIOTIS, S.T., 2007, Neoichnology of scarab beetle larvae: modern analogues for backfilled trace fossils: Geological Society of America Abstracts with Programs, v. 39, p. 54.

CROWSON, R. A., 1981, The Biology of the Coleoptera: Academic Press, New York, 802 p.

DALTHORP, D., NYROP, J., and VILLANI, M. G., 2000, Spatial ecology of the Japanese beetle, *Popillia japonica*: Entomologia Experimentalis et Applicata, v. 96, p. 129–139.

DUBOIS, M.K., and GOLDSTEIN, R.H., 2005, Accommodation model for Wolfcamp (Permian) redbeds at the updip margin of North America's largest onshore gas field: Kansas Geological Survey Open File Report 2005-25, http://www.kgs.ku.edu/PRS/AAPG2005/2005-25/index.html. Checked August 1, 2007.

D'ALESSANDRO, A., and BROMLEY, R.G., 1987, Meniscate trace fossils and the *Muensteria-Taenidium* problem: Palaeontology, v. 30, p. 743–763.

DURINGER, P., BRUNET, M., CAMBEFORT, Y., LIKIUS, A., MACKAYE, H.T., SCHUSTER, M., and VIGNAUD, P., 2000, First discovery of fossil dung beetle brood balls and nests in the Chadian Pliocene australopithecine levels: Lethaia, v. 33, p. 277–284.

EKDALE, A.A., BROMLEY, R.G., and PEMBERTON, S. G., 1984, Ichnology: the use of trace fossils in sedimentology and stratigraphy: SEPM Short Course 15, p. 1–317.

FREY, R.W., PEMBERTON, S.G., and FAGERSTROM, J.A., 1984, Morphological, ethological, and environmental significance of the ichnogenera *Scoyenia* and *Ancorichnus*: Journal of Paleontology, v. 58, p. 511–528.

GENISE, J.F., 2004, Ichnotaxonomy and ichnostratigraphy of chambered trace fossils in paleosols attributed to coleopterans, ants and termites, *in* McIlroy, D., ed., The Application of Ichnology to Paleoenvironmental and Stratigraphic Analysis: Geological Society Special Publication 228, London, p. 419–453.

GENISE, J. F., and BOWN, T.M., 1994, New Miocene scarabeid and hymenopterous nests and Early Miocene (Santacrucian) paleoenvironments, Patagonian Argentina: Ichnos, v. 3, p. 107–117.

GENISE, J.F., MÁNGANO, M.G., BUATOIS, L.A., LAZA, J.H., and VERDE, M., 2000, Insect trace fossil associations in paleosols; the *Coprinisphaera* ichnofacies: PALAIOS, v. 15, p. 49–64.

GENISE, J.F., BELLOSI, E.S., and GONZALEZ, M.G., 2004, An approach to the description and interpretation of ichnofabrics in paleosols, *in* McIlroy, D., ed., The Application of Ichnology to Paleoenvironmental and Stratigraphic Analysis: Geological Society Special Publication 228, London, p. 355–382.

GEVERS, T.W., FRAKES, L.A., EDWARDS, L. N., and MARZOLF, J. E., 1971, Trace fossils in the Lower Beacon sediments (Devonian), Darwin Mountains, southern Victoria Land, Antarctica: Journal of Paleontology, v. 45, p. 81-94.

GHENT, E.D., and HENDERSON, R.A. 1966, Petrology, sedimentation, and paleontology of Middle Miocene graded sandstones and mudstones, Kaiti Beach, Gisborne: Transactions of the Royal Society of New Zealand, Geology, v. 4, p. 147–169.

GRIMALDI, D., and ENGEL, M.S., 2005, Evolution of the Insects: Cambridge University Press, New York, NY, 755 p.

HALFFTER, G., and EDMONDS, W.D., 1982, The Nesting Behavior of Dung Beetles (Scarabaeinae): An Ecological and Evolutive Approach: Instituto de Ecología, Mexico, 176 p.

HANSKI, I., and CAMBEFORT, Y., eds., 1991, Dung Beetle Ecology: Princeton University Press, Princeton, New Jersey, 473 p.

HASIOTIS, S.T., 2002, Continental Trace Fossils: SEPM Short Course Notes 51, 132 p.

HASIOTIS, S.T., 2003, Complex ichnofossils of solitary and social soil organisms; understanding their evolution and roles in terrestrial paleoecosystems, *in* Miller, W., ed., New interpretations of complex trace fossils: Palaeogeography, Palaeoclimatology, Palaeoecology, v. 192, p. 259–320.

HASIOTIS, S. T., 2004, Reconnaissance of Upper Jurassic Morrison Formation ichnofossils, Rocky Mountain region, USA: environmental, stratigraphic, and climatic significance of terrestrial and freshwater ichnocoenoses: Sedimentary Geology, v. 167, p. 277–368.

HASIOTIS, S. T., 2007. Continental ichnology: fundamental processes and controls on trace-fossil distribution. In, Miller, W. III (ed.), Trace Fossils—Concepts, Problems, Prospects, Elsevier Press, p. 268–284.

HASIOTIS, S.T., and BOWN, T.M., 1992, Invertebrate trace fossils; The backbone of continental ichnology, *in* Maples, C.G., and West, R.R., eds., Trace Fossils: Short Courses in Paleontology, Number 5: The Paleontological Society, Knoxville, TN, p. 64–104.

HASIOTIS, S. T., and DUBIEL, R. F. 1994. Ichnofossil tiering in Triassic alluvial paleosols: Implications for Pangean continental rocks and paleoclimate: *in* Beauchamp, B., Embry, A. F., and Glass, D., eds., Pangea: Global Environments and Resources. Canadian Society of Petroleum Geologists Memoir, v. 17, p. 311–317.

HASIOTIS, S. T., ASLAN, A., and BOWN, T. M., 1993, Origin, architecture, and paleoecology of the early Eocene continental ichnofossil *Scaphichnium hamatum*—integration of ichnology and paleopedology: Ichnos, v. 3, p. 1–9.

HASIOTIS, S. T., KRAUS, M. J., and DEMKO, T. M., 2007. Climate controls on continental trace fossils. In, Miller, W. III (ed.), Trace Fossils—Concepts, Problems, Prospects, Elsevier Press, p. 172–195.

HOLE, F. D., 1981. Effects of animals on soil. Geoderma, v. 25, p. 75–112.

HUNT, T., BERGSTEN, J., LEVKANICOVA, Z., PAPADOPOULOU, A., ST. JOHN, O., WILD, R., HAMMOND, P.M., AHRENS, D., BALKE, M., CATERINO, M.S., GÓMEZ-ZURITA, J., RIBERA, I., BARRACOUGH, T.G., BOCAKOVA, M., BOCAK, L., VOGLER, A.P., 2007., A comprehensive phylogeny of beetles reveals the evolutionary origins of a superradiation. Science, v. 318, p. 1913–1916.

JOHNSTON, P. A., EBERTH, D. A., AND ANDERSON, P. K., 1996, Alleged vertebrate eggs from Upper Cretaceous redbeds, Gobi Desert, are fossil insect (Coleoptera) pupal chambers: *Fictovichnus* new ichnogenus: Canadian Journal of Earth Sciences, v. 33, p. 511–525.

KEIGHLEY, D.G., and PICKERILL, R., 1994, The ichnogenus *Beaconites* and its distinction from *Ancorichnus* and *Taenidium*: Palaeontology, v. 37, p. 305–337.

KRAUS, M. J., 1999, Paleosols in clastic sedimentary rocks: their geologic applications: Earth Science Reviews, v. 47, p. 41–70.

KRAUS, M. J., and HASIOTIS, S. T., 2006. Significance of different modes of rhizolith preservation to interpreting paleoenvironmental and paleohydrologic settings: examples from Paleogene paleosols, Bighorn basin, Wyoming: Journal of Sedimentary Research, v. 76, p. 633–646.

KRELL, F.T. 2000, The fossil record of Mesozoic and Tertiary Scarabaeoidea (Coleoptera: Polyphaga): Invertebrate Taxonomy, v. 14, p. 871–905.

KRELL, F.T., 2006, Fossil record of Scarabaeoidea (Coleoptera: Polyphaga): Coleopterists Society Monograph Number 5, p. 120–143.

KUKALOVÁ-PECK, J, and WILLMANN, R.,1990, Lower Permian “mecopteroid-like” insects from central Europe (Insecta, Endopterygota): Canadian Journal of Earth Science, v. 27, p. 459–468.

LAZA, J.H., 2006, Dung-beetle fossil brood balls: The ichnogenera *Coprinisphaera* Sauer and *Quirogaichnus* (Coprinisphaeridae): Ichnos, v. 13, p. 217–235.

MCCOLLOCH, J.W., HAYES, W.P., and BRYSON, H. R., 1928, Hibernation of certain scarabaeids and their *Tiphia* parasites: Ecology, v. 9, p. 34–42.

MERCHANT, M., BILES, S., and MOTT, D., 2004, White grubs in Texas turfgrass: Texas A & M University Extension Entomology E-publication E-211, http://insects.tamu.edu/extension/publications/html/e211.html. Checked August 1, 2007.

O'GEEN, A.T., and BUSACCA, A.J., 2001, Faunal burrows as indicators of paleo-vegetation in eastern Washington, USA: Palaeogeography, Palaeoclimatology, Palaeoecology, v. 169, p. 23–37.

O’GEEN, A. T., MCDANIEL, P. A., AND BUSACCA, A. J., 2002, Cicada burrows as indicators of paleosols in the inland Pacific Northwest: Soil Science Society of America Journal, v. 66, p. 1584–1586.

POTTER, D. A., 1983, Effect of soil moisture on oviposition, water absorption, and survival of Southern Masked Chafer (Coleoptera: Scarabaeidae) eggs: Environmental Entomology, v. 12, p. 1223–1227.

POTTER, D.A., 1998, Destructive Turfgrass Insects: Biology, Diagnosis, and Control: Ann Arbor Press, Chelsea, Michigan, 344 p.

POTTER, D.A., and GORDON, F.C., 1984, Susceptibility of *Cyclocephala immaculata* (Coleoptera: Scarabaeidae) eggs and immature to heat and drought in turfgrass: Environmental Entomology, v. 13, p. 794–799.

POTTER, D.A., POWELL, A.J., SPICER, P.G. and WILLIAMS, D.W., 1996, Cultural practices affect root-feeding white grubs (Coleoptera: Scarabaeidae) in turfgrass: Journal of Economic Entomology, v. 89, p. 156–164.

RASNITSYN, A.P., and QUICKE, D.L.J., 2002, History of Insects: Kluwer Academic Publishers, Norwell, MA, 517 p.

RATCLIFFE, B.C., and FAGERSTROM, J.A., 1980, Invertebrate Lebensspuren of Holocene floodplains: their morphology, origin and paleoecological significance: Journal of Paleontology, v. 54, p. 614–630.

RETALLACK, G.J., 2001a, *Scoyenia* burrows from Ordovician paleosols of the Juniata Formation in Pennsylvania: Paleontology, v. 44, p. 209–235.

RETALLACK, G.J., 2001b. Soils of the Past: An Introduction to Paleopedology, Second Edition: Blackwell Science, Oxford. 404 p.

RICHTER, P.O., 1966, White Grubs and Their Allies: Oregon State University Press, Corvallis, 219 p.

ROGERS, M.E., and POTTER, D.A., 2002, Kairomones from scarabaeid grubs and their frass as cues in below-ground host location by the parasitoids *Tiphia vernalis* and *Tiphia pygidialis*: Entomologia Experimentalis et Applicata, v. 102, p. 307–314.

SAUER, W., 1955, *Coprinisphaera ecuadorensis*, un fósil singular del Pleistoceno: Boletín del Instituto de Ciencias Naturales, Universidad Central del Ecuador, v. 1, p. 123–129.

SAVRDA, C.E., BLANTON-HOOKS, A.D., COLLIER, J.W., DRAKE, R.A., GRAVES, R.L., HALL, A.G., NELSON, A.I., SLONE, J.C., WILLIAMS, D.D., and WOOD, H.A., 2000, *Taenidium* and associated ichnofossils in fluvial deposits, Cretaceous Tuscaloosa Formation, eastern Alabama, U.S.A.: Ichnos, v. 7, p. 227–242.

SCHWERTMANN, U., 1993, Relations between iron oxides, soil color, and soil formation: Journal of Soil Science, v. 31, p. 51–69.

SMITH, J. J., AND HASIOTIS, S. T., 2008, Traces and burrowing behaviors of the cicada nymph *Cicadetta calliope*: Neoichnology and paleoecological significance of extant soil-dwelling insects: PALAIOS, in press.

SMITH, J.J., HASIOTIS, S.T., WOODY, D.T., and KRAUS, M.J., submitted 2008, *Naktodemasis bowni*: New ichnogenus and ichnospecies for adhesive meniscate burrows (AMB), and paleoenvironmental implications, Paleogene Willwood Formation, Bighorn Basin, Wyoming: Journal of Paleontology, 43 manuscript pages.

SMITH, R. M. H., AND MASON, T. R., 1998, Sedimentary environments and trace fossils of Tertiary oasis deposits in the central Namib Desert, Namibia: PALAIOS, v. 13, p. 547–559.

SQUIRES, R.L., and ADVOCATE, D.M., 1984, Meniscate burrows from Miocene lacustrine-fluvial deposits, Diligencia Formation, Orocopia Mountains, southern California: Journal of Paleontology, v. 58, p. 593–597.

VEPRASKAS, M.J., 1999, Redoximorphic features for identifying aquic conditions, North Carolina Agricultural Research Service, Technical Bulletin, 301, 33 p.

VERDE, M., UBILLA, M., JIMENEZ, J. J., and GENISE, J. F., 2007, A new earthworm trace fossil from paleosols: Aestivation chambers from the late Pleistocene Sopas Formation of Uruguay: Palaeogeography, Palaeoclimatology, Palaeoecology, v. 243, p. 339–347.

VITTUM, P.J., VILLANI, M.G., and TASHIRO, H., 1999, Turfgrass Insects of the United States and Canada: Cornell University Press, Ithaca, New York, 422 p.

LENGERKEN, H. VON,1954. Die Brutfürsorge und Brutpflegeinstinkte der Käfer: Akademische Verlagsgesellshaft Geest & Portig K.–G., Leipzig, Germany, 283 p.

WILLIS, E. R., and ROTH, L.M., 1962. Soil and moisture relations of *Scaptocoris divergins* Troeschner (Hemiptera: Cynidae). Annals of the Entomological Society of America 55, 21–32.

ZENGER, J.T., and GIBB T.J., 2001, Identification and impact of egg predators of *Cyclocephala lurida* and *Popillia japonica* (Coleoptera: Scarabaeidae) in turfgrass: Environmental Entomology, v. 30, p. 425–430.

CHAPTER FIVE. SUMMARY AND CONCLUSIONS

By integrating paleopedology, ichnotaxonomy, and neoichnology, this study takes a multidisciplinary approach to reconstructing the paleoenvironmental conditions of the Hugoton Basin area in the Lower Permian of western Kansas. Continental intervals in upper Council Grove Group contain features that indicate paleosol formation occurred under variable climatic conditions. Composite paleosols are the result of numerous 5th-order climatic and eustatic cycles occurring within the time frame of larger 4th-order cycles, juxtaposing both wet and dry indicators within individual paleosol units. Pedogenic features provide evidence that climate varied between semiarid and temperate, and likely did not reach arid conditions for extended periods of time. Quantitative indexing of pedogenic features in core allowed trends across formations to be seen; this data indicates that climate varied across formations and points to progressively wetter conditions during sea-level fall over the span of larger 3rd-order cycles.

As evidenced by abundant assemblages of continental trace fossils, paleosols were repeatedly colonized by soil-dwelling organisms during their formation. Trace fossils are most similar to *Naktodemasis bowni*, but trace fossil morphologies are unique enough to warrant the erection of a new ichnospecies—the name proposed here is *Naktodemasis krausi*. *N. krausi* shares with *N. bowni* cylindrical cross-sections, tortuous axes, meniscate fill, and thin linings, but is distinguished by the smooth transitions between packets of internal menisci with, unlike the angular offset between packets seen in *N. bowni*.

Experiments with modern insect larvae provide a convincing analog for *Naktodemasis* trace fossils. The burrows of masked chafer beetle larvae are similar enough to

Permian traces that they can be used to make inferences about the behavior, ecology, and burrowing mechanism of Permian tracemakers. These types of insect larvae have specific moisture requirements and cannot survive in extremely dry or fully saturated conditions. These tolerances suggest that Permian soil moisture during the interval of bioturbation fell within a similar range, of approximately 20-40%. Detailed study of chafer burrowing behavior revealed a unique, previously undescribed burrowing mechanism that is applicable to the Permian deposits described here, as well as many other instances of backfilled trace fossils in the geologic record. Contrary to some hypotheses of earlier workers, this study demonstrates conclusively that meniscate backfilled burrows can be produced in subaerial conditions in terrestrial environments.

Appendix 1: Indices of paleosol features by formation

Speiser Shale:

Depth from top of Speiser	XHC II	May Beaty II	D Alex II	Stuart II	XHC MI	May Beaty MI	D Alex MI	Stuart MI	XHC GI	May Beaty GI
0	20	A	A0	A	0	0	0	0	95	100
0.5	A5	A	A0	A	1	0	0	0	50	80
1	A	A		A	0	1		0	10	20
1.5	A	A		A	2	5		3	3	0
2	A	A	A0	A	1	5	0	0	4	0
2.5	A	A1	A0	A	0	0	0	0	3	7
3	A	A1	A0	A	1	0	0	0	5	10
3.5	A	A	A0	A	0	2	0	0	2	3
4	A	A	A	A	0	3	0	0	2	0
4.5	A	A	A	A	0	1	0	1	3	2
5	A	A	A	A	0	1	0	1	5	2
5.5	A	A	A	A	0	2	1	0	5	0
6	A	A	A	A7	0	7	1	0	3	0
6.5	A	A	A2	A10	0	7	0	0	10	2
7	A	A2	A	A.5	2	7	0	0	15	10
7.5	A	A	A1	A.5	1	5	0	0	15	95
8	A	A	A3	A.5	0	2	0	0	10	20
8.5	A	A	A1	A	0	4	0	0	7	15
9	A	A2	A3	A	0	7	0	0	3	50
9.5	A	A3	A5	A	0	5	0	0	2	30
10	A	A1	A1	A	0	1	0	0	1	3
10.5	A	A10	A	A2	0	0	0	7	3	2
11	A	A1	A3	A1	15	0	0	0	40	0
11.5	A	A	A	99	15	0	0	0	0	0
12	A	A	A	95	25	0	0	0	0	0
12.5	A	A15	A	5	17	2	0	1	0	10
13	A	A80	A	25	15	2	0	0.5	0	7
13.5	A	A15	97	15	10	2	0.5	2	0	2
14	A	A7	A	30	3	0.5	0	1	0	3
14.5	A	A40	A	80	10	1	0	0.5	0	30
15	A	A5	7	99	5	1	50	0	0	2
15.5	A5	A	0?	A	7	1	40	1	2	0
16	A1	A	0	A	2	1	80	0	3	0
16.5	A1	0?	0	A0?	5	1	50	0.5	7	5
17	A35	A	0/A0	A0?	5	1	10	0	50	0
17.5	A40		A	70?	3		0	0	15	
18	A10		A	50?	5		0	1	3	
18.5	A1		A	30?	0		5	30	1	
19	A		A0	A?	0		25	0	0	
19.5	A		A	A?	0		10	0	0	
20	A		A	A	0		10	0.5	0	

20.5	A2		A	A	3		0	5	1	
21	A5			A?	2			10	5	
21.5	A1				1				2	
22	A7				2				5	
22.5	A7				2				7	
23	A				0				0	
23.5	A				0				0	
24	A				0				0	
24.5	A				1				0	
25	A				0				0	
25.5	A				1				0	
26	2				7				0	
26.5	A15 or 15				5				5	
27	A15				3				3	
27.5	A10				5				2	
28	A				4				0	
28.5	A				3				0	
29	A1				1				1	
29.5	A				0				0	
30	A				0				0	
30.5	A				1				0	
31	A				0				0	
31.5	A				1				0	
32	A				1				2	
32.5	0?				2				3	
33	1				2				30	
33.5	A?				3				85	
34	A				3				100	
34.5	A				30				100	
35										

Speiser Shale (continued):

Depth from top of Speiser	D Alex GI	Stuart GI	XHC RI	May Beaty RI	D Alex RI	Stuart RI	XHC CI	May Beaty CI	D Alex CI	Stuart CI
0	100	100	5	0	0	0	0	0	0	0
0.5	100	100	10	0	0	0	0	0	0	0
1		100	10	0		0	0	1		0
1.5		90	0	0		0	0	0		0
2	100	5	0	0	0	0	0	5	0	0
2.5	100	5	7	1	0	0	0	3	0	0
3	100	1	5	0	0	1	0	5	0	0
3.5	100	0.5	0	3	0	0	0	10	0	0
4	100	0	5	0	0	0	0	6	0	0
4.5	100	0.5	2	3	0	0	0	1	0	0

5	1	0	5	3	1	1	0	1	0	0
5.5	2	1	5	0	1	7	0	1	0	0
6	2	5	3	0	2	10	0	1	1	0
6.5	15	15	0	0	0	3	0	10	3	0
7	15	0.5	0	0	0	15	0	7	1	0
7.5	17	0	10	0	2	3	1	0	2	0
8	10	0	7	7	5	0	0	0	0	0
8.5	15	0	7	15	15	0	0	0	0	0
9	15	1	10	50	7	0.5	0	0	0	0
9.5	15	0.5	5	30	5	0.5	0	0	0	0
10	5	25	0	3	5	0	0	0	3	0.5
10.5	4	20	0	0	4	0	0	0	0	0
11	5	8	0	0	1	2	0	0	0	0
11.5	1	0.5	0	0	1	0.5	0	0	0	0
12	1	1	0	0	1	2	0	0	0	0
12.5	25	10	0	0	0.5	3	0	0	0	0
13	95	0	0	1	1	2	0	0	0	0
13.5	3	0.5	0	0	1	7	0	0	0	0
14	0.5	0.5	0	1	1	4	0	0	0	0
14.5	10	1	0	1	7	0.5	0	0	0	0
15	50	25	0	1	0	0	0	0	0	1.5
15.5	60	80	0	1	0	1	0	0	0	0.5
16	20	100	0	1	0	0	0	0	0	0
16.5	50	100	0	0	0	0	0	30	0	0
17	60	100	0	1	0	0	0	0	0	0
17.5	100	95	0		0	0	0		0	0
18	100	100	3		0	0	0		0	0
18.5	100	100	1		0	0	0		0	0
19	90	100	0		0	0	0		0	0
19.5	2	100	0		0	0	0		0	13
20	2	100	0		0	2	0		0	50
20.5	90	100	0		0	0	0		0	1
21		100	0			0	0			0?
21.5			0				0			
22			5				0			
22.5			7				0			
23			0				0			
23.5			0				0			
24			0				0			
24.5			0				0			
25			0				0			
25.5			0				0			
26			7				15			
26.5			5				10			
27			3				7			
27.5			5				0			
28			4				0			
28.5			3				0			

29			1				0			
29.5			0				0			
30			0				0			
30.5			0				0			
31			0				1			
31.5			0				50			
32			1				40			
32.5			1				1			
33			2				2			
33.5			3				0			
34			3				0			
34.5			0				0			
35										

Blue Rapids Shale:

Depth from top of Blue Rapids	XHC II	May Beaty II	D Alex II	Stuart II	Prater II	XHC MI	May Beaty MI
0	A		A	A	A	0	
0.5	A	A0	A	A	A	0	0
1	A	A0	A0	A		0	0
1.5	A	A0	A0	A	A0	0	0
2	A	A	A	A		0	0
2.5	A	A	A	A	A	2	0
3	A		A	A	A3	2	
3.5	A		A	A	A10	2	
4	A2	A	A	A	A20	5	0
4.5	A	A0	A	A0?	A5	3	0
5	A0	A	A	A	A2	7	5
5.5	A0	A	A	A	A2	5	5
6	A0	A	A	A	A2	10	20
6.5	A	A	A	A	A	20	15
7	A	A	A1	A	A	20	10
7.5	A	A	A	A	A?	10	10
8	A	A	A	A	A/0	3	7
8.5	A		A	A5	A/0	?	
9	A		A	A	A	1	
9.5	A	A	A1	A	A/0	1	7
10	A	A0	A	A	A/0	1	2
10.5	A	A0	A	A2	A1/0	10	3
11	A	A	A	A1	A/0	15	2
11.5	A	A	A	A	A/0	5	2
12	A	A	A2	A		25	2
12.5	A	A	A	A		15	5
13	A	A	A4	A		7	5
13.5	A	A	A	A		5	4
14	A20	A	A	A?		1	0

14.5	A	A	A	A		0	1
15	A	A	A1			0	0
15.5	A3		A			0	
16	A5					0	
16.5	A0					1	
17	0?	A				10	0
17.5	A5	A				7	0
18	A60	A				7	0.5
18.5	A100	A				5	0
19	A90					2	
19.5	A100					1	
20	A100					1	
20.5	A85					0	
21	A100					1	
21.5	A100					0	
22	A100					0	
22.5	A					0	
23	A					0	
23.5	A					5	
24	A					3	
24.5	A					2	
25	A					1	
25.5	A1					3	
26	A100					2	
26.5	A					1	
27	A1					2	
27.5	A1					1	
28	A0					2	
28.5	A					0	
29	?					1	
29.5	A					1	
30	A					3	
30.5	A					0	
31	A					0	
31.5	A					0	
32	A					1	
32.5	?					1	

Blue Rapids Shale (continued):

Depth from top of Blue Rapids	D Alex MI	Stuart MI	Prater MI	XHC GI	May Beaty GI	D Alex GI	Stuart GI	Prater GI
0	0	0	0	100		100	100	40
0.5	0	7	0	90	100	100	100	5
1	?	7		100	100	100	100	
1.5	0.5	0	0	100	50	100	85	97
2	1	0		100	0	80	0	
2.5	10	0.5	0	5	1	7	0	10
3	2	0	0	3		3	0	0

3.5	1	0	1	3		6	0	5
4	0.5	0	0	2	5	2	5	0
4.5	1	1	0	15	15	2	1	0.5
5	0	7	0	3	2	0	0.5	0.5
5.5	0	15	0	1	1	0	0.25	4
6	1	5	0	2	1	3	30	2
6.5	1	4	7	5	0	1	1	20
7	0	15	6	7	0	3	0	45
7.5	1	5	15	5	0	3	2	3
8	7	5	2	2	0	4	1	70
8.5	40	10	1	1		30	1	100
9	45	7	1	?		25	1	100
9.5	15	5	1	?	100	0	0.5	95
10	7	3	2	0	100	5	0.25	1
10.5	4	7	1	1	100	30	0	5
11	7	2	2	1	50	15	0	7
11.5	4	3	0	0	2	1	0	10
12	7	2		0	0	7	0	
12.5	0	1		0	0	0	0	
13	5	0.5		0	0	2	0	
13.5	5	0.5		0	0	0	0	
14	4	7		1	0	0	30	
14.5	2	0		80	0	0	80	
15	70			93	50	0		
15.5	?			97		0		
16				85				
16.5				99				
17				50	0			
17.5				20	0			
18				15	1			
18.5				10	1			
19				2				
19.5				2				
20				50				
20.5				20				
21				60				
21.5				0				
22				1				
22.5				0				
23				0				
23.5				0				
24				0				
24.5				0				
25				0				
25.5				0				
26				0				
26.5				0				
27				0				
27.5				0				
28				0				
28.5				30				
29				90				
29.5				1				

30				0				
30.5				0				
31				0				
31.5				1				
32				2				
32.5				80				

Blue Rapids Shale (continued):

Depth from top of Blue Rapids	XHC RI	May Beaty RI	D Alex RI	Stuart RI	Prater RI	XHC CI	May Beaty CI	D Alex CI	Stuart CI	Prater CI
0	0		0	0	2	0		0	0	0
0.5	0	0	0	0	0	0	0	0	0	1
1	0	0	0	0		0	0	?	0	
1.5	0	1	0	0	20/0	0	1	5?	0	1
2	0	0	0	0		0	0	5	0	
2.5	5	0	0	0	0	5	1	0	0	1
3	100		0	0	0	7		0	0	5
3.5	100		0	0	3	5		0	0	15
4	100	R	0	0	0	3	0	0	0	85
4.5	100	R	0	100?	2	0	7	0	0	50
5	7	0	0	0	3	0	0	0	0	15
5.5	5	0	0	0	R/2	0	0	0	0	10
6	7	0	0	0	R	0	0	0	0	5
6.5	5	R	0	0	0	0	0	0	0	0.5
7	2	0	0	0	0	0	0	0.5	0	0
7.5	0	0	0	2	R	0	0	0.5	0.25	0.5
8	0	0	0	3?	0	0	0	0	0	0
8.5	0		0	0?	0	0		0	0	0
9	?		0	0?	0	0		0	0	0
9.5	?	0	0	0	0	0	0	0	0	0
10	?	0	0	0	1	0	0	0	0	0
10.5	1	0	0	0	1	0	0	0	0	0
11	2	0	0	0	1/R	0	0	0	0	0
11.5	3	0	0	0	0	0	0	0	0	0
12	1	0	0	0		1	0	0	0	
12.5	1	0	0	0		1	0	0	0	
13	0	0	0	0		0	0	0	0	
13.5	0	0	0	0.5		1	0	0	0	
14	0	0	0	0		5	0	0	0	
14.5	0	0	0	0		1	0	0	0	
15	0	0	0			0	0	0		
15.5	0		0?			0		0?		
16	1					0				
16.5	1					0				
17	2	0				0	1			
17.5	0	0				0	1			
18	0	0				0	10			
18.5	0	0				0	5			

19	0					0				
19.5	0					0				
20	0					0				
20.5	0					0				
21	0					0				
21.5	0					0				
22	0					0				
22.5	0					0				
23	0					0				
23.5	0					0				
24	0					0				
24.5	0					0				
25	0					0				
25.5	0					0				
26	0					0				
26.5	0					0				
27	0					0				
27.5	0					0				
28	0					0				
28.5	3					0				
29	0					0				
29.5	1					3				
30	0					0				
30.5	0					0				
31	0					0				
31.5	0					0				
32	2					0				
32.5	2					0				

Easly Creek Shale:

Depth from top of Easly Creek	XHC II	MBE2 II	D Alex II	Stuart II	Prater II	XHC MI	MBE2 MI
0	A	?	0	A	A	0	0?
0.5	A	?	99	98	A	2	0
1	A	98	A	A	A1	0	0
1.5	A	A	A	A	A	2	0
2	A	A	A	A	97	1	0
2.5	A	A	A	A	A	0	0.5
3	A	A	A1	A		0	0
3.5	A10	A	A	A	A	0	0.5
4	A5	A	A1	A	A	0	0
4.5	A	A	A	A	A	1	0
5	A	A15	A	A1	A1	20	0
5.5	A	A70	A	A	A1	5	0
6	A	A	A	A	A	15	0.5
6.5	A	A	A	A	A	25	0.5
7	A	A	A	A	A0?	15	5

7.5	A	A	A	A	A	5	1
8	A	A	A	A		4	1
8.5	A	A	A	A		40	15
9	A	A	A			70	10
9.5	A	A	A			70	0
10	A	A	A			30	0
10.5	A	A	A			25	0
11	A	A				75	0
11.5	A	A				50	0
12	A	A				25	0
12.5	A	A5				10	0
13	A2	A10				3	0
13.5	A10	A5				7	0
14	A10	A				10	0
14.5	A	A1				40	0
15	A	A				5	1
15.5	A	A				25	0
16	A	A2				10	0
16.5	A	A				5	2
17	A1					5	
17.5	A					4	
18	A					2	
18.5	A					2	
19	A					0	
19.5	0					0	
20	0					0	
20.5	2					0	
21	1					0	
21.5	1					0	
22	A					7	
22.5	A					3	
23	A					0	
23.5	A					0	
24	A					0	
24.5	A					0	

Easly Creek Shale (continued):

Depth from top of Easly Creek	D Alex MI	Stuart MI	Prater MI	XHC GI	MBE2 GI	D Alex GI	Stuart GI	Prater GI
0	0	0	0	7	100	60	100	100
0.5	0	0	2	2	95	0	100	50
1	0	0	0	0	10	0.5	70	15
1.5	0	0.5	2	0	3	0	2	7
2	0	0	0	5	5	0	0	30
2.5	0	0?	0	2	2	0	0	2
3	0	0?		0	2	0	10	

3.5	0	0	0	1	0.5	0.5	1	0
4	0	0	0	1	0	0	0	1
4.5	0	0	0	20	10	0	0	1
5	0	0	4	100	1	1	0	0.5
5.5	2	0	0	15	2	0	0.5	0
6	0	0	0.5	7	5	0.5	0	1
6.5	0	0	0.5	1	5	0	0	0.5
7	0	0	0.5	3	100	0	7	7
7.5	0	0	0.5	1	7	0	7	75
8	1	1		3	5	0	2	
8.5	0	60		2	5	0	15	
9	0			0	70	2		
9.5	0			0	0.5	0.5		
10	0			1	0.5	3		
10.5	0			7	0.5	95		
11				0	0.5			
11.5				20	0.5			
12				25	99			
12.5				7	0.5			
13				2	1			
13.5				3	25			
14				1	1			
14.5				1	0			
15				2	5			
15.5				5	1			
16				2	3			
16.5				3	1			
17				10				
17.5				7				
18				1				
18.5				10				
19				20				
19.5				0				
20				7				
20.5				25				
21				5				
21.5				15				
22				0				
22.5				0				
23				0				
23.5				0				
24				1				
24.5				2				

Easly Creek Shale (continued):

Depth from top of Easly Creek	XHC RI	MBE2 RI	D Alex RI	Stuart RI	Prater RI	XHC CI	MBE2 CI	D Alex CI	Stuart CI	Prater CI
0	0	0	0	0	0	7	0	0	0	0
0.5	R	0	0	0	0	1	0	0	1	0
1	R	0	0.5	0	0	0	10	0	5	5
1.5	R	50	0	0	0	0	5	0	1	0
2	0	100	0	0	0	0	8	3	2	0
2.5	1	15	0	0.5	0	0	5	3	4	0
3	R	15	0	0		0	2	4	7	
3.5	R	20	0.5	0	0	0	2	0.5	2?	5
4	0	20	0.5	1/R	0.5	0	7	1	10	7
4.5	0	10	0	R/0	0	0	0	0	15	0
5	0	5	0.5	0	0	0	5	0	25	0
5.5	0	3	0	0	0.5	0	20	0	15	0
6	0	2	0.5	0	8	0	0	0	3	0
6.5	2	4	0	2	0.5	0	1	0	4	0
7	0	0	0	5	7	0	25	0	5	0
7.5	0	2	0	10	1	?	10	0	10	0
8	R	80	0?	0		100?	0	0	0	
8.5	0	70	0?	R		?	0	0	0	
9	0	1	40			3	0	4		
9.5	0	0	25			0	0.5	7		
10	1	0	0			0	0.5	7		
10.5	10	0	0			0	0.5	10		
11	5	0				10	0.5			
11.5	10	0				40	0.5			
12	1	0				0	15			
12.5	5	0				0	15			
13	3	0				0	20			
13.5	2	0				0	5			
14	2	R				0	2			
14.5	0	R				0	0			
15	0	2				0	0			
15.5	0	5				0	2			
16	1	R				0	10			
16.5	0	R				0	5			
17	20					2				
17.5	3					0				
18	1					2				
18.5	100					7?				
19	80					0				
19.5	7					0				
20	0					0				
20.5	20					0				

21	20					0				
21.5	40					0				
22	5					0				
22.5	1					0				
23	3					0				
23.5	1					0				
24	1					0				
24.5	1					0				

A = homogeneous sediment (percent bioturbated not quantifiable)

II = percent covered by identifiable burrowing

MI = percent covered by anhydrite

GI = percent covered by gleying

RI = percent covered by root traces

CI = percent covered by carbonate

Appendix 2: Individual measurements of burrow diameters and orientations

Possible Orientations	Number of burrows of a given orientation	Percent of total	Categorized orientation	Percent of total
T	360	62.28373702	Horizontal	76.47058824
V/T	9	1.557093426	Vertical	11.41868512
SV	41	7.093425606	Subvertical	7.612456747
H	58	10.03460208	Subhorizontal	4.498269896
V	52	8.996539792		
T/H	5	0.865051903		
H/V (KINK)	2	0.346020761		
SH	26	4.498269896		
T/V	3	0.519031142		
H/T	18	3.114186851	T	62.28373702
HV (KINK)	1	0.173010381	H or SH	18.51211073
SV/T	3	0.519031142	V or SV	17.12802768

Range of possible diameters	Number of burrows of a given diameter	Range of possible diameters	Number of burrows of a given diameter	Range of possible diameters	Number of burrows of a given diameter
0.01	0	0.48	8	0.95	0
0.02	0	0.49	4	0.96	0
0.03	0	0.5	15	0.97	0
0.04	0	0.51	15	0.98	0
0.05	0	0.52	11	0.99	0
0.06	0	0.53	9	1	0
0.07	0	0.54	5	1.01	0
0.08	0	0.55	13	1.02	0
0.09	1	0.56	7	1.03	0
0.1	0	0.57	4	1.04	0
0.11	0	0.58	4	1.05	0
0.12	0	0.59	3	1.06	1
0.13	3	0.6	4	1.07	0
0.14	1	0.61	9	1.08	0
0.15	0	0.62	4	1.09	0
0.16	3	0.63	3	1.1	0
0.17	2	0.64	0	1.11	0
0.18	5	0.65	6	1.12	0
0.19	4	0.66	5	1.13	0

0.2	8	0.67	3	1.14	0
0.21	3	0.68	1	1.15	0
0.22	4	0.69	1	1.16	0
0.23	7	0.7	1	1.17	0
0.24	9	0.71	1	1.18	0
0.25	18	0.72	1	1.19	0
0.26	9	0.73	1	1.2	0
0.27	18	0.74	3	1.21	0
0.28	8	0.75	1	1.22	0
0.29	10	0.76	0	1.23	0
0.3	17	0.77	0	1.24	0
0.31	18	0.78	0	1.25	0
0.32	16	0.79	0	1.26	0
0.33	12	0.8	2	1.27	0
0.34	8	0.81	0	1.28	0
0.35	24	0.82	0	1.29	0
0.36	19	0.83	0	1.3	0
0.37	16	0.84	0	1.31	0
0.38	16	0.85	0	1.32	0
0.39	15	0.86	0		
0.4	12	0.87	0		
0.41	12	0.88	0		
0.42	15	0.89	0		
0.43	16	0.9	0		
0.44	10	0.91	0		
0.45	22	0.92	0		
0.46	17	0.93	0		
0.47	14	0.94	0		

Trace Diameters in cm	Orientation	Trace Diameters in cm	Orientation	Trace Diameters in cm	Orientation
0.42	T	0.65	V	0.25	T
0.55	V/T	0.43	T	0.6	T
0.23	SV	0.41	T/H	0.56	SH
0.59	SV	0.53	T	0.32	T
0.52	T	0.34	T	0.45	T
0.36	T	0.51	T/V	0.24	SV
0.61	SV	0.45	H	0.39	H
0.37	T	0.5	V/SV	0.35	T
0.54	H	0.26	SV	0.16	T

0.43	V	0.55	V	0.25	V/T
0.34	T	0.6	SV	0.49	
0.28	SH	0.68	V	0.23	T
0.53	H	0.92	V	0.35	T/H
0.53	T	0.36	T	0.5	T/H
0.23	T	0.72	V	0.48	T
0.3	T	0.77	V	0.2	T
0.25	T	0.73	T	0.14	T
0.35	SV	0.48	T	0.37	V
0.29	SV	0.42	T	0.65	T
0.62	T	0.53	T	0.48	T
0.61	V	0.53	T	0.19	SH
0.3	T	0.44	SV	0.36	H/T
0.5	T/H	0.42	V	0.55	T
0.3	SV	0.43	H/T	0.51	T
0.38	T	0.53	V/T	0.47	T
0.53	V	0.21	T	0.66	T
0.48	SV	0.25	H/T	0.23	T
0.47	T	0.73	V	0.35	T
0.49	T	0.41	T	0.36	T
0.36	T	0.25	H	0.39	T
0.31	T	0.3	SV	0.55	SV
0.45	SV	0.57	SV	0.2	H/T
0.59	SV	0.56	T	0.18	T
0.37	T	0.22	T	0.17	T
0.59	T	0.47	H/T	0.18	T
0.72	SV	0.24	V	0.17	T
0.43	H	0.42	T	0.25	T
0.42	SV	0.38	H	0.4	H
0.4	V	0.31	T	0.66	H/T
0.29	H	0.23	T	0.31	T
0.6	H/V (KINK)	0.42	T	0.35	T
0.63	SH	0.21	T	0.3	T
0.51	T	0.22	V	1.06	V
0.65	SV	0.16	T	0.74	T
0.39	H	0.13	T	0.61	T
0.29	T	0.22	T	0.36	T
0.45	H	0.51	T	0.8	SV
0.6	T	0.29	SH	0.24	V
0.8	V	0.39	T	0.39	T
0.4	SV	0.41	T	0.33	T
0.19	T	0.34	SH	0.25	T

0.26	T	0.22	T	0.45	T
0.37	T	0.35	T	0.45	T
0.26	SV	0.55	T	0.48	T
0.36	T	0.31	H	0.5	SH
0.19	T	0.34	T	0.3	H
0.43	T	0.29	SH	0.46	T
0.46	SV/T	0.4	SH	0.27	T
0.2	T	0.39	SV	0.4	T
0.46	T	0.38	T	0.91	T
0.47	H/T	0.37	H	0.23	SH
0.28	H	0.36	V	0.63	V
0.43	T	0.53	T	0.37	SH
0.65	T	0.3	V	0.44	H
0.24	T	0.61	T	0.55	SH
0.66	SV/T	0.59	T	0.35	T
0.46	H/T	0.45	H/T	0.46	T
0.5	T	0.62	V	0.32	T
0.35	T	0.48	V	0.43	T
0.27	T	0.52	T	0.33	T
0.45	T	0.45		0.2	T
0.18	V	0.35		0.33	T
0.43	T	0.46	T	0.38	T
0.51	T	0.41		0.3	SV
0.43	T	0.45		0.3	T
0.48	H	0.6	SV	0.61	V
0.31	T	0.45	T	0.39	T
0.65	V	0.43	T	0.61	T
0.27	T	0.45	T	0.52	T
0.72	SV	0.37	T	0.28	T
0.68	T	0.35	T	0.35	T
0.52	T	0.5	T	0.3	T
0.47	T	0.52	T	0.44	T
0.65	T	0.5	T	0.37	SV
0.27	T	0.53	T	0.46	T
0.65	T	0.45	H	0.38	H
0.25	H	0.32	T	0.55	T
0.3	T	0.51	V	0.2	T
0.27	T	0.47	T	0.25	T
0.4	SH	0.27	T	0.29	H
0.24	H	0.42	T	0.21	T
0.56	T	0.42	T	0.37	T
0.37	T	0.42	H	0.24	T
0.33	T	0.44	T	0.32	H

0.34	SH	0.44	T	0.28	T
0.25	T	0.41	T	0.32	T
0.39	T	0.41	T	0.26	SV
0.32	H	0.56	H/T	0.36	H/T
0.13	T	0.53	T	0.36	T
0.25	T	0.61	T	0.44	H
0.36	T	0.27	T	0.33	T
0.25	T	0.37	SV/T	0.31	T
0.35	T	0.37	H	0.66	SV
0.27	H	0.3	T	0.45	V
0.43	T	0.53	H	0.49	SV
0.55	T	0.35	T	0.44	SH
0.61	T	0.62	H/T	0.58	T
0.38	T	0.52	T	0.56	V
0.35	T	0.32	T	0.25	SV
0.5	T	0.27	T	0.29	T
0.38	H	0.36	T	0.25	T
0.52	T	0.51	H	0.32	T
0.45	T	0.43	T	0.32	T
0.47	H	0.47	T	0.24	T
0.46	T	0.26	T	0.5	T
0.33	H	0.5	H/V (KINK)	0.52	T
0.26	T	0.5	T	0.32	T
0.27	T	0.25	H	0.51	T
0.57	V	0.29	T	0.24	T
0.45	T	0.41	T	0.2	SH
0.46	H/T	0.27	T	0.3	T
0.5	T	0.51	T	0.31	T
0.37	T	0.34	T	0.59	V
0.65	V/SV	0.52	T	0.34	SV
0.35	V/T	0.35	T	0.41	V
0.48	T	0.49	V/T	0.6	T
0.45	T	0.55	H	0.36	T
0.7	V	0.41	T	0.3	T
0.56	T	0.29	V	0.46	T
0.35	T	0.63	H	0.31	T
0.67	V	0.36	T	0.43	T
0.58	T	0.25	T	0.31	T
0.38	T	0.35	T	0.54	V
0.19	T	0.29	H	0.52	V
0.27	T	0.23	H	0.5	V
0.45	T	0.51	T	0.53	V

0.33	V/T	0.4	T	0.47	T
0.71	SV	0.25	T/H	0.33	SH
0.33	T	0.54	H	0.43	T
0.4	T	0.31	T	0.2	H
0.61	V	0.18	T	0.55	T
0.44	T	0.51	T	0.67	V
0.23	T	0.32	T	0.46	T
0.42	T	0.16	T	0.38	T
0.5	SV	0.39	T	0.46	T
0.2	T	0.45	T	0.39	T
0.13	T	0.31	T	0.32	T
0.09	T	0.51	H/T	0.36	SV
0.45	H	0.46	SV	0.45	T
0.32	T	0.31	T	0.44	T
0.3	T	0.31	T	0.36	T
0.5	T	0.28	T	0.59	H/T
0.49	T	0.66	V/T	0.27	H
0.29	T	0.38	T	0.27	SH
0.38	T	0.61	H	0.3	T
0.38	SV	0.38	T	0.37	T
0.43	SH	0.41	H	0.43	H
0.3	T	0.4	T	0.35	H
0.61	V	0.23	H/T	0.25	SH
0.55	T	0.27	SH	0.33	SH
0.52	T	0.75	V/T	0.43	SH
0.54	T	0.43	V	0.36	T
0.37	T	0.3	V	0.32	SH
0.35	T	0.4	H	0.4	T
0.38		0.35	H	0.3	T
0.42	SH	0.6	V	0.47	T
0.32	T	0.47	T	0.39	T
0.36	T	0.42	V	0.44	T
0.54	V	0.63	V	0.31	T
0.62	T	0.31	H	0.5	T/V
0.33	T	0.32	V	0.36	T
0.55	T	0.74	V	0.42	SV
0.69	T	0.57	T	0.39	T
0.46	T	0.27	H/T	0.31	T
0.46	T	0.39	V/T	0.3	T
0.31	T	0.24	H	0.41	T
0.45	T	0.67	T	0.35	T
0.51	SV	0.27	H	0.26	T
0.51	H	0.26	T	0.39	T

0.31	SV	0.42	T	0.34	T
0.57	T	0.42	T	0.58	T
0.36	T	0.55	SV	0.46	T
0.39	T	0.62	T	0.46	T
0.36	T	0.58	SV/SH (KINK)	0.28	T
0.38	T	0.37	T	0.47	T
0.27	H	0.4	H/T	0.47	T
0.37	T	0.74	T	0.28	T
0.48	T	0.38	T	0.26	T
0.25	T	0.53	T	0.37	T
0.34	H	0.52	T	0.35	V
0.42	T	0.51	H	0.35	T
0.56	T/V	0.54	V/SV	0.47	H
0.47	H				
0.45	T				
0.4	V				
0.55	V/SV				
0.42	V/SV				
0.28	T				
0.18	T				
0.41	H				
0.28	T				
0.35	T				
0.82	HV (KINK)				
0.51	T				
0.33	SH				
0.38	T				

Appendix 3: Burrow diameters by core and formation

XHC								
0.42	0.33	0.45	0.31	0.13	0.16	0.91	0.3	0.49
0.55	0.8	0.5	0.34	0.25	0.25	0.23	0.27	0.36
0.23	0.4	0.26	0.29	0.36	0.49	0.63	0.4	0.31
0.59	0.19	0.55	0.4	0.25	0.23	0.37	0.24	0.45
0.52	0.26	0.6	0.39	0.35	0.35	0.44	0.56	0.59
0.36	0.37	0.68	0.38	0.27	0.5	0.55	0.37	0.37
0.61	0.26	0.92	0.37	0.43	0.48	0.35	0.33	0.59
0.37	0.36	0.36	0.36	0.55	0.2	0.46	0.34	0.72
0.54	0.19	0.72	0.53	0.61	0.14	0.32	0.25	0.43
0.43	0.43	0.77	0.3	0.38	0.37	0.43	0.51	0.42
0.34	0.46	0.73	0.61	0.35	0.65	0.33	0.34	0.4
0.28	0.2	0.48	0.59	0.3	0.48	0.2	0.22	0.29
0.53	0.46	0.42	0.45	0.44	0.19	0.33	0.35	0.61
0.53	0.47	0.53	0.62	0.37	0.36	0.38	0.55	0.3
0.23	0.28	0.53	0.48	0.46	0.55	0.3	0.6	0.5
0.3	0.43	0.44	0.52	0.38	0.51	0.3	0.63	0.3
0.25	0.65	0.42	0.45	0.55	0.47	0.61	0.51	0.38
0.35	0.24	0.43	0.35	0.2	0.66	0.39	0.65	0.53
0.29	0.66	0.53	0.46	0.25	0.23	0.61	0.39	0.48
0.62	0.46	0.21	0.41	0.29	0.35	0.52	0.29	0.47
0.6	0.65	0.43	0.41	0.53	0.34	0.51	0.38	0.29
0.27	0.45	0.35	0.39	0.24	0.45	0.32	0.56	0.6
0.48	0.47	0.52	0.32	0.25	0.43	0.22	0.5	0.39
0.31	0.24	0.5	0.44	0.4	0.51	0.4	0.46	0.35
0.65	0.42	0.53	0.41	0.66	0.25	0.41	0.39	0.82
0.27	0.38	0.45	0.35	0.31	0.17			
0.72	0.31	0.32	0.39	0.35	0.28			
0.68	0.23	0.51	0.33	0.3				
0.52	0.42	0.47	0.25	1.06				
0.47	0.21	0.27	0.45	0.74				
0.65	0.22	0.42	0.45	0.61				
0.27	0.16	0.42	0.48	0.36				
0.65	0.13	0.42	0.5	0.8				
0.25	0.22	0.44	0.3	0.24				
0.5	0.25	0.45	0.21	0.36				
0.35	0.73	0.6	0.37	0.39				

0.27	0.41	0.45	0.24	0.55				
0.45	0.25	0.43	0.32	0.2				
0.18	0.3	0.45	0.28	0.18				
0.43	0.57	0.37	0.32	0.17				
0.51	0.56	0.35	0.28	0.18				
MBE2								
0.5	0.45	0.47	0.43	0.35	0.37	0.29	0.49	0.33
0.38	0.33	0.26	0.31	0.48	0.37	0.63	0.44	0.31
0.52	0.71	0.5	0.18	0.45	0.3	0.36	0.58	0.66
0.45	0.33	0.5	0.51	0.7	0.53	0.25	0.56	0.45
0.47	0.4	0.25	0.32	0.56	0.35	0.35	0.25	0.52
0.46	0.61	0.29	0.16	0.35	0.62	0.29	0.29	0.35
0.33	0.44	0.41	0.18	0.67	0.52	0.23	0.25	0.49
0.26	0.23	0.27	0.26	0.58	0.32	0.51	0.32	0.55
0.27	0.42	0.51	0.36	0.38	0.27	0.4	0.32	0.41
0.57	0.41	0.34	0.36	0.19	0.36	0.25	0.24	0.61
0.45	0.41	0.52	0.44	0.27	0.51	0.54	0.5	0.27
0.46	0.56	0.37						
0.5	0.53	0.65						
D ALEX								
0.32	0.38	0.62	0.52	0.55	0.36	0.49	0.32	0.55
0.51	0.28	0.33	0.5	0.52	0.3	0.29	0.36	0.67
0.24	0.5	0.55	0.53	0.54	0.46	0.38	0.54	0.46
0.2	0.2	0.69	0.47	0.37	0.31	0.38	0.45	0.32
0.3	0.13	0.46	0.33	0.35	0.43	0.43	0.51	0.3
0.31	0.09	0.46	0.43	0.38	0.31	0.3	0.51	0.5
0.59	0.45	0.31	0.2	0.42	0.54	0.61	0.6	0.41
0.34								
STUART								
0.31	0.61	0.26	0.45	0.31	0.25	0.4	0.38	0.24
0.57	0.38	0.42	0.31	0.32	0.34	0.35	0.53	0.67
0.36	0.41	0.42	0.51	0.74	0.42	0.6	0.52	0.27
0.39	0.4	0.55	0.46	0.57	0.56	0.47	0.51	0.28
0.36	0.23	0.62	0.31	0.27	0.42	0.42	0.54	0.66
0.38	0.27	0.58	0.31	0.39	0.39	0.63	0.55	0.38
0.27	0.75	0.37	0.48	0.3	0.74	0.37	0.43	0.4
PRATER								
0.46	0.47	0.28	0.3	0.27	0.28	0.32	0.58	0.33

0.39	0.39	0.26	0.41	0.3	0.47	0.4	0.46	0.43
0.32	0.44	0.37	0.35	0.37	0.47	0.3	0.46	0.36
0.36	0.31	0.35	0.26	0.43	0.36	0.42	0.4	0.47
0.45	0.5	0.35	0.39	0.35	0.59	0.39	0.31	0.45
0.44	0.36	0.47	0.34	0.25	0.27			
SPEISER								
0.42	0.47	0.25	0.45	0.43	0.38	0.61	0.35	0.72
0.55	0.42	0.29	0.46	0.42	0.28	0.38	0.62	0.77
0.23	0.63	0.41	0.5	0.4	0.5	0.41	0.52	0.5
0.59	0.31	0.27	0.37	0.29	0.2	0.4	0.32	0.38
0.52	0.32	0.51	0.65	0.6	0.13	0.23	0.27	0.52
0.36	0.74	0.34	0.35	0.63	0.09	0.27	0.36	0.45
0.61	0.57	0.52	0.48	0.51	0.45	0.75	0.51	0.47
0.37	0.27	0.35	0.45	0.65	0.32	0.43	0.43	0.46
0.54	0.39	0.49	0.7	0.39	0.3	0.3	0.47	0.33
0.43	0.32	0.55	0.56	0.29	0.5	0.4	0.26	0.26
0.34	0.51	0.41	0.35	0.45	0.49	0.35	0.5	0.27
0.28	0.24	0.31	0.67	0.6	0.29	0.6	0.5	0.57
0.53	0.2	0.57	0.58	0.65	0.38	0.5	0.31	0.56
0.53	0.3	0.36	0.38	0.43	0.38	0.53	0.51	0.53
0.23	0.31	0.39	0.19	0.41	0.43	0.47	0.46	0.61
0.3	0.59	0.36	0.27	0.53	0.3	0.33	0.31	0.27
0.25	0.34	0.38	0.45	0.34	0.61	0.43	0.31	0.37
0.35	0.41	0.27	0.33	0.51	0.55	0.2	0.28	0.37
0.29	0.6	0.37	0.71	0.45	0.52	0.55	0.66	0.3
0.62	0.36	0.48	0.33	0.5	0.54	0.67	0.38	0.53
0.61	0.3	0.25	0.4	0.26	0.37	0.46	0.36	0.72
0.3	0.46	0.34	0.61	0.55	0.45	0.47	0.54	0.39
0.5	0.31	0.42	0.44	0.6	0.59	0.49	0.52	0.45
0.3	0.43	0.56	0.23	0.68	0.37	0.36	0.41	0.53
0.38	0.31	0.42	0.42	0.92	0.59	0.31	0.41	0.48
BLUE RAPIDS								
0.73	0.25	0.24	0.5	0.38	0.39	0.69	0.68	0.43
0.48	0.51	0.33	0.48	0.53	0.41	0.46	0.52	0.35
0.42	0.34	0.8	0.2	0.52	0.25	0.46	0.47	0.25
0.53	0.22	0.4	0.14	0.51	0.6	0.24	0.65	0.33
0.53	0.35	0.19	0.37	0.54	0.56	0.67	0.27	0.43

0.44	0.55	0.26	0.65	0.46	0.32	0.27	0.65	0.36
0.42	0.31	0.37	0.48	0.39	0.45	0.26	0.25	0.32
0.43	0.34	0.26	0.19	0.32	0.24	0.42	0.3	0.4
0.53	0.29	0.36	0.36	0.36	0.39	0.42	0.27	0.3
0.21	0.4	0.19	0.55	0.45	0.35	0.55	0.4	0.47
0.25	0.39	0.43	0.51	0.44	0.16	0.62	0.24	0.39
0.73	0.38	0.46	0.47	0.36	0.25	0.58	0.56	0.44
0.41	0.37	0.2	0.66	0.59	0.49	0.37	0.37	0.31
0.25	0.36	0.46	0.23	0.27	0.23	0.4	0.33	0.5
0.3	0.53	0.47	0.35	0.27	0.35	0.74	0.34	0.36
0.57	0.3	0.28	0.36	0.3	0.33	0.27	0.36	0.42
0.56	0.61	0.43	0.39	0.37	0.55	0.72	0.8	0.39
0.22	0.59	0.65	0.55	0.22	0.38	0.43	0.31	0.38
0.47	0.29	0.24	0.2	0.16	0.42	0.51	0.35	0.82
0.24	0.63	0.66	0.18	0.13	0.32	0.43	0.3	0.25
0.42	0.36	0.46	0.17	0.22	0.36	0.48	1.06	0.4
0.38	0.25	0.5	0.18	0.51	0.54	0.31	0.74	0.66
0.31	0.35	0.35	0.17	0.29	0.62	0.65	0.61	0.18
0.23	0.29	0.27	0.21	0.35	0.42	0.23	0.45	
EASLY CREEK								
0.45	0.56	0.28	0.54	0.45	0.44	0.34	0.26	0.35
0.62	0.25	0.26	0.31	0.51	0.33	0.58	0.36	0.26
0.48	0.29	0.37	0.18	0.51	0.31	0.46	0.36	0.39
0.52	0.25	0.35	0.51	0.55	0.66	0.46	0.5	0.47
0.45	0.32	0.35	0.32	0.31	0.45	0.28	0.52	0.45
0.35	0.32	0.47	0.16	0.3	0.49	0.47	0.31	0.58
0.46	0.24	0.4	0.18	0.41	0.44	0.47	0.25	0.4
0.51								